SYNTHESIS, STRUCTURE, AND REACTIVITY OF HYDRIDE AND PHOSPHIDE COMPLEXES OF HAFNIUM AND ZIRCONIUM

Thesis by

Dean Michael Roddick

In Partial Fulfillment of the requirements

for the Degree of

Doctor of Philosophy

California Institute of Technology

Pasadena, California

1984

(Submitted January 30, 1984)

Acknowledgements

I would like to thank a number of people, past and present, for their friendship and help during my stay at Caltech: from Mike Fryzuk, who introduced me to high-vacuum line techniques, to the present Bercaw crew (Alan, Tippy and his gismos, the 3 R's *et al.*, etc.) who provided an intellectually(?) stimulating environment for me in the latter part of my graduate career. I would also like to thank Don for the moussaka, and Eric for his unflagging support of the California Golden Bears.

In addition to members of the Bercaw group, there are several members of the Caltech community whose friendship and support deserve mention: George Spies, for his kindness and numerous jump starts, Dan Straus, for his companionship and advice, and Jeff Peake, for lasting more than 6 months as a roommate. Special thanks also to Bernie Santarsiero for all of his help, time, and patience, both in crystallographic work and in extracurricular activities.

I am particularly grateful for the financial support and occasional good advice of John Bercaw, both prior to and during my graduate career, without which thesis writing itself would be impossible. Finally, I would like to thank Nancy, who both professionally and personally has had a profound impact on my life.

Abstract

A series of alkyl hydride complexes $Cp^*_2Hf(H)R$ (R= Et, CH_2CHMe_2, CH_2CH_2Ph; Cp^*= η-C_5Me_5) have been prepared by reaction of $Cp^*_2HfH_2$ with the appropriate olefin. The reactions of these compounds with H_2 and C_2H_4 follow those of the previously reported zirconium isobutyl hydride, $Cp^*_2Zr(H)CH_2CHMe_2$, giving $Cp^*_2HfH_2$ and metallacyclopentane $Cp^*_2Hf\overline{CH_2CH_2CH_2CH_2}$, respectively, plus one equivalent alkane. All alkyl hydrides examined exhibit high thermal stability and decompose only slowly at 80°C. The thermolysis of $Cp^*_2Hf(H)CH_2CHMe_2$ yields a 1:1 mixture of $Cp^*_2HfH_2$ and a metallacyclobutane complex $Cp^*_2Hf\overline{CH_2CH(Me)CH_2}$. A proposed mechanism for the formation of $Cp^*_2HfCH_2CH(Me)CH_2$ is given, involving initial γ-H abstraction from the isobutyl methyls of $Cp^*_2Hf(H)CH_2CHMe_2$. $Cp^*_2HfH_2$ also reacts cleanly with t-butylacetylene to form a remarkably stable alkenyl hydride complex, $Cp^*_2Hf(H)CH{=}CH^tBu$. The reactivity of $Cp^*_2Hf(H)CH{=}CH^tBu$ with H_2 and C_2H_4 is similar to that observed for the related alkyl hydrides. The hydride complexes $Cp^*_2Hf(H)Ph$ and $Cp^*_2Hf(H)CH_2CMe_3$ have been conveniently prepared by the metathesis of $Cp^*_2HfH_2$ with PhLi and $LiCH_2CMe_3$, respectively.

$Cp^*_2HfH_2$ reacts cleanly with allene to form the π-allyl hydride $Cp^*_2Hf(H)(\eta^3\text{-}CH_2CHCH_2)$. ^1H and ^{13}C NMR data as well as labeling studies indicate that $Cp^*_2Hf(H)(\eta^3\text{-}CH_2CHCH_2)$ is highly fluxional, and isostructural to $Cp^*_2Zr(H)(\eta^3\text{-}CH_2CHCH_2)$. The crystal structure of $Cp^*_2Hf(H)(\eta^3\text{-}CH_2CHCH_2)$ is presented. The

coordination of the allyl ligand is confirmed to be trihapto, with notably asymmetric Hf-C(allyl) distances (2.38, 2.48, 2.57 A). The final R index is 0.049. The hydride ligand has been reliably located, and represents the first structurally characterized example of a terminal Hf–H bond.

$Cp^*_2Zr(H)CH_2CHMe_2$ has been shown to react cleanly with CO to form the enolate hydride $Cp^*_2Zr(H)OCH{=}CHCHMe_2$. A proposed mechanism for formation of $Cp^*_2Zr(H)OCH{=}CHCHMe_2$ involves hydride migration via the initially formed acyl hydride $Cp^*_2Zr(H)(\eta^2\text{-}C(O)CH_2CHMe_2)$ to give a π-coordinated aldehyde complex $Cp^*_2Zr(\eta^2\text{-}OCHCH_2CHMe_2)$, which subsequently β-H eliminates to give the observed product. Support for the intermediacy of a π-aldehyde complex in this transformation is provided by the reaction of $Cp^*_2M(H)CH_2CHMe_2$ (M= Zr, Hf) with excess CO under controlled conditions to give moderately stable π-aldehyde carbonyl complexes $Cp^*_2M(CO)(\eta^2\text{-}OCHCH_2CHMe_2)$. Thermolysis of $Cp^*_2Hf(CO)(\eta^2\text{-}OCH\text{-}CH_2CHMe_2)$ results in a novel coupling reaction to form the enediolate $Cp^*_2Hf\overline{OC(CH_2CHMe_2)CHO}$. The coordinatively unsaturated zirconium π-aldehyde intermediate $Cp^*_2Zr(\eta^2\text{-}OHCCH_2\text{-}CHMe_2)$ is also implicated in the reactions of acyl hydride $Cp^*_2Zr(H)(\eta^2\text{-}C(O)CH_2CHMe_2)$ with trapping substrates C_2H_4, $MeC{\equiv}CMe$, H_2, and $HC{\equiv}C^tBu$ upon warming to give $Cp^*_2Zr\overline{(OCH(\text{-}CH_2CHMe_2)CH_2CH_2)}$, $Cp^*_2Zr\overline{(OCH(CH_2CHMe_2)C(Me){=}C(Me))}$, $Cp^*_2Zr\text{-}(H)OCH_2CH_2CHMe_2$, and $Cp^*_2Zr(C{\equiv}C^tBu)OCH_2CH_2CHMe_2$, respectively. Carbonylation of the alkenyl hydride $Cp^*_2Hf(H)CH{=}C\text{-}H^tBu$ did not yield an aldehyde complex, but rather the

metallacycle $Cp^*_2Hf(OHC{=}CHCH(^tBu))$. Mechanistic interpretations of these and related reactions are presented.

A series of mono-ring, terminal phosphido complexes of hafnium have been prepared. Reaction of Cp^*HfCl_3 with one equivalent or excess LiP^tBu_2 yields deeply-colored phosphide complexes $Cp^*HfCl_2(P^tBu_2)$ and $Cp^*HfCl(P^tBu_2)_2$, respectively. Alkyl and aryl derivatives of $Cp^*HfCl_2(P^tBu_2)$, $Cp^*HfR(Y)(P^tBu_2)$ (R=Y=Me; Y=Cl, R-CH_2CMe, CH_2Ph, Ph), are prepared either by direct alkylation, or from the corresponding chloro-alkyls $Cp^*Cl_nR_{3-n}$. $Cp^*HfMe_2(P^tBu_2)$ reacts slowly with H_2 to form a highly insoluble methyl hydridophosphide dimer, $[Cp^*HfMe(\mu\text{-}H)(\mu\text{-}P^tBu_2)]_2$. The crystal structure of $[Cp^*HfMe(\mu\text{-}H)(\mu\text{-}P^tBu_2)]_2$ reveals a symmetric-bridged Hf_2P_2 core with Hf–P distances of 2.805, 2.807 A. The hydride ligands have been tentatively located and form an assymetric Hf_2H_2 bridge (Hf–H= 2.12, 2.33 A) orthogonal to the planar Hf_2P_2 moiety. The final R index is 0.066. Hydrogenolysis of alkyl derivatives $Cp^*HfClR(P^tBu_2)$ (R= CH_2CMe_3, CH_2Ph) affords an analogous chloro-hydridophosphide dimer, $[Cp^*HfCl(\mu\text{-}H)(\mu\text{-}P^tBu_2)]_2$. Treatment of $Cp^*HfCl(P^tBu_2)_2$ with H_2 leads to rapid cleavage of Hf–P bonds and formation of $[Cp^*HfCl(\mu\text{-}H)(\mu\text{-}P^tBu_2]_2$. $Cp^*HfCl_2(P^tBu_2)$ also reacts with H_2, albeit slower, to give products derived from initially-formed Cp^*HfCl_2H.

The relatively low Hf–P bond energy suggested by hydrogenolysis reactions in these systems is further indicated by the reaction of $Cp^*HfCl_2(P^tBu_2)$ with CO to

form the CO-insertion product, $Cp^*HfCl_2(\eta^2\text{-}C(O)P^tBu_2)$. The crystal structure of $Cp^*HfCl_2(\eta^2\text{-}C(O)P^tBu_2)$ exhibits dihapto carboxyphosphide functionality, with Hf—C = 2.203 and Hf—O = 2.117 A. The P—C(acyl) bond is 0.08 A shorter than P—C(alkyl) values, and suggests a significant P—π interaction. This has been confirmed by variable temperature studies, which reveal a substantial (10.7 kcal/mol) barrier to rotation about the P—C(acyl) bond.

Table of Contents

Chapter I

Synthesis and Reactivity of Alkyl, Alkenyl, and Aryl Derivatives of Permethylhafnocene Dihydride.

Introduction

Transition metal complexes bearing cis hydride and alkyl ligands comprise an important class of organometallic compounds. Typically, the thermal stability of such complexes is quite low, and as a consequence systematic study of the reactivity associated with alkyl hydride complexes has been limited.[1] McAlister, Erwin, and Bercaw have reported the facile insertion of isobutylene into the Zr-H bonds of $Cp^*_2ZrH_2$ to form the isobutyl hydride complex $Cp^*_2Zr(H)CH_2CHMe_2$ (1).[2] In contrast to the majority of reported alkyl hydride complexes, the thermal stability of 1 is exceptionally high ($t_{½}$(74°C) = 2.7 h) and has permitted detailed study of its reaction chemistry.[2,3]

The unusual stability of 1 suggested to us the opportunity to examine in some detail the reaction chemistry of related hydrido complexes derived from the third row analog to $Cp^*_2ZrH_2$, $Cp^*_2HfH_2$ (2).[4] Accordingly, we have prepared a series of hafnium (IV) alkyl, alkenyl, and aryl hydride complexes, the synthesis and reactivity of which is reported herein.

Results and Discussion

(1) Synthesis and Reactivity of Hafnium Alkyl Hydrides

Solutions of $Cp^*_2HfH_2$ (2) react smoothly with ethylene, styrene or isobutylene to afford the corres-

ponding alkyl hydride complexes quantitatively (^{1}H NMR), as shown in equation 1. This formal insertion reaction of an

$$Cp^*_2HfH_2 + H_2C{=}CRR' \longrightarrow Cp^*_2Hf(H)CH_2CHRR' \qquad (1)$$

3, R = R' = H

4, R = R' = Me

5, R = H; R' = Ph

olefin into a Hf-H bond is facile for ethylene and styrene, proceeding to completion in minutes at 25°C. In contrast, the reaction of 2 with isobutylene requires more forcing conditions (80°C, hours) and excess olefin to effect the insertion; this is perhaps due to increased steric interactions between the disubstituted olefin and the C_5Me_5 rings of 2. Infrared and ^{1}H NMR data (Table I) are in accord with the formulation of 3, 4 and 5 as alkyl hydride complexes. Reaction of 3, 4, and 5 with excess ethylene induces reductive elimination of alkane with formation of the metallacycle complex $Cp^*_2\overline{Hf(CH_2CH_2CH_2CH_2)}$ (6) (equation 2).

$$Cp^*_2Hf(H)CH_2CHRR' \xrightarrow{\text{xs. } C_2H_4} Cp^*_2Hf\langle\text{cyclohexane}\rangle + CH_3CHRR' \qquad (2)$$

3, 4, 5 — 6

Additionally, these alkyl hydride complexes are subject to hydrogenolysis under mild (1 atm H_2, 20°C, <1 h) conditions

to afford the parent dihydride, 2, and the corresponding alkane (equation 3). Reactions 2 and 3 have been examined

$$\underset{\textbf{3, 4, 5}}{Cp^*_2Hf(H)CH_2CHRR'} \xrightarrow{H_2} Cp^*_2HfH_2 + CH_3CHRR' \qquad (3)$$

in detail for the related $Cp^*_2Zr(H)CH_2CHMe_2$ system, and mechanistic aspects of these reactions have been previously discussed.[3]

Complexes 3, 4, and 5 exhibit remarkable thermal stability, undergoing little decomposition after hours at 80°C. This stability is exceptional when compared to most cis alkyl hydride complexes, and is somewhat greater than that observed for analogous zirconium alkyl hydride 1, as might be expected.[5] Prolonged thermolysis of $Cp^*_2Hf(H)CH_2CH_3$ in benzene solution at 80°C cleanly yields (^{1}H NMR) a 2:1 mixture of dihydride 2 and metallacyclopentane 6 plus one equivalent ethane (equation 4). Observation of 6

$$\underset{\textbf{3}}{3Cp^*_2Hf(H)CH_2CH_3} \xrightarrow{\Delta} \underset{\textbf{7}}{Cp^*_2HfH_2} + \underset{\textbf{6}}{Cp^*_2Hf\langle\bigcirc\rangle} + C_2H_6 \qquad (4)$$

implies the intermediacy of C_2H_4 in thermolysis of 3: loss of ethylene from 3 to form dihydride 2 followed by ethylene-promoted reductive elimination of alkane from 3 as

in equation 2 is consistent with the observed product distribution in reaction 4 (Scheme I).

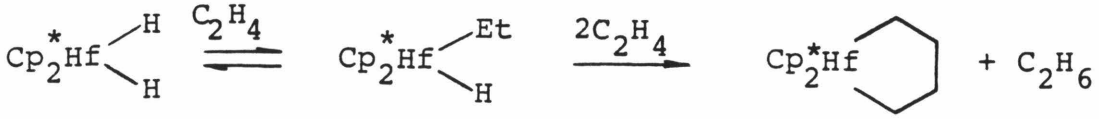

2 3 6

Scheme I

The thermolysis of $Cp^*Zr(H)CH_2CHMe_2$ (1) is reported to yield isobutane plus products derived from thermal decomposition of initially formed $(C_5(CH_3)_5)(C_5(CH_3)_4CH_2)$-ZrH.[6] In contrast, thermolysis of benzene or toluene solutions of isobutyl hydride 4 at 110°C yields a 1:1 mixture of dihydride 2 and metallacyclobutane $Cp^*_2\overline{HfCH_2CH(CH_3)CH_2}$ (7) plus one equivalent isobutane (equation 5). When the thermolysis is carried out in the

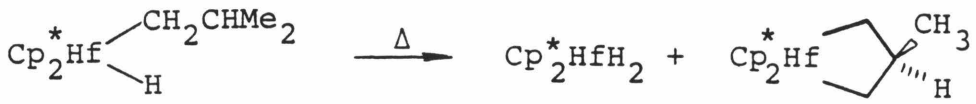

4 2 7

(5)

presence of excess isobutylene, 7 is quantitatively produced (^{1}H NMR), and may be isolated as an analytically pure, off-white crystalline solid in 62% yield. The formulation of 7 is confirmed by solution molecular weight (C_6D_6, calc.: 505, found: 486), and by ^{1}H and ^{13}C NMR data, which compare closely to data for analogous, titanacyclobutane complexes.[7]

A reaction similar to 5 has recently been reported for the related bis-alkyl actinides $Cp^*_2ThR_2$ (R = CH_2CMe_3, CH_2SiMe_3) (equation 6).[8] Labeling studies have shown this

(6)

X = C, Si

reaction to proceed via γ-hydrogen abstraction.[9] By analogy, a mechanism to account for the formation of 7 in reaction 5 is given in Scheme II.[10] Alternatively, formation of 7 could proceed via the intermediacy of the bis-alkyl $Cp^*_2Hf(CH_2CHMe_2)_2$, obtained from the disproportionation of **4**. However, at 80°C, a temperature where **4** is the sole observable reactant species in solution, the rate of thermolysis of **4** is essentially olefin independent, and

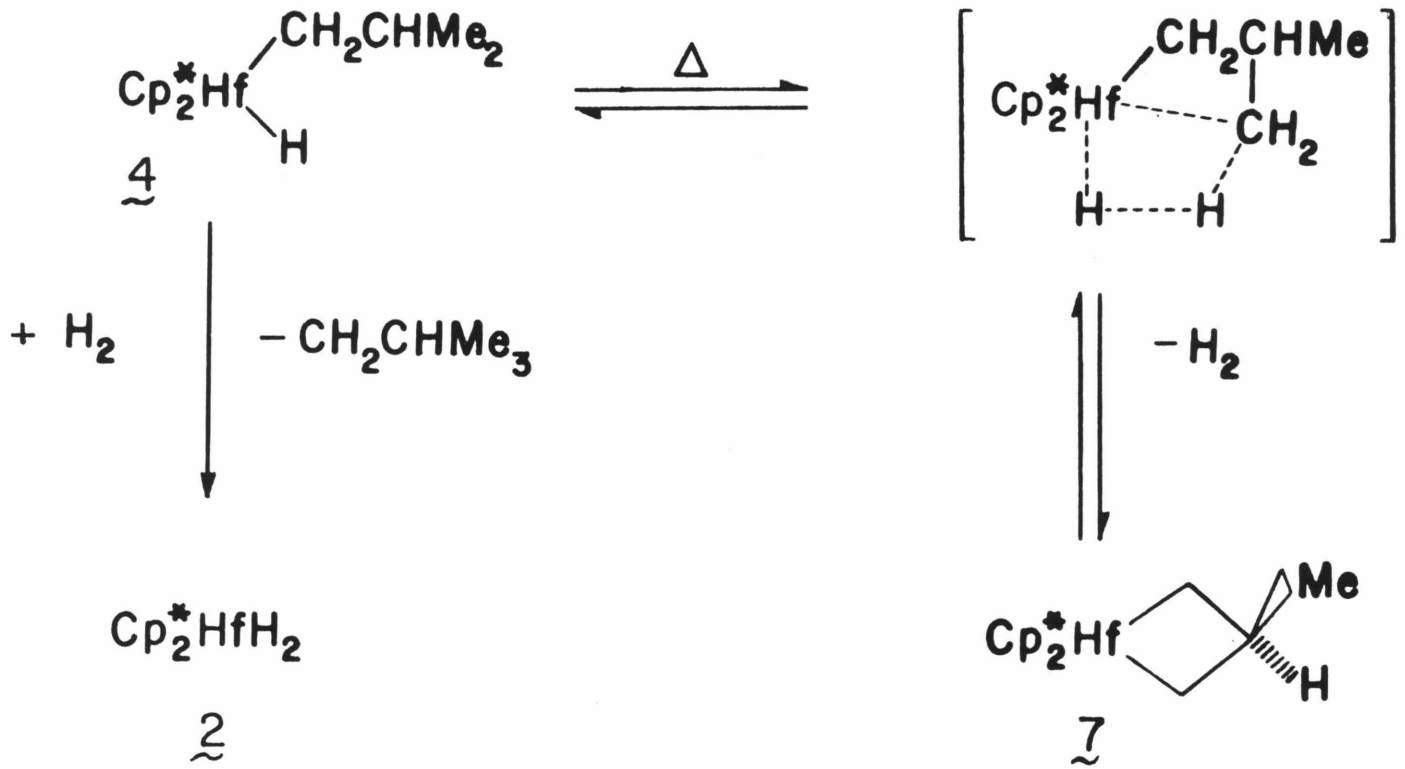
CH2CHMe2
Cp*2Hf
H
4
Δ
CH2CHMe
Cp*2Hf
CH2
H
H
+ H2
– CH2CHMe3
– H2
Cp*2HfH2
2
Cp*2Hf
Me
H
7

Scheme II

would thus appear to rule out γ-hydrogen abstraction from $Cp^*_2Hf(CH_2CHMe_3)_2$ as a significant route to 7. The reversibility of γ-hydrogen abstraction shown in Scheme II is confirmed by the facile reaction of 7 with H_2 at 25°C to form dihydride 2 plus isobutane (equation 7).

7 2

The thermal stability of 7 is substantially greater than that reported for normal ring group IV metallacyclobutane complexes $Cp_2M\overline{CH_2C(CH_3)_2CH_2}$ ($t_{½}$(25°C) for M=Ti: 1-2 h; Zr: 3 h; Hf: 9 d),[11] with negligible decomposition (^{1}H NMR) after days at 115°C. Significantly, solutions of 7 thermolyzed in the presence of excess ethylene remain similarly unchanged. This lack of reactivity is noteworthy, in light of the extensive metathesis activity observed for titanacyclobutanes,[7] and appears to reflect the inaccessibility of the methylidene propene complex 8 in reactions of 7.

7 8

(2) Synthesis and Reactivity of $Cp^*_2Hf(H)CH=CH^tBu$

A reaction related to the regioselective insertions of unactivated olefins into Hf-H bonds discussed in the previous section in the corresponding insertion involving unactivated acetylenes. Toluene solutions of **2** react rapidly with one equivalent of t-butylacetylene at ambient temperature to yield $Cp^*_2Hf(H)CH=CH^tBu$ (**9**) (equation 8),

$$Cp^*_2HfH_2 + HC{\equiv}C^tBu \longrightarrow Cp^*_2Hf(H)CH=CH^tBu \qquad (8)$$

2 **9**

isolable as a colorless, crystalline solid. Infrared (ν(Hf-H = 1625 cm^{-1}; ν(Hf-D) = 1155 cm^{-1}; ν(C=C) = 1560 cm^{-1}) and ^1H NMR ($^3J_{HH}$ = 21 Hz, $C\underline{H}=C\underline{H}CMe_3$) spectroscopic data support the formulation of **9** as a trans alkenyl hydride complex. Attempts to prepare other alkenyl hydride complexes using less bulky terminal acetylenes such as HC≡CMe or HC≡CPh resulted instead in doubly-inserted products.[12] The alkenyl hydride **9** is somewhat more thermally stable than alkyl hydrides **3**, **4** and **5**, with benzene solutions of **9** under 1 atm of N_2 showing no noticeable decomposition after days at 125°C. It is somewhat surprising that while much attention has been focused on the role of alkyl hydride complexes in olefin

hydrogenations, there have been relatively few studies of the corresponding acetylene systems. Moreover, although several reports have appeared concerning reactions of metal dihydrides with acetylenes,[13] reaction 8 represents to our knowledge the first unambiguous example of a metal hydride addition to an unactivated acetylenic bond to form a stable cis-alkenyl hydride complex.

Solutions of **9** react cleanly with ethylene to yield $Cp^*Hf(Et)(CH{=}CH^tBu)$ (**10**) as a colorless oil, as shown in equation 9. Solution infrared and ^1H NMR identify **10** as

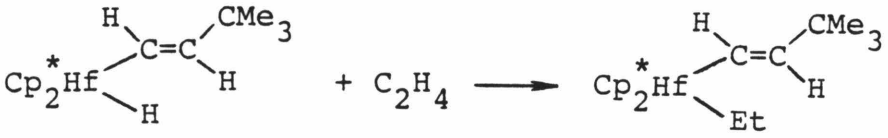

(9)

the product of ethylene insertion into the Hf-H bond of **9**. Reaction 9 contrasts with that of $Cp^*_2Zr(H)CH_2CHMe_2$ (**1**) and ethylene, where ethylene insertion into the Zr-H bond has been shown to be reversible with the equilibrium lying toward **1** and C_2H_4.[3] Thermolysis of **10** in the presence of excess ethylene results in quantitative generation of **6** and neohexane (80°C, 6 h), according to equation 10. Analogously to reaction 3, **9** reacts with H_2 in stepwise

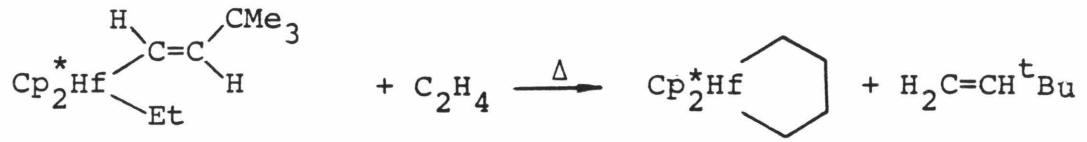

10 **6** (10)

fashion[14] to yield the dihydride **2** and neohexane (80% conversion after 72 h at 25°C, 3 atm H_2) (equation 11).

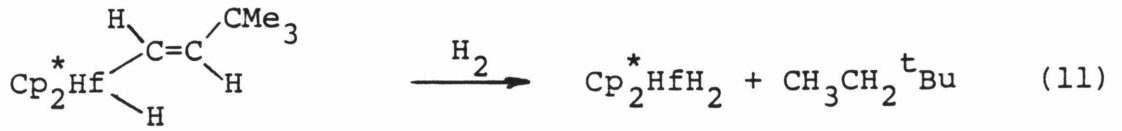

9 **2**

(3) Reaction of $Cp^*_2HfH_2$ (2) with RLi (R = Ph, CH_2CMe_3)

The synthetic procedures described in the preceding sections (equations 1 and 8) are necessarily limited to formation of hydrocarbon products with β-hydrogen functionality, and are thus inappropriate for the synthesis of phenyl and neopentyl derivatives of **2**. Consideration of the pronounced hydricity of Zr-H and Hf-H bonds[15] suggested a degree of uninegative, halogen-like character for the hydride ligands of **2**. Thus, by analogy to the ready metathesis of transition metal halides with alkyllithium reagents, it was hoped that $Cp^*_2HfH_2$ would exhibit similar metathetical reactivity. Indeed, treatment of toluene

solutions of 2 with one equivalent PhLi provides a novel route to the phenyl hydride $Cp^*_2Hf(H)Ph$ (11) as shown in equation 12. The thermal stability of 11 is comparable to

$$Cp^*_2HfH_2 + PhLi \longrightarrow Cp^*_2Hf(H)Ph + LiH \qquad (12)$$

that of alkenyl hydride 9, with no decomposition evident after days at 125°C. Similarly, reaction of 2 with one equivalent $LiCH_2CMe_3$ yields $Cp^*_2Hf(H)CH_2CMe_3$ (12), together with ~10% of two uncharacterized sideproducts (equation 13). Reactions 12 and 13 demonstrate the marked

$$Cp^*_2HfH_2 + LiCH_2CMe_3 \longrightarrow Cp^*_2Hf(H)CH_2CMe_3 + LiH \qquad (13)$$

hydridic character of group IV metal hydrides relative to metal hydrides to the right in the periodic table, which typically deprotonate in the presence of strong bases. For example, Cp_2MH_2 (M = Mo, W) reacts with n-BnLi to give a lithiated tetramer, $[Cp_2M(H)Li]_4$ plus butane (equation 14).[16] It should be noted, however, that the

$$Cp_2MH_2 + \underline{n}\text{-BnLi} \longrightarrow \tfrac{1}{4}[Cp_2W(H)Li]_4 + C_4H_{10} \qquad (14)$$
$$M = Mo, W$$

coordinative unsaturation of $Cp^*_2HfH_2$ provides for a direct metal-alkyl anion interaction using the vacant equatorial

$1a_1$ LUMO.[17] This interaction is not available for the 18 electron Cp_2WH_2, and may be responsible in part for the contrasting reactivities observed.

Conclusion

A series of bis-(pentamethylcyclopentadienyl)-hafnium (IV) hydrido complexes have been prepared, encompassing a range of hydrocarbon ligand types: alkyl (with and without β-hydrogens), alkenyl, and aryl. Facile insertion of olefinic and acetylenic bonds into Hf-H bonds provides a general route to a variety of alkylhydride derivatives of **2**. Additionally, hydride ligands of **2** undergo ready metathesis with alkyl and aryllithium reagents to give derivatives of **2** not obtainable via simple insertion.

While the reactions reported in this chapter in many ways parallel those of the related Cp^*_2Zr system, some significant differences in reactivity are evidenced. In particular, thermolysis of alkyl hydride $Cp^*_2Hf(H)CH_2CHMe_2$ (**4**) affords a product derived <u>not</u> from formal reductive elimination of alkane, as observed for $Cp^*_2Zr(H)CH_2CHMe_2$ (**1**), but rather from an alternate pathway γ-abstraction to form metallacycle **7** by which **4** avoids reduction of the metal center. An important factor to be considered in comparing the reactivities of zirconium and hafnium systems is the relative energetics of the M(IV) → M(II) couple.

Reactions involving the Zr(IV) $\longrightarrow$ Zr(II) are anticipated to be much more energetically accessible than analogous reactions involving hafnium; thus, mechanisms which circumvent such couples are undoubtedly preferred for hafnium.

TABLE I. NMR[a] AND IR[b] DATA

Compound	IR	Assignment	Nucleus	Chemical Shift	Coupling
$Cp^*_2Hf(H)CH_2CH_3$ (3)	ν(Hf-H) 1630	$C_5(C\underline{H}_3)_5$	^1H	1.90 s	
		$C\underline{H}_2CH_3$		0.03 q	^3J = 8
		$CH_2C\underline{H}_3$		0.68 t	^3J = 8
		$Hf\underline{H}$		12.41 s,br	
$Cp^*_2Hf(H)CH_2CHMe_2$ (4)	ν(Hf-H) 1636	$C_5(C\underline{H}_3)_5$	^1H	1.96 s	
		$C\underline{H}_2CHMe_2$		-0.21 d	^3J = 6
		$CH_2C\underline{H}Me_2$		1.02 d	^3J = 6
		$Hf\underline{H}$		13.64 s,br	
$Cp^*_2Hf(H)CH_2CH_2Ph$ (5)	ν(Hf-H) 1620	$C_5(C\underline{H}_3)_5$	^1H	1.93 s	
		$C\underline{H}_2CH_2Ph$		0.30 m	
		$CH_2C\underline{H}_2Ph$		Not observed	
		$CH_2CH_2\underline{Ph}$		7.30 m	
		$Hf\underline{H}$		13.71 s,br	
$Cp^*_2Hf(CH_2CH_2CH_2CH_2)$ (6)		$C_5(C\underline{H}_3)_5$	^1H	1.84 s	
		$C\underline{H}_2CH_2CH_2C\underline{H}_2$		0.44 m	
		$CH_2C\underline{H}_2C\underline{H}_2CH_2$		2.10 m	

TABLE I (cont'd)

Compound	IR	Assignment	Nucleus	Chemical Shift	Coupling
$Cp^*_2\overline{HfCH_2CH(CH_3)CH_2}$ (7)[c]		$C_5(C\underline{H}_3)_5$	^1H	1.72, 1.87 s	
		$CH_2CH(C\underline{H}_3)CH_2$		1.54 d	
		$C\underline{H}_2CH(CH_3)C\underline{H}_2$		0.79 dd	^2J, ^3J = 12
				1.27 dd	^2J=12, ^3J=9.5
		$\underline{C}_5(CH_3)_5$	^{13}C	114.74, 115.46	
		$C_5(\underline{C}H_3)_5$		10.89, 11.80 q	^1J = 126
		$CH_2CH(\underline{C}H_3)CH_2$		7.45 q	^1J = 129
		$CH_2\underline{C}H(CH_3)CH_2$		23.57 d	^1J = 120
		$\underline{C}H_2CH(CH_3)\underline{C}H_2$		68.21 t	^1J = 127
$Cp^*_2Hf(H)CH{=}CH^tBu$ (9)	ν(Hf-H) 1625	$C_5(C\underline{H}_3)_5$	^1H	1.91 s	
	ν(Hf-D) 1155	$C\underline{H}{=}CH^tBu$		5.80 d	^3J = 21
	ν(C=C) 1560	$CH{=}\underline{CH}^tBu$		4.81 d	^3J = 21
		$CH{=}CH^t\underline{Bu}$		1.09 s	
		$Hf\underline{H}$		12.83 s,br	
$Cp^*_2Hf(Et)CH{=}CH^tBu$ (10)	ν(C=C) 1558[d]	$C_5(C\underline{H}_3)_5$	^1H	1.78 s	
		$C\underline{H}{=}CH^tBu$		5.23 d	^3J = 19
		$CH{=}C\underline{H}^tBu$		4.87 d	^3J = 19
		$CH{=}CH^t\underline{Bu}$		1.07 s	
		$C\underline{H}_2CH_3$		-0.08 q	^3J = 7.5
		$CH_2C\underline{H}_3$		1.29 t	^3J = 7.5

TABLE I (cont'd)

Compound	IR	Assignment	Nucleus	Chemical Shift	Coupling
$Cp^*_2Hf(H)Ph$ (11)	ν(Hf-H) 1630	$C_5(C\underline{H}_3)_5$	^1H	1.78 s	
		<u>Ph</u>		6.67, 6.98 m	
		Hf<u>H</u>		13.14 s,br	
$Cp^*_2Hf(H)CH_2CMe_3$ (12)	ν(Hf-H) 1630	$C_5(C\underline{H}_3)_5$	^1H	1.96 s	
		$C\underline{H}_2CMe_3$		-0.16 s	
		$CH_2C\underline{Me}_3$		1.20 s	
		Hf<u>H</u>		14.04 s	

[a] ^1H (90 MHz) and ^{13}C (22.5 MHz) NMR spectra taken in benzene-$\underline{d}_6$ at ambient temperature. Chemical shifts are reported in δ relative to internal TMS or residual protons or carbons in solvent. Coupling constants are reported in Hz.

[b] IR spectra obtained as Nujol mulls except where indicated. Values are given in Hz. The complete spectra are detailed in the Experimental Section.

[c] ^1H NMR spectrum obtained at 500 MHz.

[d] IR spectrum obtained for neat oil.

[e] IR spectrum obtained for C_6D_6 solution.

Experimental Section

General Considerations. All manipulations were carried out by using either high vacuum line or glovebox techniques. Solvents were purified by vacuum transfer first from $LiAlH_4$ or benzophenone ketyl and then from "titanocene", prepared as described earlier.[18] Hydrogen was purified by passage over MnO on vermiculite[19] and activated 4-Å molecular sieves. Ethylene and isobutylene (Matheson) were used directly from the cylinder. All other reagents were degassed and transferred from molecular sieves or used as received. Elemental analyses were determined by Alfred Bernhardt, Dornis and Kolbe, and C.I.T. Analytical Laboratories.

^1H NMR spectra were recorded with Varian EM-390, JEOL FX90Q, or Bruker 500 MHz spectrometers. ^{13}C NMR spectra were recorded with a JEOL FX90Q spectrometer. Infrared spectra were measured on a Beckman 4240 spectrometer as Nujol nulls unless otherwise noted and are reported in cm^{-1}.

Many reactions were carried out in sealed NMR tubes and monitored by NMR spectroscopy. A typical example is the reaction of $Cp^*_2Hf(H)CH_2CHMe_2$ (**4**) with H_2 : 30 mg (0.06 mmol) of **4** was placed in an NMR tube sealed to a 14/20 ground glass joint and fitted with a teflon needle adapter. Benzene-$\underline{d}_6$ was vacuum transferred into the tube

at -78°C, 1 atm H_2 admitted, the tube cooled to -196°C and then sealed with a torch.

Procedures. $Cp^*_2Hf(H)CH_2CH_3$ (3). A solution of 0.60 g (1.25 mmol) $Cp^*_2HfH_2$ in 15 ml petroleum ether was stirred at room temperature under 200 torr ethylene for 1 hour. Excess ethylene was removed and the solution was concentrated and cooled to -78°C. Filtration and drying in vacuo yielded 0.39 g (61%) of 3. IR: 1630 (br), 1488, 1022, 919, 802, 778. Anal. Calcd. for $C_{22}H_{36}Hf$: C, 55.15; H, 7.57; Hf, 37.26. Found: C, 55.03; H, 7.42; Hf, 37.10.

$Cp^*_2Hf(H)CH_2CHMe_2$ (4). A thick-walled glass reaction vessel with a teflon needle valve was charged with 1.0 g (2.0 mmol) Cp^*HfH_2, 5 ml toluene, and 8 mmol isobutylene and stirred at 80°C for 2 days. Volatiles were removed in vacuo; workup with petroleum ether afforded 0.795 g (71%) of white crystalline 4. IR: 1636 (br), 1302, 1155, 1028, 805, 770. Anal. Calcd. for $C_{24}H_{40}Hf$: C, 56.85; H, 7.95; Hf, 35.20. Found: C, 56.68; H, 8.12; Hf, 34.94.

$Cp^*_2Hf(H)CH_2CH_2Ph$ (5). To a stirred solution of 0.41 g (0.91 mmol) Cp^*HfH_2 in 15 ml toluene at -78°C was added 110 μl (0.96 mmol) styrene via syringe under argon counterflow. The solution was warmed to room temperature, stirred an additional 30 minutes, and worked up with petroleum

ether to give 0.36 g (71%) of white crystalline **5** (>95% pure, ^{1}H NMR). IR: 3060, 1620 (br), 1492, 1053, 1030, 975, 806, 776.

$Cp^*_2Hf(CH_2CH_2CH_2CH_2)$ **(6).** The procedure for **4** was followed except 1.0 g (2.22 mmol) Cp^*HfH_2, 10 ml toluene, and 72.6 mmol C_2H_4 were stirred at 80°C for 24 hours. Workup with petroleum ether afforded 0.80 g (61%) of off-white metallacyclopentane **6**. IR: 1490, 1022, 993. Anal. Calcd. for $C_{24}H_{38}Hf$: C, 57.08; H, 7.58; Hf, 35.34. Found: C, 57.06; H, 7.59; Hf, 35.43.

$Cp^*_2Hf(CH_2CH(CH_3)CH_2)$ **(7).** The procedure for **4** was followed except 1.01g(2.24 mmol) Cp^*HfH_2, 10 ml toluene, and 9 mmol isobutylene were stirred at 115°C for ten days. Petroleum ether workup yielded 0.685 g (62%) of off-white crystalline **7**. ^{1}H NMR of the workup residue indicated >90% **7**, with traces of **2** and **4**. IR: 1490, 1298, 1053, 1023, 978, 938. Anal. Calcd. for $C_{24}H_{38}Hf$: C, 57.08; H, 7.58. Found: C, 56.86; H, 7.51.

$Cp^*_2Hf(H)CH{=}CH^tBu$ **(9).** To a solution of 1.0 g (2.22 mmol) Cp_2HfH_2 in 15 ml petroleum ether was condensed 2.50 mmol t-butylacetylene at -196°C. The reaction mixture was stirred for 30 minutes at -78°C and allowed to warm to room temperature. Concentration, cooling to -78°C, and

filtration afforded 0.56 g (47%) of white crystalline **9**. IR: 1624 (br), 1560, 1490, 1360, 1252, 1218, 1204, 1064, 1026, 1005, 805. Anal. Calcd. for $C_{26}H_{42}Hf$: C, 58.58; H, 7.94; H, 33.48. Found: C, 58.32; H, 7.89; Hf, 33.26.

$Cp^*_2Hf(Et)CH=CH^tBu$ (10). To a solution of 0.66 g (1.24 mmol) $Cp^*_2Hf(H)CH=CH^tBu$ in 10 ml toluene was condensed 3.0 mmol ethylene at -196°C. The reaction mixture was warmed to room temperature and stirred for 2 days. Removal of the volatiles *in vacuo* left a colorless oil, identified by ^1H NMR as >95 mol % **10**. IR: 1558, 1490, 1357, 1250, 1215, 1200, 1060, 1021, 1000, 801.

$Cp^*_2Hf(H)Ph$ (11). To a solution of 3.02 g (6.7 mmol) of $Cp^*_2HfH_2$ in 60 ml petroleum ether at -78°C was syringed 3.3 ml (7.3 mmol) of 2.2 M phenyllithium (70:30 cyclohexane/diethyl ether solution, Aldrich). The reaction mixture was allowed to warm to room temperature with stirring. After 18 hours, the solution was filtered, concentrated, and cooled to -78°C. The resulting white crystalline precipitate was filtered off and dried *in vacuo*, giving 1.82 g (52%) of **11**. IR: 3045, 1650 (br), 1568, 1487, 1414, 1238, 1059, 1050, 1023, 804, 785, 726, 710. Anal. Calcd. for $C_{26}H_{36}Hf$: C, 59.25; H, 6.88. Found: C, 58.93; H, 6.89.

$\underline{Cp^*_2Hf(H)CH_2CMe_3}$ **(12).** Cp_2HfH_2 (0.50 g, 1.1 mmol) and $LiCH_2CMe_3$ (0.088 g, 1.1 mmol) were placed in a flask, and 10 ml of petroleum ether was distilled in at -78°C. The reaction mixture was warmed to room temperature and stirred for 12 hours. Concentration and cooling to -78°C afforded 0.24 g (42%) of **12**, approximately 90% pure by ^1H NMR. IR: 1635, 1485, 1400, 1354, 1204, 1083, 1022, 774, 693.

References

(1) Some notable exceptions are: (a) Norton, J. R. Acc. Chem. Res. **1979**, 12, 139. (b) Halpern, J. Ibid. **1982**, 15, 332. (c) Gell, K. I.; Schwartz, J. J. Am. Chem. Soc. **1978**, 100, 3246.

(2) Manriquez, J. M.; McAlister, D. R.; Sanner, R. D.; Bercaw, J. E. J. Am. Chem. Soc. **1978**, 100, 2716.

(3) McAlister, D. R.; Erwin, D. K.; Bercaw, J. E. J. Am. Chem. Soc. **1978**, 100, 5966.

(4) Roddick, D. M.; Fryzuk, M. D.; Seidler, P. F.; Hillhouse, G. L.; Bercaw, J. E., manuscript in preparation.

(5) Similar stability trends for zirconium and hafnium complexes have been noted: (a) Planalp, R. P.; Andersen, R. A.; Zalkin, A. Organometallics **1983**, 2, 16. (b) Cardin, D. J.; Lappert, M. F.; Raston, C. L.; Riley, P. I. "Comprehensive Organometallic Chemistry"; Wilkinson, G., ed.; Pergamon Press: New York, **1982**, Vol. 3, 559-634.

(6) Manriquez, J. M., Ph.D. Thesis, California Institute of Technology, **1976**.

(7) Howard, T. R.; Lee, J. B.; Grubbs, R. H. J. Am. Chem. Soc. **1980**, 102, 6877.

(8) Bruno, J. W.; Marks, T. J.; Day, V. W. J. Am. Chem. Soc. **1982**, 104, 7357.

(9) Whereas labeling studies[8] appear to exclude α-abstraction or homolytic bond scission processes, it should be noted that ring methyl C-H abstraction[3] has not been ruled out. The detailed mechanism of reaction 6 is currently under investigation in our group: Bulls, A. R., work in progress.

(10) The possible intermediacy of $(C_5Me_5)(C_5Me_4CH_2)HfH$,[4] formed via initial reductive elimination of isobutane from **4**, in reaction 5 has been addressed: thermolysis of $(C_5Me_5)(C_5Me_4CH_2)HfH$ in the presence of isobutylene results solely in "tuck-in" products analogous to those reported for zirconium.[6]

(11) Seetz, J. W. F. L.; Schat, G.; Akkerman, O. S.; Bickelhaupt, F. Angew. Chem., Int. Ed. Engl. **1983**, 22, 248.

(12) (a) McGrady, N. D.; McDade, C.; Bercaw, J. E. "Organometallic Compounds", Shapiro, B. L., ed.; Texas A&M University Press: College Station, Texas, **1983**; pp. 46-85. (b) Roddick, D. M., unpublished results.

(13) (a) Nakamura, A.; Otsuka, S. J. Am. Chem. Soc. **1972**, 94, 1886; ibid., **1973**, 95, 7262. (b) Longato, B.; Bresadola, S. Inorg. Chem. **1982**, 21, 168.

(14) Monitoring of reaction 11 by ^1H NMR indicated the presence of free neohexene during early stages of the hydrogenation.

(15) Bercaw, J. E. "Transition Metal Hydrides", Bau, R., ed.; Adv. Chem. Ser. 167; American Chemical Society: Washington, D.C., 1978, pp. 136-148.

(16) Francis, B. R.; Green, M. L. H.; Luong-thi, T.; Moser, G. A. J. C. S. Dalton, 1976, 1339.

(17) Lauher, J. W.; Hoffmann, R. J. Am. Chem. Soc. 1976, 98, 1729.

(18) Marvich, R. H.; Brintzinger, H. H. J. Am. Chem. Soc. 1971, 94, 2046.

(19) Brown, T. L.; Dickerhoof, D. W.; Bafus D. A.; Morgan, G. L. Rev. Sci. Instrum. 1962, 33, 491.

Chapter II

Synthesis and Structural Characterization of $Cp^*_2Hf(H)(\eta^3\text{-}CH_2CHCH_2)$.

Introduction

Transition metal complexes containing allylic ligands comprise an important class of reactive organometallic complexes. In particular, π-allyl hydride complexes have been implicated as key intermediates in a number of metal-assisted hydrocarbon rearrangements[1] and, therefore, are of considerable interest. Some time ago, the early transition metal π-allyl hydride complexes $Cp^*_2Zr(H)(\eta^3\text{-}CH_2\text{-}CHCH_2)$ (1) and $Cp^*_2Zr(H)(\eta^3\text{-}CH_2CHCHMe)$ (2) were prepared in our laboratories (equations 1 and 2).[2]

$$Cp^*_2ZrH_2 + H_2C{=}C{=}CH_2 \longrightarrow Cp^*_2Zr(H)(\eta^3\text{-}CH_2CHCH_2) \quad (1)$$

or

$$\tfrac{1}{2}\{Cp^*_2ZrN_2\}_2N_2 + H_2C{=}CHCH_3 \longrightarrow Cp^*_2Zr(H)(\eta^3\text{-}CH_2CHCH_2)$$

$$\tfrac{1}{2}\{Cp^*_2ZrN_2\}_2N_2 + H_2C{=}CHCH_2Me \longrightarrow Cp^*_2Zr(H)(\eta^3\text{-}CH_2CHCHMe) \quad (2)$$

The thermal stabilities of 1 and 2 are quite high, and have permitted the reaction chemistry and fluxional behavior of these complexes to be studied in detail.

In this chapter we report the synthesis and structural characterization of the hafnium analogue to 1, $Cp^*_2Hf(H)(\eta^3\text{-}CH_2CHCH_2)$ (3). Spectroscopic data indicate that allyl hydrides 1 and 3 are isostructural; consequently, the X-ray structural study of 3 provides

useful information pertaining to the bonding in these complexes, as well as insight into the dynamic processes operative in these molecules.

Results and Discussion

Treatment of petroleum ether solutions of $Cp^*_2HfH_2$ with one equivalent of allene readily afforded analytically pure, white crystalline $Cp^*_2Hf(H)(\eta^3\text{-}CH_2CHCH_2)$ (3) in good yield (62%) (equation 3).

$$Cp^*_2HfH_2 + H_2C{=}C{=}CH_2 \longrightarrow \underset{\mathbf{3}}{Cp^*_2Hf(H)(\eta^3\text{-}CH_2CHCH_2)} \qquad (3)$$

3 has been characterized by its ^1H and ^{13}C NMR spectra, which compare closely to that of 1 (Table I). Although π coordination of allyl ligands in complexes 1 and 2 was clearly established by infrared data, IR spectra of 3 display a number of bands in the diagnostic hydride/allyl region (see Experimental Section) and could not be reliably assigned.

As was the case for zirconium allyls 1 and 2, ^1H and ^{13}C NMR data indicate the 3 is fluxional. Thus, ambient temperature ^1H NMR spectra exhibit a single resonance for both ($\eta^5\text{-}C_5Me_5$) rings at 1.78 pm, and a quartet of doublets at 3.48 ppm ($^3J_{HH}$ ave = 12.5, 2.1 Hz) for the central allyl proton. Although the terminal allyl protons were not located, ^{13}C NMR reveals a single resonance at 57.17 ppm (triplet, $^1J_{HC}$ = 155.2 Hz) attributable to the terminal allyl carbons consistent with a rapid equilibration of allyl CH_2 groups. The small 2.1 Hz splitting observed for $CH_2\underline{CH}CH_2$ arises from coupling to the hydride ligand, which

appears as a broad singlet at 3.58 ppm. The equivalence of (η^5-C_5Me_5) proton and carbon and allyl terminal carbon resonances of 3 can be rationalized analogously to the zirconium allyls 1 and 2,[2b] in terms of a rapid η^3-η^1 interchange and syn-anti equilibration as shown in Scheme 1.

The dynamic nature of 3 has been confirmed by variable temperature 90 MHz ^{1}H NMR. Upon cooling, the (η^5-C_5Me_5) singlet for 3 broadens and coalesces at -69°C. At -80°C, ^{1}H NMR of 3 displays a pair of singlets for the inequivalent (η^5-C_5Me_5) groups at 1.72 and 1.83 ppm with $\Delta\nu$ = 11.0 ± 0.5 Hz, consistent with a groundstate η^3-allyl structure (<u>vide infra</u>). From these values, $\Delta G^{\ddagger}$(-69°C) for equilibration of permethylring groups of 3 is calculated[3] to be 10.5 ± 0.1 kcal mol^{-1}. Surprisingly, this value is somewhat less than the corresponding barrier found for zirconium analog 1 of 12.5 kcal mol^{-1} (T_c = -8°C).[4] In light of the complexity of Scheme 1, it is not clear what factors are responsible for this equilibration process and the observed ordering of 1 and 3.

At elevated temperature (80°C) the central allyl proton of 1 appears as a sextet in the ^{1}H NMR, indicative of an exchange process equilibrating the four terminal allyl protons and the hydride ligand. This observation has been rationalized in terms of a rapid alkyl hydride $\rightleftharpoons$ propene complex equilibrim, as shown in Scheme 2. In contrast, ^{1}H NMR spectra of 3 exhibit no changes up to

Scheme I

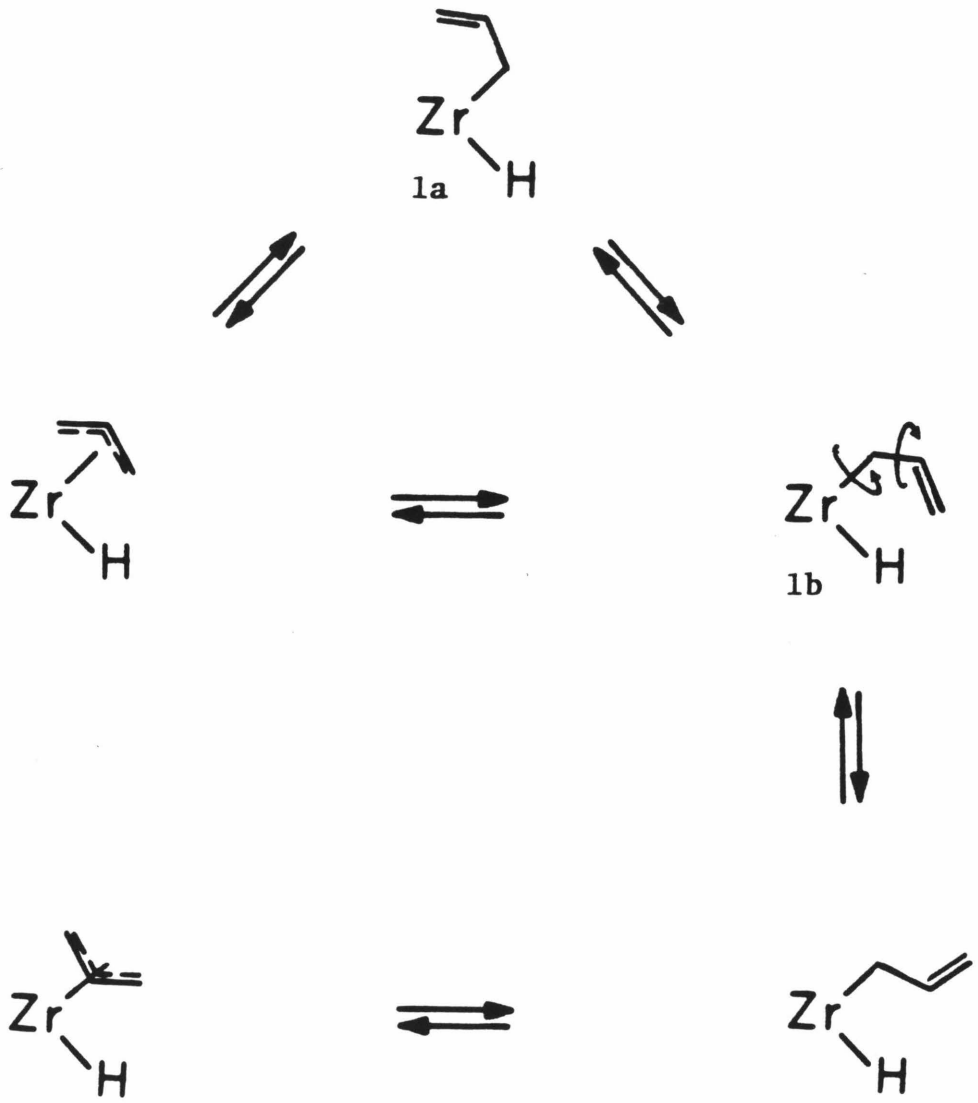

Scheme 2

decomposition (125°C). Although dynamic NMR behavior was not observed for **3**, the tautomerism in Scheme 2 has been demonstrated on the chemical timescale for $Cp^*_2Hf(H)(\eta^3\text{-}CH_2\text{-}CHCH_2)$ by the complete scrambling of deuterium in $Cp^*_2Hf(D)(\eta^3\text{-}CH_2CDCH_2)$ (prepared by reaction of $CpHfD_2$ with allene at -30°C (^1H NMR)) into the terminal allyl positions after 15 minutes at room temperature (equation 4).

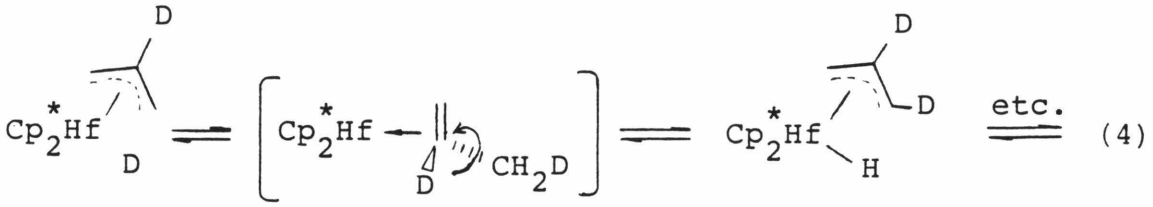

(4)

Crystallographic Results and Discussion

The molecular structure of $Cp^*_2Hf(H)(\eta^3\text{-}CH_2CHCH_2)$ (**3**) is presented in Figure 1, a stereo view in Figure 2, and a skeletal view of the immediate ligation about the hafnium with relevant bond distances and bond angles is given in Figure 3. The hafnium atom in **3** adopts the familiar pseudotetrahedral "bent sandwich" Cp_2MX_2 configuration, if $(\eta^5\text{-}C_5Me_5)$ ligands and X = H $(\eta^3\text{-}CH_2CHCH_2)$ are considered to occupy single coordination sites. The Hf-ring centroid distances of 2.243 and 2.233 Å and the ring centroid-Hf-ring centroid angle of 137.5° (Tables III and IV) are greater than typically found for unsubstituted bis(cyclopentadienyl)hafnium complexes, but compare closely to

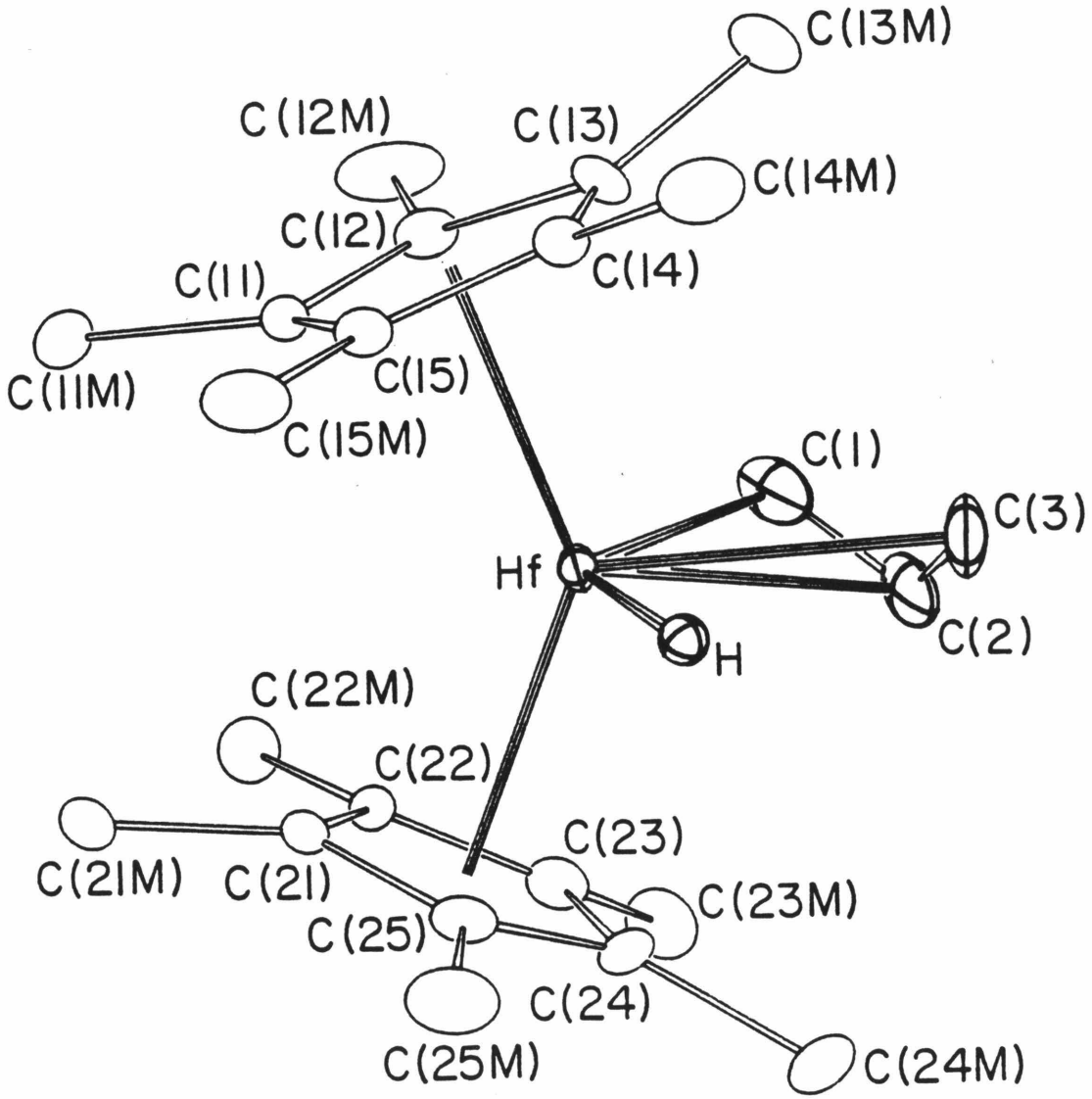

Figure 1. Structure of $Cp^*_2Hf(H)(\eta^3\text{-}CH_2CHCH_2)$ (3).

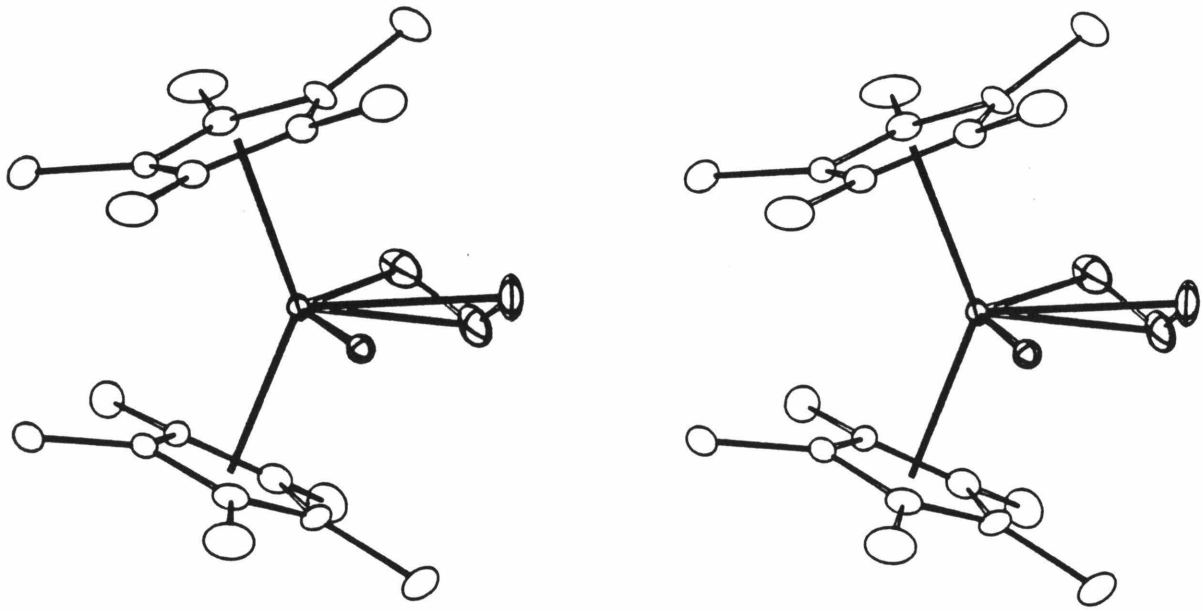

Figure 2. Stereo view of $Cp^*_2Hf(H)(\eta^3\text{-}CH_2CHCH_2)$ (3).

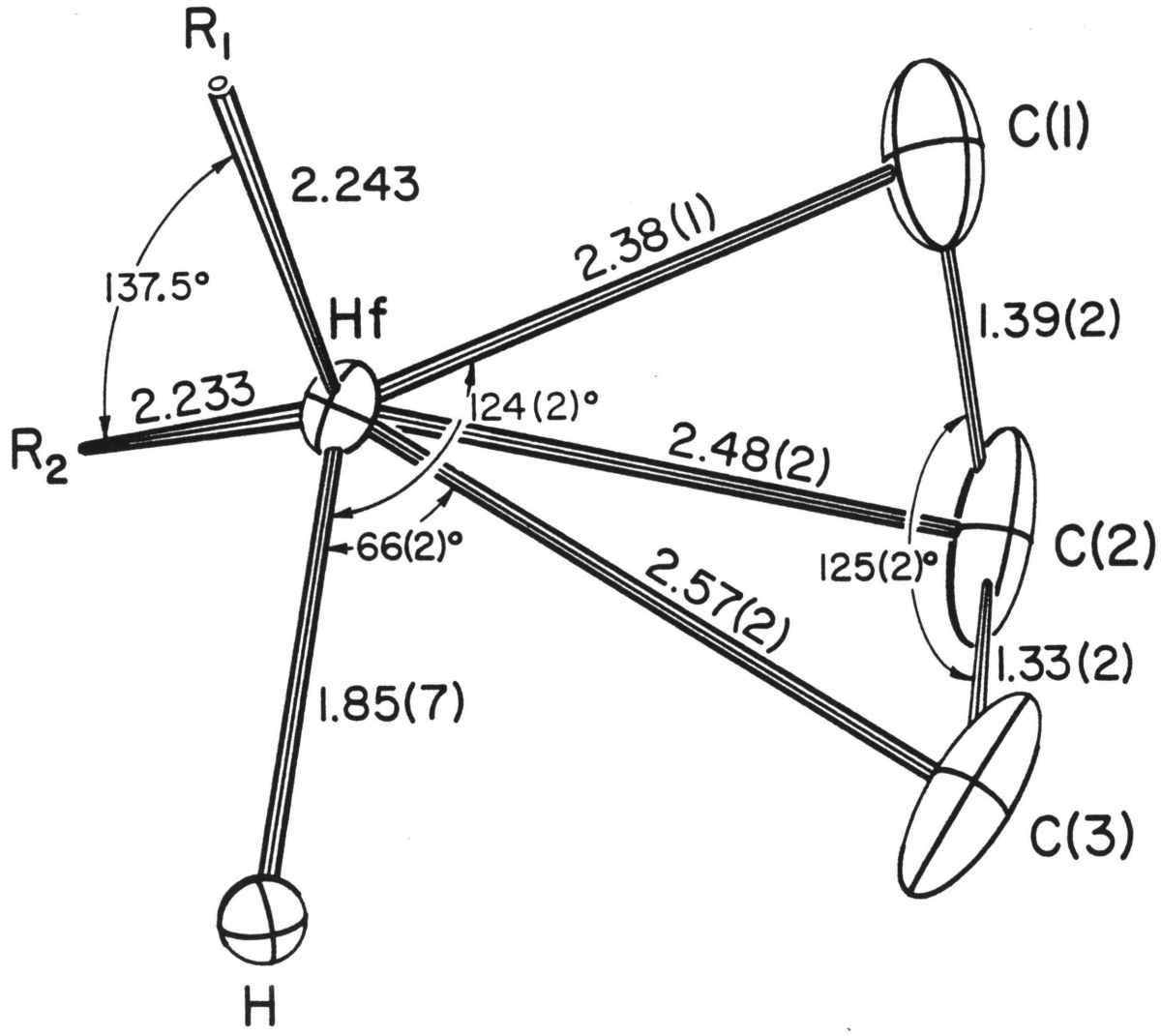

Figure 3. Skeletal view of $Cp^*_2Hf(H)(\eta^3\text{-}CH_2CHCH_2)$ (3), with selected bond distances (Å) and angles (°).

values for permethylzirconocenes $\{Cp^*_2ZrN_2\}_2N_2$ (2.232 Å; 141.3°)[5] and $Cp^*_2Zr(C(O)CHPMe_3)H$ (2.251, 2.258 Å; 138.9°).[6]

The inner-ring carbons of 3 are coplanar (Table V), and the small variations observed for Hf-C(ring) distances (2.448(7)-2.563(10) Å) are not unusual for pentahapto coordination. As observed previously for other bent permethylmetallocene structures, the ring methyl groups are displaced out of the cyclopentadienyl ligand planes away from the metal center. The observed displacements correlate well with inter-ring and ring-allyl C-C nonbonding distances (Table VI), with the shortest ring methyl nonbonding distances C(1)-C(23M) = 3.21(2) Å, C(11M)-C(21M) = 3.25(2) Å, C(2)-C(23M) = 3.30(2) Å, and C(1)-C(13M) = 3.40(2) Å involving methyl carbons having the greatest deviations from planarity. A further indication of steric crowding in 3 is the staggering of the (η^5-C_5Me_5) (see Figures 1 and 2). This serves to not only minimize inter-ring methyl contacts, but also successfully avoids severe steric interactions with the allyl ligand.

The allyl bonding in 3 is somewhat unusual. Although the allyl moiety is clearly π-bond, the Hf-allyl bonding is notably asymmetric, with the Hf-carbon (central) distance (2.48(2) Å) intermediate between terminal distances Hf-C(1) = 2.38(2) Å and Hf-C(3) = 2.57(2) Å. This contrasts with other reported transition metal allyl structures, where metal-carbon(central) distances are typically shorter than the respective metal-carbon(terminal) distances. Complex 3

also apparently exhibits an asymmetry in the C-C bonds of the allyl group (C(1)-C(2) = 1.39(2) Å, C(2)-C(3) = 1.33(2) Å). Taken together, these observed bond length variations suggest a degree of η^1-(σ)allyl character for $Cp^*_2Hf(H)(\eta^3\text{-}CH_2CHCH_2)$ (canonical form **1b**).[7] This result is consistent with the observed dynamic equilibria (<u>vide supra</u>) for complexes **1**, **2** and **3**, presumed to involve intermediates such as **Ia** and **1b** (Scheme 1). The apparent preference for canonical form **1b** over **Ia** is reminiscent of group IV η^2-acyl metallocene structures, where interaction of an acyl oxygen lone pair with the empty, central equatorial low-lying orbital of the bent sandwich moiety (**IIa**) is the thermodynamically favored isomer.[8] Alternatively, a steric interaction between the C(3) allyl

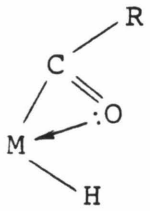

IIa

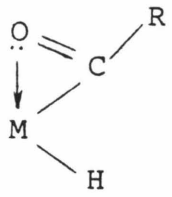

IIb

carbon and the hydride ligand (H-C(3) = 2.48(7) Å) may contribute to the observed asymmetry.

The bonding geometries for a number of metal-(η^3-allyl) complexes have been compared using a set of parameters described by Ibers[9] (Figure 4). The value of D, the distance from Hf to the centroid of the allyl group (A), for 3 (2.25 Å) differs by 0.11 Å from that in $Cp_2Ti(\eta^3\text{-}CH_2CHCH_2)$ (2.14 Å),[10] and is in accord with the difference in metal radii (Hf: 1.44 Å, Ti: 1.32 Å; Δ = 0.12 Å).[11] The tilt angle τ, defined as the angle subtended by the Hf-A and C(2)-A vectors, is 117°, within the range observed for other π-allyl structures (100-125°). The value of β, the angle between the Hf-A and the C(1)-C(3) vectors in 3, 96°C, is somewhat larger than β angles of 90-93° found in other π-allyl complexes, however, and reflects the allyl bonding asymmetry previously noted.

The hydride ligand in 3 is of interest, as it represents the first structurally characterized terminal Hf-H bond. The observed bondlength, 1.85(7) Å, is somewhat shorter than bridging Hf-H values for $Hf(BH_4)_4$ (2.06(2) Å),[12] $(\eta^5\text{-}C_5H_4CH_3)_2Hf(BH_4)_2$ (2.069(7), 2.120(8) Å),[13] and $Cp^*HfMe(\mu\text{-}H)(\mu\text{-}P^tBu_2)_2$ (2.12(13), 2.33(13) Å),[14] and compares closely to terminal Zr-H values for $Cp^*_2\overline{Zr(H)CH_2P(CH_3)_2CH_2}$ (1.88(4) Å)[15] and $Cp^*_2Zr(C(O)CH\text{-}PMe_3)H$ (1.89(2) Å).[15]

TABLE I. NMR[a] DATA

Compound; Solvent and Temperature	Assignment	Nucleus	Chemical Shift	Coupling
$Cp^*_2Zr(H)(\eta^3\text{-}CH_2CHCH_2)$	$C_5(C\underline{H}_3)_5$	^1H	1.72 s	
Toluene-$\underline{d}_8$, +25°	$CH_2C\underline{H}CH_2$		3.47 quint	$^3J_{ave}$ = 12
	$C\underline{H}_2CHC\underline{H}_2$		not observed	
	$Zr\underline{H}$		3.88 s, br	
Toluene-$\underline{d}_8$, -55°	$C_5(C\underline{H}_3)_5$		1.64, 1.75 s	
	$CH_2C\underline{H}CH_2$		3.47 m	
	$C\underline{H}_2CHC\underline{H}_2$		1.06 d	J = 13.7
	$C\underline{H}_2CHC\underline{H}_2$		1.36 d	J = 17.1
	$C\underline{H}_2CHC\underline{H}_2$		2.15 d	J = 8.5
	$C\underline{H}_2CHC\underline{H}_2$		not observed	
	$Zr\underline{H}$		3.91 d	J = 10.1
Toluene-$\underline{d}_8$, +65	$\underline{C}_5(CH_3)_5$	$^{13}C\{^1H\}$	111.3	
	$C_5(\underline{C}H_3)_5$		12.4	
	$\underline{C}H_2C\underline{H}CH_2$		58.1	
	$CH_2\underline{C}HCH_2$		116.5	

TABLE I (cont'd)

Compound; Solvent and Temperature	Assignment	Nucleus	Chemical Shift	Coupling
$Cp^*_2Hf(H)(\eta^3\text{-}CH_2CHCH_2)$ (3)	$C_5(C\underline{H}_3)_5$	^1H	1.78 s	
Benzene-$\underline{d}_6$, +34°	$CH_2C\underline{H}CH_2$		3.48 quint of d	J_{ave} = 12.5, 2.1
	$C\underline{H}_2CHC\underline{H}_2$		not observed	
	$Hf\underline{H}$		3.58 s, br	
Toluene-$\underline{d}_8$, -80°	$C_5(C\underline{H}_3)_5$		1.72, 1.81 s, br	
	$CH_2C\underline{H}CH_2$		not observed	
	$C\underline{H}_2CHC\underline{H}_2$		not observed	
	$Hf\underline{H}$		3.41 s, br	
Benzene-$\underline{d}_6$, +25°	$\underline{C}_5(CH_3)_5$	^{13}C	109.9 s	
	$C_5(\underline{C}H_3)_5$		11.7 q	^1J = 126
	$\underline{C}H_2CH\underline{C}H_2$		57.2 t	^1J = 155
	$CH_2\underline{C}HCH_2$		114.4 d	^1J = 139

[a] ^1H (90 MHz) and ^{13}C (22.5 MHz) chemical shifts are reported in δ relative to internal TMS or residual protons or carbons in solvent. Coupling constants are reported in Hz.

Experimental Section

General Considerations. All manipulations were performed using either glove box or high vacuum line techniques as described previously.[16] $Cp^*_2HfH_2$ and $Cp^*_2HfD_2$ were prepared using established procedures.[17] Allene was used directly from the cylinder. Elemental analysis of 3 was determined by Alfred Bernhardt Analytical Laboratories.

^1H NMR spectra were recorded using Varian EM-390 and Bruker 500 MHz spectrometers. ^{13}C NMR spectra were obtained using a JEOL FW90Q spectrometer. Infrared spectra were measured on a Beckman 4240 spectrometer as nujol nulls and are reported in cm^{-1}.

Procedures. $Cp^*_2Hf(H)(\eta^3\text{-}CH_2CHCH_2)$ (3). To 0.500 g (1.10 mmol) Cp^*HfH_2 in 15 ml petroleum ether at -78°C was condensed 1.16 mmol allene. After warming to room temperature, the solution was stirred for one hour, then concentrated to ca. 5 ml and cooled to -78°C. Filtration and drying in vacuo afforded 0.338 g (62%) of white, crystalline $Cp^*_2Hf(H)(\eta^3\text{-}CH_2CHCH_2)$ (3). IR: 1648, 1615(sh), 1583, 1530, 1490, 1268, 1212, 1023, 1005, 850(st), 812, 740, 710, 653. Anal. Calcd. for $C_{23}H_{36}Hf$: C, 56.26; H, 7.39. Found: C, 56.22; H, 7.31.

Structure Determination for $Cp^*_2Hf(H)(\eta^3\text{-}CH_2CHCH_2)$ (3).

A large single crystal obtained by slow crystallization from n-octane solution was mounted approximately along the b-axis in a glass capillary under N_2. A series of oscillation and Weissenberg photographs indicated monoclinic symmetry; the space group $P2_1/c$ was inferred from systematic absences in the diffractometer data. Data were collected on a locally-modified Syntex $P2_1$ diffractometer with graphite monochromator. The unit cell parameters (Table II) were obtained by least squares refinement of 15 2θ values ($39 < 2\theta < 45^o$), where each 2θ value was an average of two measurements of $\pm 2\theta$. Intensity data was corrected for a 2% linear decay, as indicated by the three check reflections, and the data were reduced to F_o^2; the form factors for H are from Stewart et. al,[18] and reference 19 for the other atoms, and that for Hf was corrected for anomalous dispersion. The details on data collection are included in Table II.

The position of the Hf atom was derived from the Patterson map, and a series of Fourier maps phased on Hf revealed the remaining non-hydrogen atoms of the molecule. Least-squares refinement of atom coordinates and U's, minimizing $\Sigma\omega[F^2-(F_c/k)^2]^2$, gave R = 0.076. All ring methyl H-atoms and the hydride were located from difference maps. Allyl H-atoms were not reliably located and were placed at trigonal positions in the allyl carbon plane. All H-atoms except the hydride were introduced into the

model with fixed coordinates and isotropic U's. Refinement of all carbon atoms in the Hf complex with anisotropic U_{ij}'s, and the hydride atom with isotropic U using all the data (3716 reflections) led to R = 0.049 and S = 2.51, with refinement of secondary extinction giving coeff. = $0.10(2)\times10^{-6}$. The final ΔF map showed a symmetric pair of peaks associated with the Hf atom ($\sim 2e^{-}/\text{Å}^3$, 1.2 Å from Hf). Bond distances and bond angles are given in Tables III and IV, respectively. Final atomic coordinates and U_{ij}'s are given in Table VII. Hydrogen atom coordinates and U's are given in Table VIII. All calculations were carried out on a VAX 11/780 computer using the CRYRM system of programs.

TABLE II. Crystal and Intensity Collection Data for $Cp^*_2Hf(H)(\eta^3\text{-}CH_2CHCH_2)$ (**3**).

Formula	$C_{23}H_{36}Hf$			
Formula weight	491.03 g/mol			
Space group	$P2_1/c$			
a	8.7533(16) Å			
b	14.165(4) Å			
c	17.5438(21) Å			
β	104.810(12)°			
V	2103.0(8) $Å^3$			
Z	4			
D_{calc}	1.55(1) g/cm^3			
Crystal size	0.45 x 0.50 x 0.53			
λ	0.71069 Å (MoKᾱ)			
μ	4.92 mm^{-1}			
Scan range	1.0° below $K\alpha_1$, 1.0° above $K\alpha_2$			
2θ limits, scan rate,	3-30°	3.91°/min	1.0	1179(+h,+k,±l)
backgrd time/scan time,	30-40°	2.02°/min	1.0	1303(+h,+k,±l)
number of reflections	3-30°	3.91°/min	1.0	1981(+h,±k,±l)
	29-40°	2.02°/min	1.0	2799(+h,±k,±l)
	39-50°	2.02°/min	1.0	3928(+h,±k,±l)
Total number of averaged data	3716 (3537 $F_o^2 > 0$)			
Refinement on	F_o^2			
Final number of parameters	221			
Final agreement				
R ($F_o^2 > 0$)	0.049 (3537)†			
R'	0.039 (2885)			
S	2.51 (3716)			

†Typical R-value, number of reflns used in sums given in parentheses. R' refers to R-value calculated for reflns with $F_o^2 > 3\sigma_{F^2}$. S is the goodness of fit.

Table III. Bond Lengths for $Cp^*_2Hf(H)(\eta^3\text{-}CH_2CHCH_2)$ (Å).

Hf–H	1.85(7)	C(14)–C(15)	1.396(12)
Hf–C(1)	2.381(15)	C(11)–C(11M)	1.520(15)
Hf–C(2)	2.481(17)	C(12)–C(12M)	1.465(16)
Hf–C(3)	2.566(17)	C(13)–C(13M)	1.486(18)
Hf–C(11)	2.537(9)	C(14)–C(14M)	1.496(15)
Hf–C(12)	2.532(9)	C(15)–C(15M)	1.516(14)
Hf–C(13)	2.563(10)	C(21)–C(22)	1.396(11)
Hf–C(14)	2.554(9)	C(21)–C(25)	1.387(12)
Hf–C(15)	2.523(8)	C(22)–C(23)	1.361(12)
Hf–C(21)	2.509(8)	C(23)–C(24)	1.408(15)
Hf–C(22)	2.488(7)	C(24)–C(25)	1.428(14)
Hf–C(23)	2.563(10)	C(21)–C(21M)	1.495(13)
Hf–C(24)	2.560(11)	C(22)–C(22M)	1.518(13)
Hf–C(25)	2.526(9)	C(23)–C(23M)	1.511(16)
C(1)–C(2)	1.388(23)	C(24)–C(24M)	1.516(17)
C(2)–C(3)	1.334(24)	C(25)–C(25M)	1.492(15)
C(11)–C(12)	1.390(12)	Hf–[a]R_1	2.243
C(11)–C(15)	1.383(12)	Hf–R_2	2.233
C(12)–C(13)	1.457(13)	Hf–A	2.253
C(13)–C(14)	1.397(14)		

[a]R_1≡ ring centroid of first Cp^*-ring [atoms C(11)—C(15M)]; R_2≡ ring centroid of second Cp^*-ring [atoms C(21)—C(25M)]; A≡ centroid of allyl group [atoms C(1)—C(3)].

Table IV. Bond angles for $Cp^*_2Hf(H)(\eta^3\text{-}CH_2CHCH_2)$ (°).

[a]R_1–Hf–R_2	137.5	C(11M)–C(11)–C(15)	125.7(8)
A–Hf–R_1	111.5	C(12M)–C(12)–C(13)	126.3(9)
A–Hf–R_2	108.6	C(12M)–C(12)–C(11)	126.2(9)
H–Hf–R_1	97.9	C(13M)–C(13)–C(14)	126.6(10)
H–Hf–R_2	92.9	C(13M)–C(13)–C(12)	125.0(10)
H–Hf–A	93.5	C(14M)–C(14)–C(15)	126.4(9)
H–Hf–C(1)	124(2)	C(14M)–C(14)–C(13)	124.3(9)
H–Hf–C(2)	92(2)	C(15M)–C(15)–C(11)	127.1(8)
H–Hf–C(3)	66(2)	C(15M)–C(15)–C(14)	124.0(8)
C(1)–C(2)–C(3)	125.1(20)	C(21M)–C(21)–C(22)	126.5(7)
C(15)–C(11)–C(12)	110.0(8)	C(21M)–C(21)–C(25)	124.0(8)
C(13)–C(12)–C(11)	106.1(8)	C(22M)–C(22)–C(23)	123.2(8)
C(14)–C(13)–C(12)	107.0(10)	C(22M)–C(22)–C(21)	125.9(7)
C(15)–C(14)–C(13)	108.7(8)	C(23M)–C(23)–C(24)	123.0(9)
C(11)–C(15)–C(14)	108.1(7)	C(23M)–C(23)–C(22)	127.8(9)
C(25)–C(21)–C(22)	107.5(7)	C(24M)–C(24)–C(25)	123.4(10)
C(23)–C(22)–C(21)	109.7(7)	C(24M)–C(24)–C(23)	129.8(10)
C(24)–C(23)–C(22)	108.3(8)	C(25M)–C(25)–C(21)	125.5(9)
C(25)–C(24)–C(23)	106.5(9)	C(25M)–C(25)–C(24)	125.8(9)
C(21)–C(25)–C(24)	107.9(8)		
C(11M)–C(11)–C(12)	122.5(8)		

[a]$R_1 \equiv$ ring centroid of first Cp^*-ring [atoms C(11)—C(15M)];
$R_2 \equiv$ ring centroid of second Cp^*-ring [atoms C(21)—C(25M)];
A$\equiv$ centroid of allyl group [atoms C(1)—C(3)].

Table V. Least-squares planes of pentamethyl rings for 3.[a]

Atom	Deviation from plane (Å)[b]
C(11)	0.0173
C(12)	-0.0143
C(13)	0.0064
C(14)	0.0037
C(15)	-0.0130
C(11M)	0.4006
C(12M)	0.2056
C(13M)	0.3061
C(14M)	0.1846
C(15M)	0.1483
C(21)	0.0124
C(22)	-0.0171
C(23)	0.0147
C(24)	-0.0067
C(25)	-0.0035
C(21M)	0.3807
C(22M)	0.1793
C(23M)	0.2742
C(24M)	0.1131
C(25M)	0.1809

[a]Planes defined by atoms C(11)–C(15) and C(21)–C(25).

[b]A negative deviation is a deviation toward the metal atom.

Table VI. Intramolecular non-bonded distances for **3** (Å)[a]

C(1)—C(12)	3.19(2)	C(2)—C(23M)	3.30(2)
C(1)—C(13)	3.15(2)	C(3)—C(13)	3.36(2)
C(1)—C(23)	3.09(2)	C(11)—C(21)	3.38(1)
C(1)—C(23M)	3.21(2)	C(11M)—C(21M)	3.25(2)
C(1)—C(12M)	3.44(2)	H—C(14)	2.66(7)
C(1)—C(13M)	3.40(2)	H—C(24)	2.79(7)
C(2)—C(23)	3.11(2)	H—C(25)	2.47(7)
C(2)—C(24)	3.19(2)	H—C(25M)	2.74(7)
		H—C(3)	2.48(7)

[a]Listed are all C—C distances less than 3.50 Å and hydride—C distances less than 2.80 Å.

Table VII. Final non-hydrogen atom coordinates ($\times 10^4$) and Gaussian amplitudes ($\times 10^4$).

	x	y	z	U_{11}	U_{22}	U_{33}	U_{12}	U_{13}	U_{23}
Hf	2777.7(4)	1980.0(2)	1711.2(2)	393(2)	453(2)	345(2)	81(2)	138(1)	−4(2)
C(1)	26(14)	1700(13)	1532(8)	514(66)	1851(159)	910(93)	306(88)	216(62)	511(99)
C(2)	176(17)	2644(14)	1751(9)	880(99)	2005(186)	999(107)	936(121)	580(87)	612(123)
C(3)	1113(22)	2974(12)	2421(8)	1855(161)	1628(142)	854(88)	1264(133)	711(103)	217(100)
H	3865(80)	2983(49)	2280(37)	414*					
C(11)	4351(11)	464(6)	2042(4)	732(62)	470(48)	337(41)	167(45)	187(42)	63(36)
C(12)	2875(11)	281(6)	2170(5)	567(55)	439(49)	464(49)	−143(42)	−52(41)	−15(38)
C(13)	2785(11)	846(8)	2851(5)	664(64)	982(79)	534(55)	160(60)	342(50)	295(55)
C(14)	4189(12)	1361(6)	3077(5)	758(65)	483(51)	352(44)	32(47)	123(44)	−8(36)
C(15)	5134(9)	1136(6)	2571(5)	378(44)	548(53)	473(46)	−22(39)	39(37)	114(40)
C(11M)	5104(18)	−179(8)	1544(6)	1690(131)	647(69)	742(73)	489(80)	559(82)	120(56)
C(12M)	1800(19)	−483(9)	1815(7)	1614(137)	842(87)	878(87)	−559(91)	−348(89)	203(67)
C(13M)	1602(17)	713(12)	3317(8)	1155(108)	1863(157)	1224(108)	659(106)	853(94)	854(106)
C(14M)	4663(19)	1945(8)	3810(5)	2034(149)	734(68)	346(47)	139(96)	47(68)	−91(54)
C(15M)	6827(12)	1464(9)	2691(7)	498(61)	1190(97)	948(84)	−101(62)	−34(58)	475(72)
C(21)	4178(9)	2115(6)	634(4)	528(47)	495(52)	347(38)	56(41)	161(34)	76(36)
C(22)	2636(8)	1822(5)	282(4)	263(35)	413(47)	454(42)	−15(33)	46(31)	52(34)
C(23)	1612(12)	2542(8)	293(5)	620(61)	812(68)	386(47)	11(54)	33(44)	106(47)
C(24)	2477(16)	3311(7)	696(5)	1337(104)	479(57)	457(52)	351(60)	327(62)	175(41)
C(25)	4097(11)	3029(7)	904(4)	726(59)	574(52)	385(42)	−131(57)	91(40)	73(46)
C(21M)	5664(11)	1663(7)	543(5)	602(59)	897(75)	588(56)	204(52)	269(48)	276(49)
C(22M)	2166(13)	926(8)	−194(5)	952(81)	885(74)	411(49)	93(67)	24(51)	−141(52)
C(23M)	−105(13)	2614(10)	−157(7)	514(62)	1558(117)	712(70)	184(69)	−18(54)	232(71)
C(24M)	1932(20)	4301(8)	822(7)	2166(171)	679(78)	882(85)	629(96)	625(100)	301(64)
C(25M)	5476(16)	3657(8)	1233(7)	1125(100)	802(80)	850(79)	−489(74)	95(72)	−30(62)

*Refined with isotropic U.

Table VIII. Hydrogen atom coordinates ($\times 10^3$) and U's ($Å^2, \times 10^3$).

	x	*y*	*z*	*U*
H(1A)	−669	1505	1039	76
H(1B)	621	1219	1866	76
H(2B)	−451	3071	1392	76
H(3A)	1135	3625	2528	76
H(3B)	1743	2546	2794	76
H(1)	4265	−440	1085	63
H(2)	5667	−708	1845	63
H(3)	5851	187	1314	63
H(4)	679	−240	1607	63
H(5)	2094	−750	1340	63
H(6)	1781	−1000	2176	63
H(7)	714	1173	3169	63
H(8)	1131	64	3223	63
H(9)	2093	775	3890	63
H(10)	5435	1630	4229	63
H(11)	3697	2092	4003	63
H(12)	5094	2569	3697	63
H(13)	7587	1024	3032	63
H(14)	6983	2102	2954	63
H(15)	7102	1526	2184	63
H(16)	5555	956	538	63
H(17)	6570	1837	979	63
H(18)	5873	1851	39	63
H(19)	1055	962	−515	63
H(20)	2851	836	−566	63
H(21)	2291	363	146	63
H(22)	−295	3181	−492	63
H(23)	−441	2048	−511	63
H(24)	−798	2635	205	63
H(25)	2690	4783	713	63
H(26)	876	4441	477	63
H(27)	1897	4395	1379	63
H(28)	6328	3309	1634	63
H(29)	5218	4232	1490	63
H(30)	5995	3866	812	63

References

(1) (a) Parshall, G. W. "Homogeneous Catalysis", Wiley-Interscience, New York, 1980, pp. 35-37. (b) Tulip, T. H.; Ibers, J. A. J. Am. Chem. Soc. 1979, 101, 4201. (c) Bingham, D.; Hudson, B.; Webster, D.; Wells, P. B. J. Chem. Soc. Dalton 1974, 1521. (d) Keim, W. "The π-Allyl System in Catalysis" in Schrauzer, G. N., Ed., "Transition Metals in Homogeneous Catalysis", Marcel Dekker, 1971, pp. 59.92. (e) Orchin, M. Adv. Catal. 1966, 16, 1.

(2) (a) Erwin, D. K., Ph.D. Thesis, California Institute of Technology, 1979. (b) Sanner, R. D.; Erwin, D. K.; Cohen, S. A.; Roddick, D. M.; Santarsiero, B. D.; Bercaw, J. E., manuscript in preparation.

(3) Using the Eyring equation, with k_c (exchange rate at coalescence temperature (sec^{-1})) calculated from the Gutowsky-Holm relation: $k_c = \frac{\pi}{\sqrt{2}}\Delta\nu$; Gutowsky, H. S.; Holm, C. H. J. Chem. Phys. 1956, 25, 1228.

(4) Calculated using values $T_c = -8^{\circ}C$, $\Delta\nu = 9.7$ Hz.

(5) Sanner, R. D.; Manriquez, J. M.; Marsh, R. E.; Bercaw, J. E. J. Am. Chem. Soc. 1976, 98, 8351.

(6) Moore, E. J., Ph.D. Thesis, California Institute of Technology, 1984.

(7) Incipient formation of an η^1-(σ)allyl complex has been suggested for the structurally characterized iridium π-allyl complex $[Ir(\eta^3-C_3H_5)Cl(CO)(P(CH_3)_2Ph)_2][PF_6]$,[9] although bondlength variations are only possibly significant.

(8) (a) Erker, G.; Rosenfeldt, F. Angew. Chem. Int. Ed. Engl. 1978, 17, 605. (b) Ibid., J. Organomet. Chem. 1980, 188, C1.

(9) Kaduk, J. A.; Poulos, A. T.; Ibers, J. A. J. Organomet. Chem. 1977, 127, 245.

(10) Helmholdt, R. B.; Jellinek, F.; Martin, H. A.; Vos, A. Rec. Trav. Chim. Pays-Bas 1967, 86, 1263.

(11) Pauling, L. "The Nature of the Chemical Bond"; Cornell, New York, 1960; 3rd ed., pg. 256.

(12) Bernstein, E. R.; Hamilton, W. C.; Keiderling, T. A.; Kennelly, W. J.; Laplaca, S. J.; Lippard, S. J.; Marks, T. J.; Mayerle, J. J., unpublished results at Brookhaven National Laboratory (neutron structure).

(13) Johnson, P. L.; Cohen, S. A.; Mark, T. J.; Williams, J. M. J. Am. Chem. Soc. 1978, 100, 2709 (neutron structure).

(14) This thesis, Chapter 4.

(15) Santarsiero, B. D.; Moore, E. J.; Bercaw, J. E., 1982, unpublished results. See also reference 6.

(16) This thesis, Chapter 1.

(17) Roddick, D. M.; Fryzuk, M. D.; Seidler, P. F.; Hillhouse, G. L.; Bercaw, J. E., manuscript in preparation.

(18) Stewart, R. F.; Davidson, E. R.; Simpson, W. T. J. Chem. Phys. **1965**, 42, 3175.

(19) International Tables for X-Ray Crystallography, Vol. IV, **1974**, pp. 72-98.

Chapter III

Reactions of Permethylhafnocene and Permethylzirconocene Hydrides with CO. Synthesis and Reactivity Patterns of Early Transition Metal Aldehyde Complexes.

INTRODUCTION

Transition metal-mediated C-C bond-forming reactions, particularly those involving carbon monoxide and/or simple olefins, are of continuing interest in organometallic chemistry.[1] Recently, the ability of early transition metal complexes to effect a variety of stoichiometric C-C bond-forming transformations has received much attention. In particular, hydrozirconation[2] and titanocene methylene transfer,[3] which have been investigated in detail, have proven to be of considerable synthetic utility.

Work in our laboratories[4] has established a number of CO-based carbon-carbon coupling reactions (equations 1-5)

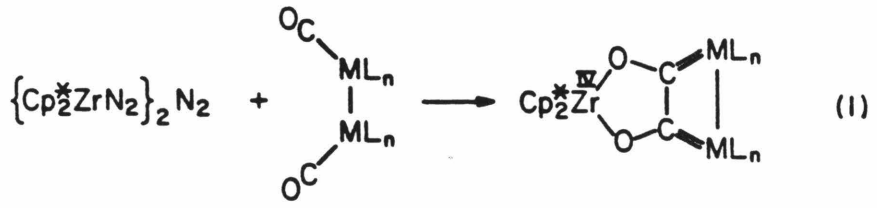

(1)

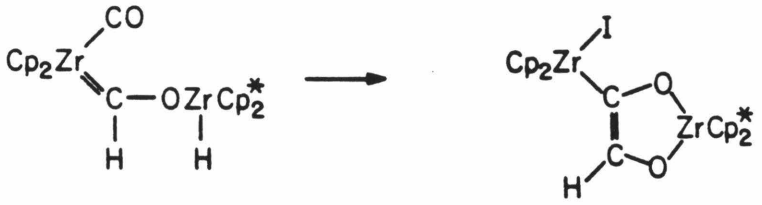

(2)

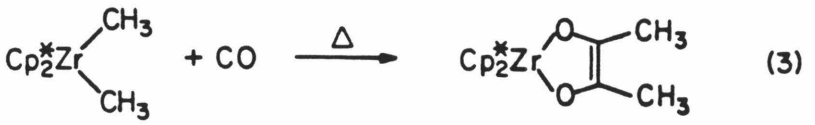

(3)

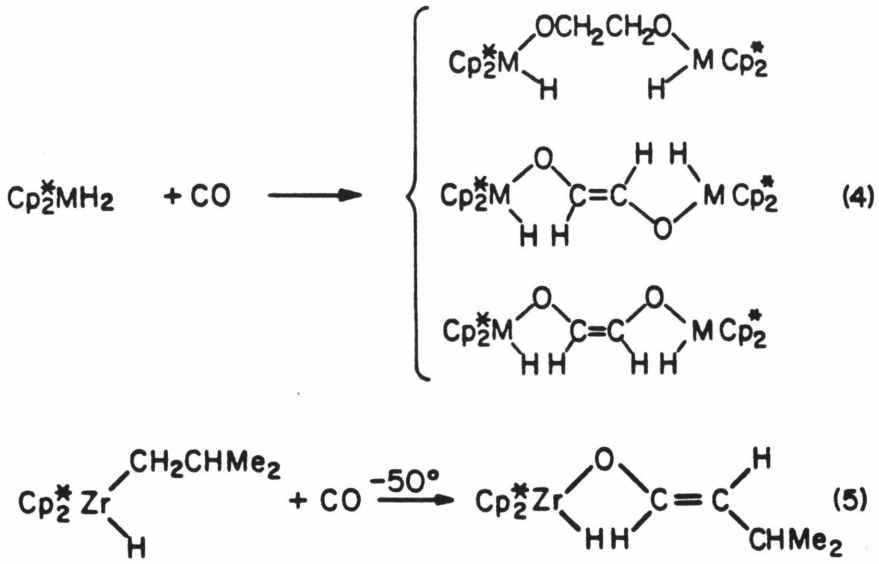

for group IV permethylmetallocene complexes. The reaction of zirconium alkyl hydride derivatives with CO is noteworthy: labeling studies have shown that carbonylation of $Cp^*_2Zr(H)CH_2CHMe_2$ proceeds via the intermediacy of aldehyde complex 2 (Scheme I), which undergoes facile β-H elimination to form the enolate hydride product 3. This

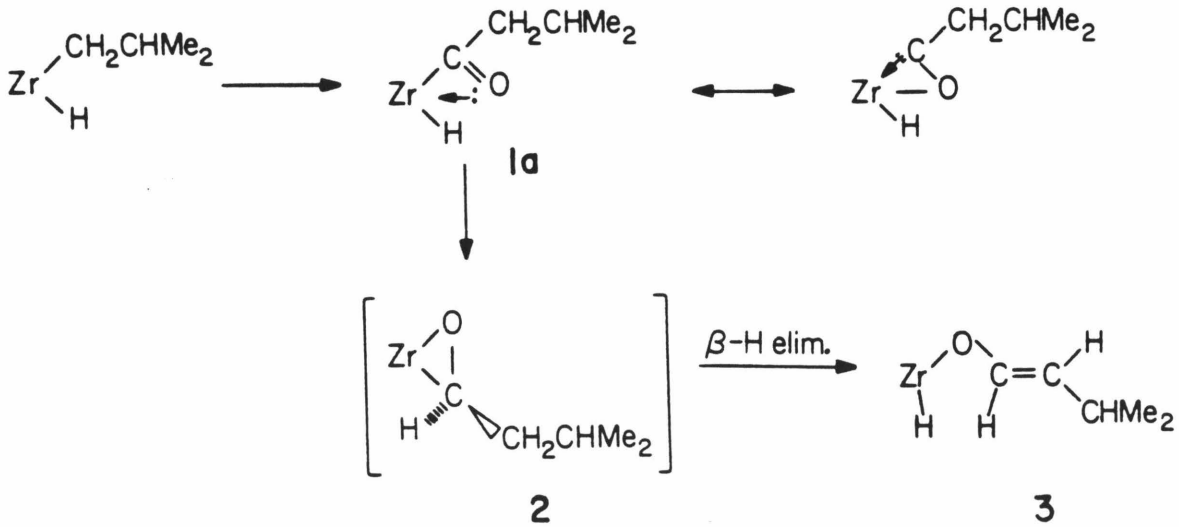

Scheme I

pattern of reactivity is unprecedented in late metal aldehyde chemistry, and was therefore of interest to us. The ready availability of a range of alkyl as well as aryl and alkenyl hydride complexes of zirconium and hafnium[5] has provided the opportunity to examine the carbonylation chemistry of zirconium and hafnium hydrocarbon derivatives in detail. The results of this study are reported in this chapter.

RESULTS

(1) Synthesis and Reactivity of $Cp^*_2M(CO)(\eta^2\text{-}O{=}CHR)$- (M=Zr, Hf; R=$CH_2CHMe_2$, Ph).

Toluene solutions of $Cp^*_2M(H)CH_2CHMe_2$ (M=Zr, Hf) are quantitatively converted at -50°C under 1 atm CO to the corresponding dihaptoacyl hydrides, $Cp^*_2MH(\eta^2\text{-}C(O)CH_2CHMe_2)$ (M=Zr : **1a**; Hf : **1b**). Characteristic ^1H NMR (Table I) and $^{13}C\{^1H\}$ NMR ($Me_2CHCH_2\underline{C}O$: 335.86 δ) spectra of **1b** are indicative of a single isomeric species at low temperature, presumably the expected kinetic product with acyl oxygen coordinated in the lateral equatorial position.[6]

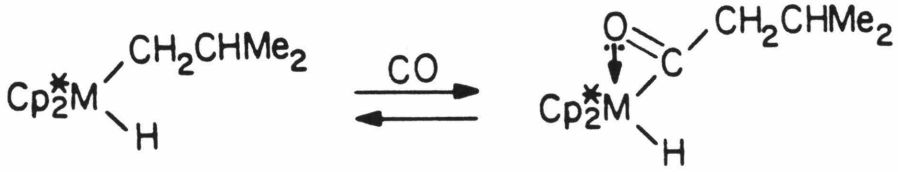

(6)

(M = Zr: 1a; Hf: 1b)

The reaction of $Cp^*_2Zr(H)CH_2CHMe_2$ with carbon monoxide at 25°C has been reported to give the enolate hydride, $Cp^*_2ZrH(OCH{=}CHCHMe_2)$ (**3**), together with a small (~5%) amount of $Cp^*_2Zr(CO)_2$.[4b] However, when solutions of **1a** and **1b** are stirred vigorously in toluene at -78°C under 1 atm CO and allowed to warm slowly to room temperature over the course

of several hours, new products **4a** and **4b** (~ 80% pure by ^{1}H NMR, with traces of enolate hydride and dicarbonyl byproducts) are obtained, which may be isolated from hexamethyldisiloxane as highly soluble, orange powders. ^{1}H and ^{13}C NMR and infrared data, as well as subsequent chemical reactivity clearly indicate **4a** and **4b** to be η^{2}-aldehyde complexes as shown below:

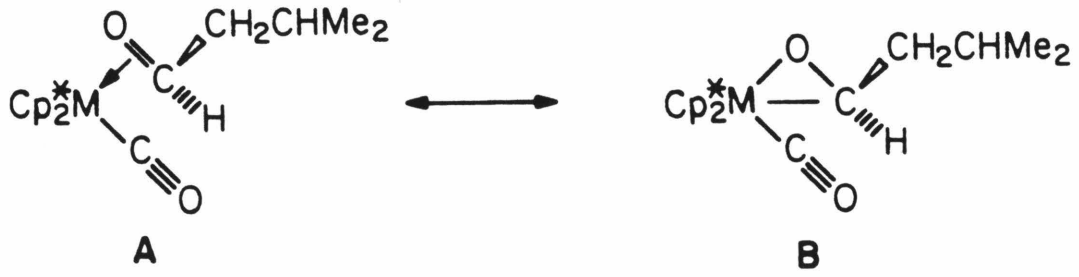

(M = Zr:4a; Hf: 4b)

The ^{1}H NMR spectrum of **4b** exhibits inequivalent η^{5}-$C_5(CH_3)_5$ methyl resonances at 1.67 δ (15H) and 1.71 δ (15H), a broad doublet at 2.21 δ (1H, $^{3}J_{HH}$ = 10 Hz) assigned to the aldehyde proton, and an overlapping pair of doublets at 1.18 δ and 1.20 δ ($^{3}J_{HH}$ = 6 Hz) due to the diastereotopic isobutyl methyl groups. The gated ^{13}C NMR of labeled **4b**, prepared from $Cp^{*}_{2}Hf(H)CH_2CHMe_2$ and ^{13}CO, shows a small coupling ($^{2}J_{CC}$ = 9.8 Hz) between terminal carbonyl (252.49 δ) and aldehyde carbonyl (dd, 84.22 δ; $^{1}J_{HC}$ = 156.2 Hz) carbons. These data are consistent with the given structure.[7] The aldehyde proton and carbonyl carbon

chemical shifts are substantially upfield from values reported for free aliphatic aldehydes;[8] however, the chemical shift of the aldehyde carbon in **4b** agrees closely with the value reported for the structurally characterized molybdenum η^2-aldehyde complex CpMo(CO)(α-2-pyridyl-2-methylaminobenzyl)(η^2-O=CHPh) (81.6 δ).[9]

The infrared spectra of **4a** and **4b** are informative, showing strong terminal carbonyl bands at 1940 and 1930 cm^{-1}, respectively. These values are significantly lower than that of the Hf(IV) adduct $Cp^*_2HfH_2(CO)$ (2036 cm^{-1}),[10] and quite similar to values for the symmetric stretching modes of $Cp^*_2Zr^{II}(CO)_2$ (1942 cm^{-1})[11] and $Cp^*_2Hf^{II}(CO)_2$ (1940 cm^{-1}),[4e] suggesting a considerable amount of electron rich M(II) character (canonical form **A**) in **4a** and **4b**. However, the absence of any additional IR bands in **4a,b** above 1200 cm^{-1} assignable to an aldehyde acyl stretch ν(C-O) is noteworthy,[12] and appears indicative of some degree of M(IV) oxymetallacyclopropane character (canonical form **B**).

Both **4a** and **4b** decompose slowly at 25°C, but may be stored indefinitely at low temperature. The carbonyl ligand is quite labile: ^{13}CO labeling studies of **4b** indicated complete label scrambling after several minutes at room temperature ($\tilde{P}(CO) \approx 2$ atm):

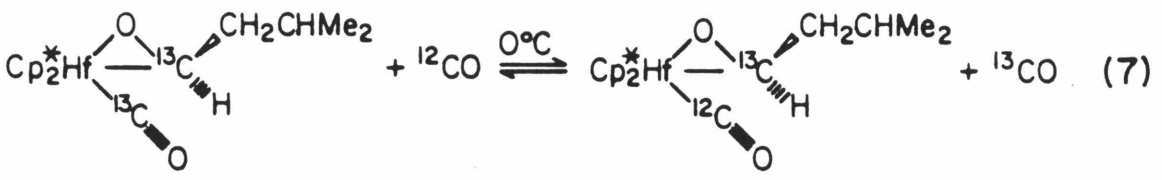

(7)

The lability of CO in **4a** is suggested by its thermolysis (80C, 1 hr), which induces clean loss of CO to generate the enolate hydride, **3**. In contrast, thermolysis of **4b** at 80°C for 1 hr effects a clean rearrangement to a new species, identified by ^{1}H and ^{13}C NMR and IR data as the cyclic enediolate $Cp^{*}_{2}HfOC(CH_2CHMe_2)=CHO$ (**5**) (equation 8).[13]

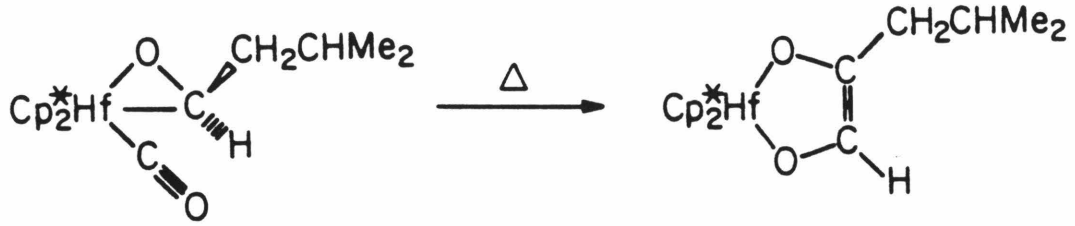

4b **5** (8)

When toluene solutions of **3b** are cooled below -10°C in the presence of 1 atm CO, a dramatic, reversible color change from orange to lime green is observed. ^{1}H NMR of this green solution indicates a quantitative conversion of **4b** to a single new species **6**. In contrast, **6** is not observed in the variable temperature ^{1}H NMR of **4b** under N_2. Likewise, the ^{1}H NMR of **4a** under N_2 or CO is essentially temperature independent. The ^{1}H NMR of **6** shows the resonance previously attributed to the aldehyde proton in **4b** shifted downfield to 4.88 δ (dd, $^{3}J_{HH}$ = 10.1, 2.7 Hz); the remaining ring and isobutyl methyl resonances in **6** are only slightly shifted from values in **4b** (Table I). The ^{13}C NMR of ^{13}CO-labeled **4b** treated with ^{13}CO at -50°C is more informative, showing the presence of three labeled resonances at 94.4 δ (dddd, J_{CC} = 13.6, 37.1 Hz; $^{1}J_{CH}$ =

136.7 Hz; $^{3}J_{CH}$ = 5.9 Hz), 213.6 δ (d, J_{CC} = 37.1 Hz), and 310.6 δ (d, J_{CC} = 13.6 Hz). Treatment of $Cp^{*}_{2}Hf(^{13}CO)(O=^{13}CHCH_{2}CHMe_{2})$ at -50°C with ^{12}CO yields a product with only the 94.4 and 213.6 pm resonances enriched, indicating that the 310.6 δ carbon is derived from ambient CO uptake. A final piece of spectroscopic data is given by the low temperature infrared spectrum (toluene, -78°C) of **6**, which shows two strong acyl bands at 1724 and 1640 cm^{-1} and no bands in the 1800-2100 cm^{-1} region. Despite the extensive spectroscopic data, no clear assignment of the structure of **6** is evident. A reasonable structure consistent with all the available data is given below:

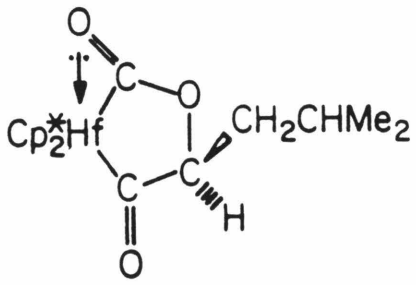

6

The isolation of aldehyde carbonyl complexes **4a** and **4b** is plagued by impurities and low yields. In order to obtain more suitable systems for study, the reaction of CO with a variety of alkyl hydrides, $Cp^{*}_{2}M(H)R$ (M=Zr, Hf; R=Et, butyl, ethyphenyl, neohexyl, neopentyl) was examined. Not surprisingly, all alkyl hydrides reacted similarly with CO, generating complexes analogous to **4** in varying yields

(40-80%), with similar thermal instabilities and intractable natures.

The reaction of CO with $Cp^*_2Hf(H)Ph$ was examined in the hope of cleanly forming a stable aldehyde product not subject to β-H elimination decomposition pathways. Solutions of $Cp^*_2Hf(H)Ph$ react surprisingly slowly with 3 atm CO over the course of several hours at 25°C to form (>95%, ^1H NMR) the benzaldehyde carbonyl $Cp^*_2Hf(CO)(\eta^2$-O=CHPh) (7), isolable in 66% yield as an analytically pure, thermally stable orange crystalline solid.

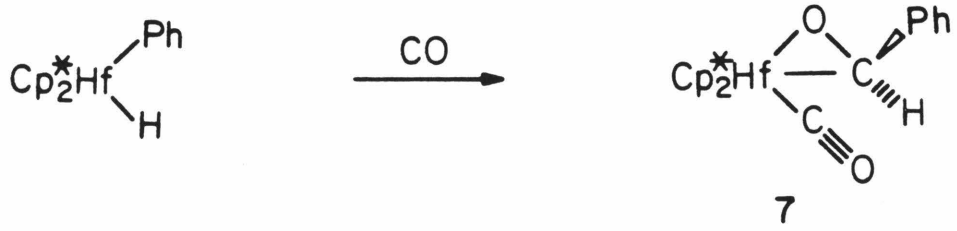

7 (9)

The monomeric formulation of 7 was confirmed by its solution molecular weight (C_6D_6, calc: 583; found: 592). Monitoring reaction 10 by ^1H NMR indicated no build up of an intermediate carbonyl adduct or acyl hydride species. Thermolysis of 7 (80°C, 12 hr) induces clean rearrangement to an enediolate complex analogous to **5**, $Cp^*_2\overline{HfOC(Ph)=CHO}$ (8). In contrast to **4b**, no spectral changes are observed when solutions of 7 are cooled under excess CO.

(2) Reaction of $Cp^*_2\overline{HfCH_2CH_2CH_2CH_2}$ with carbon monoxide.

A reaction related to equation 6 is the carbonylation of $Cp^*_2\overline{ZrCH_2CH_2CH_2CH_2}$ to give the cyclic enolate hydride, $Cp^*_2Zr(H)OC{=}CHCH_2CH_2CH_2$,[4b]. Since the mechanisms of this reaction and reaction 2 are believed to be similar, the reaction of $Cp^*_2\overline{HfCH_2CH_2CH_2CH_2}$ (9) with CO was examined in the hope of preparing a coordinated ketone complex, in analogy to the aldehyde complexes **4a,b** and **7**. The reaction of $Cp^*_2\overline{HfCH_2CH_2CH_2CH_2}$ with excess CO was monitored at low temperature by ^1H and $^{13}C\{^1H\}$ NMR. At -50°C, resonances for **9** were slowly replaced by a new set of resonances attributed to the acyl complex, $Cp^*_2\overline{Hf(\eta^2\text{-}O{=}CCH_2CH_2CH_2CH_2)}$ (**10**). The identity of **10** was confirmed by $^{13}C\{^1H\}$ NMR of the ^{13}CO labeled complex, which exhibited a single low field resonance at 344 δ characteristic of a dihaptoacyl functionality. When solutions of **10** are warmed slowly under CO, a single, isolable product is obtained, which NMR and IR (ν(C=C): 1640 cm^{-1}; ν(C-O): 1210 cm^{-1}) data show to be not the desired η^2-cyclopentanone complex, but rather the enediolate $Cp^*_2\overline{HfOCCH_2CH_2CH_2CH_2CO}$ (**11**) (equation 10).

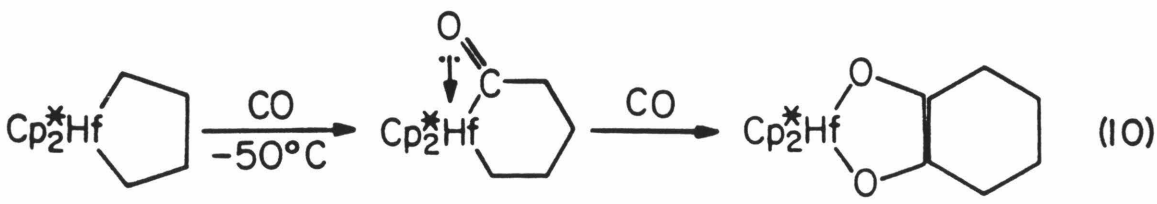

(10)

9 **10** **11**

(3) Reactions of $Cp^*_2ZrH(\eta^2\text{-}O{=}CCH_2CHMe_2)$ with C_2H_4, 2-butyne, H_2 and t-butylacetylene.

The demonstrated ability of η^2-aldehyde complexes **4b** and **7** to readily couple their aldehyde and terminal carbonyl ligands suggested that similar reactivity might be observed in complexes where CO is replaced by other suitable substrates. Attempts to trap in-situ generated zirconium aldehyde intermediate $Cp^*_2Zr(\eta^2\text{-}O{=}CHCH_2CHMe_2)$ (2) by slowly warming solutions of acyl hydride **1a** in the presence of large excesses of methylisonitrile or pyridine yielded no isolable products. However, treatment of toluene solutions of **1a** at -42°C with excess C_2H_4 and 2-butyne did quantitatively yield upon slow warming to 25°C the heterometallacycles $Cp^*_2\overline{ZrOCH(CH_2CHMe_2)CH_2CH_2}$ (12) and $Cp^*_2\overline{ZrOCH(CH_2CHMe_2)C(CH_3){=}C(CH_3)}$ (13), respectively (equation 11).

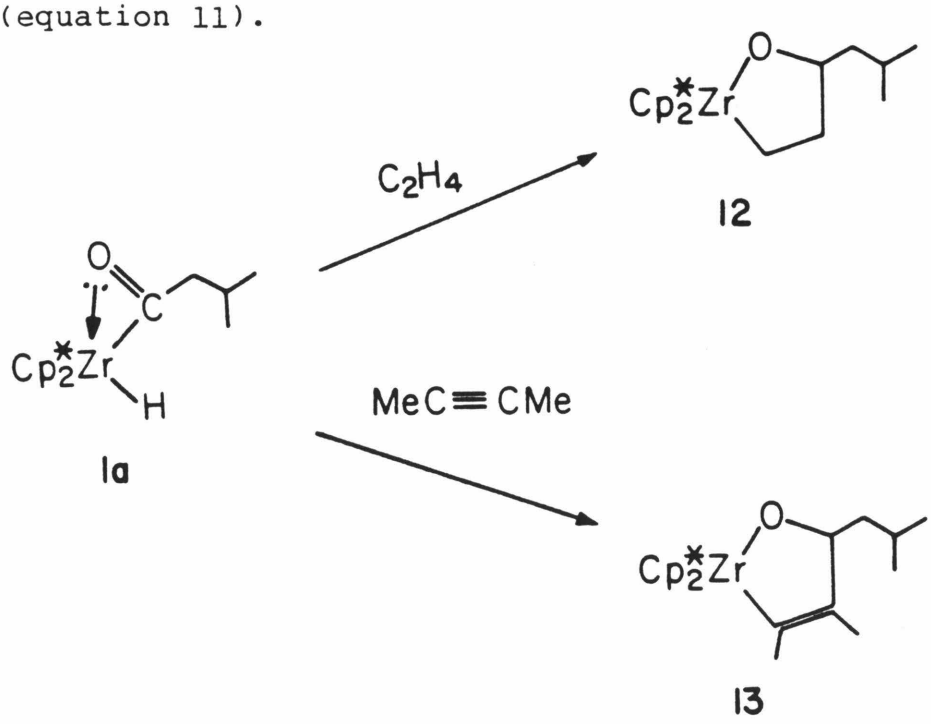

(11)

The structures of **12** and **13** were confirmed by characteristic ^{1}H and ^{13}C NMR data. In particular, the spectral data for **12** compare closely to those reported for the related titanium complex $Cp^{*}_{2}\overline{TiOCH(CH_3)CH_2CH_2}$,[14] with 6 highly coupled proton resonances (^{1}H, 500.13 MHz) observed for the ring moiety. Both **12** and **13** were isolated as analytically pure white solids.

An additional mode of reactivity for aldehyde precursor **1a** is indicated by its reactions with H_2 and t-butylacetylene upon slow warming to produce alkoxy hydride $Cp^{*}_{2}Zr(H)OCH_2CH_2CHMe_2$ (**14**) and alkoxy acetylide $Cp^{*}_{2}Zr(C{\equiv}C^{t}Bu)OCH_2CH_2CHMe_2$ (**15**), respectively (equation 12).

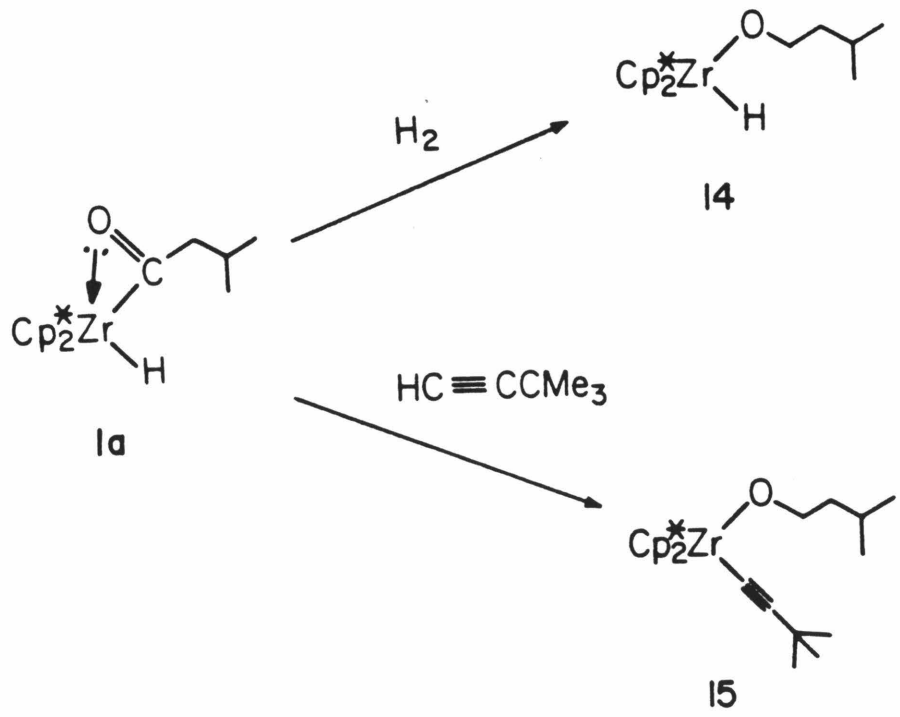

(12)

14 was isolated in good yield as a brown sublimable solid. Both **14** and **15** exhibit nearly identical ^{1}H NMR resonances attributable to the alkoxy moiety. The hydride resonance for **14** appears as a broad singlet at 5.69 δ, a relatively high field chemical shift characteristic of zirconium alkoxy-substituted hydride complexes.[4b,e] **15** was isolated as a fairly pure (>90%, ^{1}H NMR), colorless oil. The infrared spectrum reveals a 2040 cm^{-1} band assigned to the terminal acetylide group.

(4) Reactions of $Cp^*_2Hf(H)CH{=}CH^tBu$ with CO.

Like the alkyl hydride complexes examined thus far, the σ-alkenyl hydride complex $Cp^*_2Hf(H)CH{=}CH^tBu$ reacts readily with 1 atm CO at -78°C to form the vinylacyl hydride, $Cp^*_2Hf(H)(\eta^2\text{-}OCCH{=}CH^tBu)$ (**16**). The characteristic low field acyl carbon chemical shift (320.45 δ) and large vinylic proton coupling constant of 15.1 Hz suggests a dihaptoacyl structure analogous to **1b**, with the trans stereochemistry about the carbon-carbon double bond preserved.

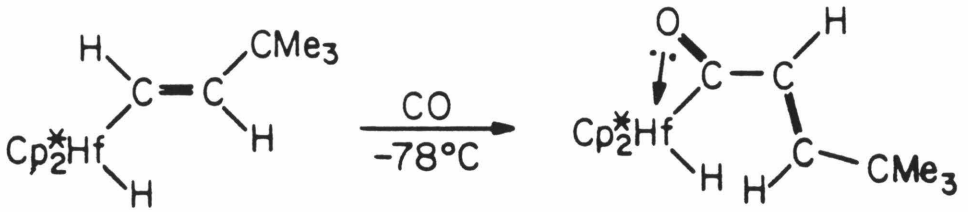

(13)

16

Thermolysis of 16 (T > -10°C) <u>in vacuo</u> induces a rearrangement to form a new metallacycle, $Cp^*_2\overline{Hf(OHC{=}CHCH(^tBu)}$ (17), isolable as a thermally unstable orange oil.

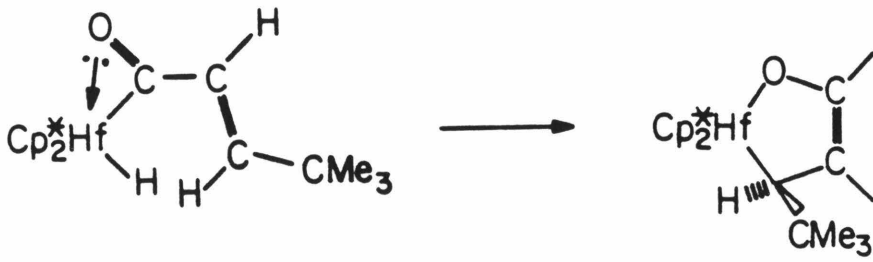

(14)

16 17

The structure of 17 is clearly established by spectroscopic data, and by its subsequent chemical reactivity. Specifically, further treatment of 17 with excess CO at 25°C quantitatively yields the insertion product, $Cp^*_2\overline{Hf(OCH{=}CHCH(^tBu)(CO)}$ (18).

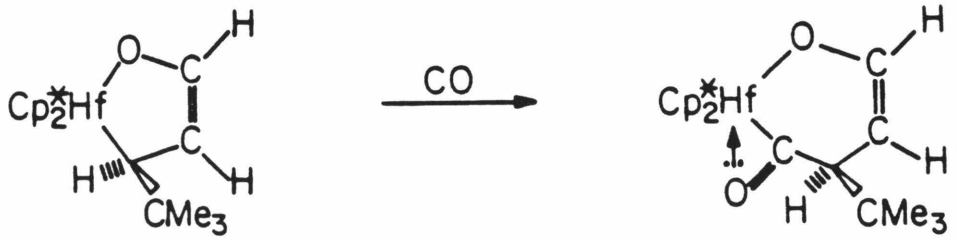

(15)

17 18

18 may be isolated from petroleum ether as an orange crystalline solid. The ^1H NMR of 18 closely resembles that of 17, the most notable difference being a downfield shift of the resonance assigned to the α-proton in 17 to 2.90 δ (pseudo triplet, J_{HH} = 6 Hz). Correct assignment of the

highly coupled vinylic and tertiary carbon proton resonances was verified by carbonylation of the deuterium labeled $Cp^*_2Hf(D)CH{=}CD^tBu$ to give $Cp^*_2\overline{HfODC{=}CHCD(^tBu)CO}$ (**18d**). The presence of an η^2-acyl functionality is indicated by IR (ν(C-O): 1610 cm^{-1}) and ^{13}C NMR of the ^{13}CO labeled compound ($\underline{C}$(acyl), 307.25 δ).

The acyl metallacycle **18** is stable at room temperature, but upon warming to 80°C rearranges via a formal 1,2 hydrogen shift to give the 7-membered ring metallacycle, $Cp^*_2\overline{HfOCH{=}CHC(^tBu){=}CHO}$ (**19**).

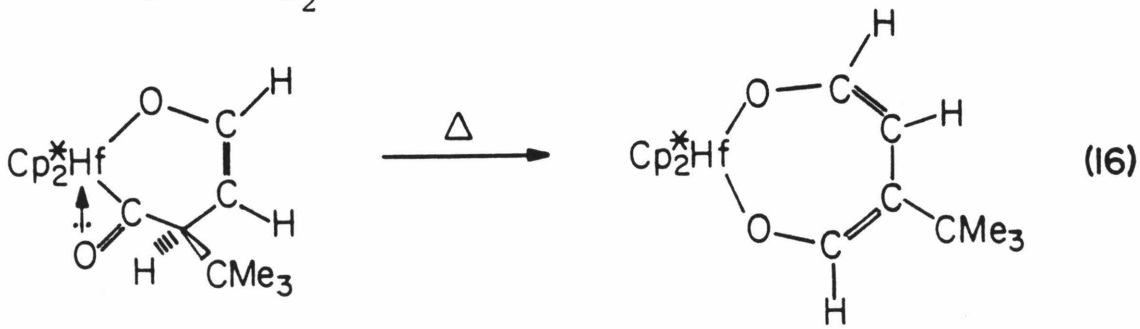

(16)

18 **19**

The thermal rearrangement of **18** to **19** obeys first-order kinetics for greater than three half lives (Figure 1), with $k = 1.5 \times 10^{-4}$ sec^{-1} at 80°C. The thermolysis of the deuterium labeled complex **18d**, which produces solely $Cp^*_2\overline{HfOCD{=}CHC(^tBu){=}CDO}$, is somewhat slower, giving a kinetic isotope effect of $k_H/k_D = 3.6$.

Figure 1

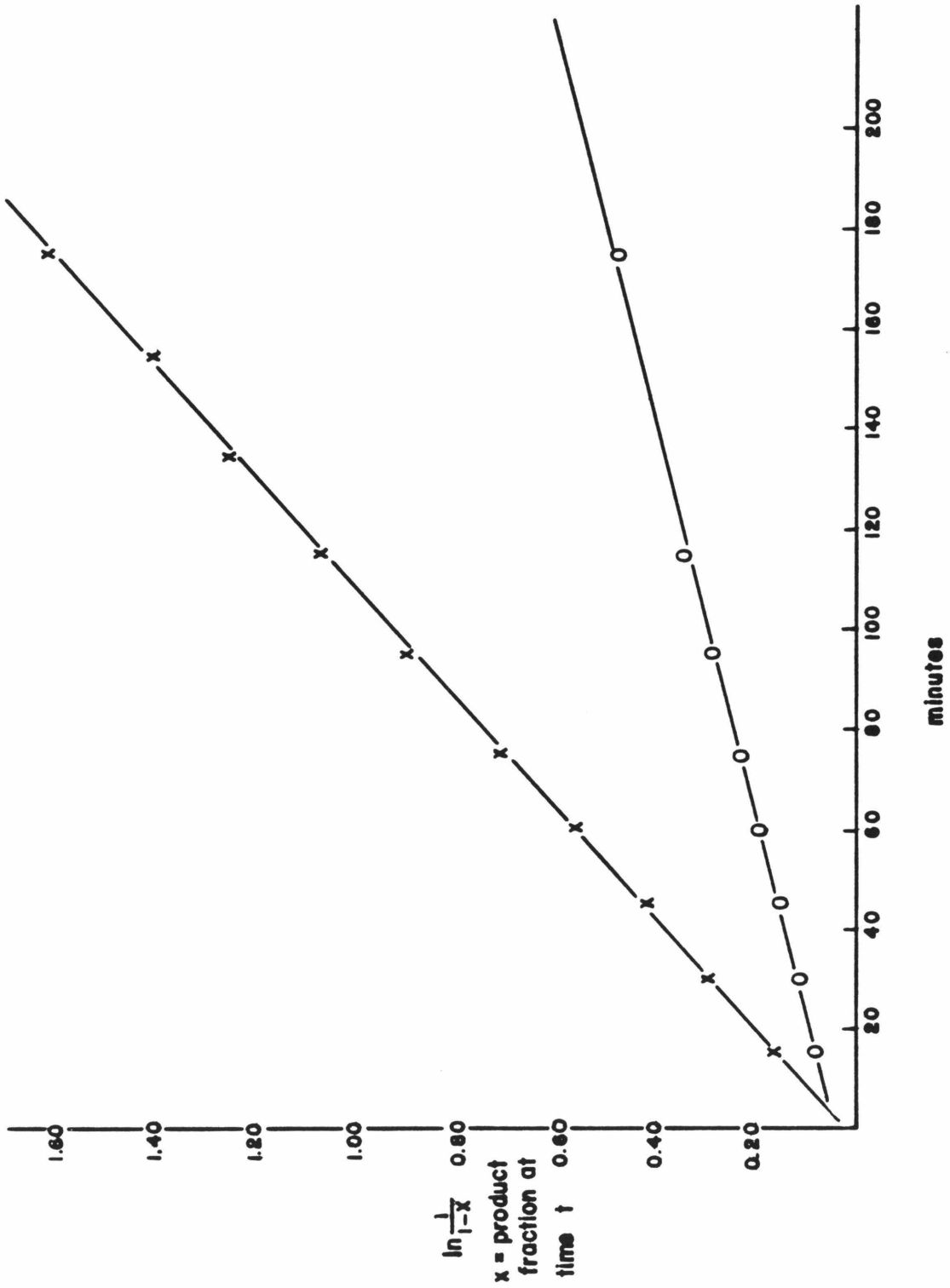
1.60
1.40
1.20
1.00
0.80
0.60
0.40
0.20
$\ln \frac{1}{1-x}$
x = product fraction at time t
20
40
60
80
100
120
140
160
180
200
minutes

DISCUSSION

The reaction chemistry of acyl hydrides **1a** and **1b** differs markedly from that of previously reported late transition metal acyl hydrides, which typically decarbonylate and subsequently release alkane,[15] or, in one instance, undergo reductive elimination of aldehyde.[16] This difference in reactivity may be readily ascribed to the oxophillic nature of coordinatively unsaturated group IV metallocenes, which encourages η^2 "oxycarbenoid" acyl coordination and directs reactivity toward final products which contain metal-oxygen bonds.

The facile migration of hydride to the acyl carbon in **1a** to form a reactive, π-bound aldehyde species, implied by earlier labeling studies, has been verified by trapping of the formally sixteen electron intermediate with CO to give an isolable aldehyde carbonyl product, **4a**. This reaction has proven general for a number of zirconium and hafnium alkyl and aryl hydride complexes.[17] The rates of reaction of the acyl hydride **1a** with CO and other trapping ligands are independent of the nature and concentration of substrate, suggesting that the products formed evolve from a common reactive intermediate, **2** (equation 17).

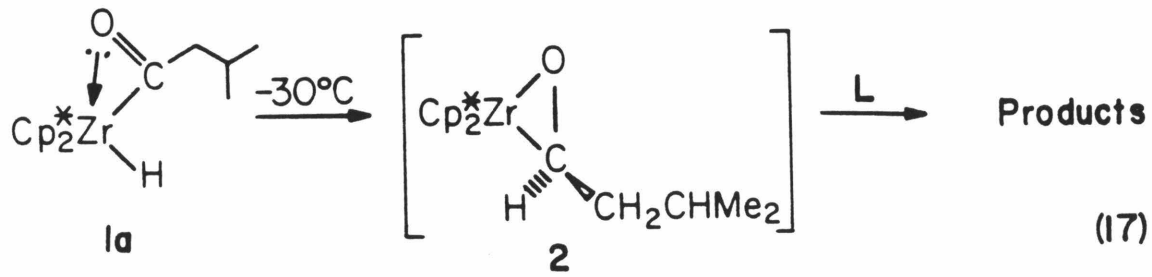

1a **2** (17)

The relatively electron rich nature of **2**, as suggested by IR data for the carbonyl adduct **4a**, is reflected in the reactivity patterns observed. The reactions of **1a** with C_2H_4 and 2-butyne (equation 11) are analogous to the reported reactions of $[Cp_2Ti(\eta^2\text{-}C(O)=CH_2]_2$, $Cp^*_2Zr(Pyr)(\eta^2\text{-}(CO)=CH_2)$[18] and $[Cp_2Zr(\eta^2\text{-}C(O)Ph_2)]_2$[19] with olefins and acetylenes, and complement the reaction of $Cp^*_2Ti(C_2H_4)$ with acetaldehyde:[20,21] in each case, facile oxidative coupling is observed to form stable, M(IV) oxymetallacyclopentane complexes (Scheme II).

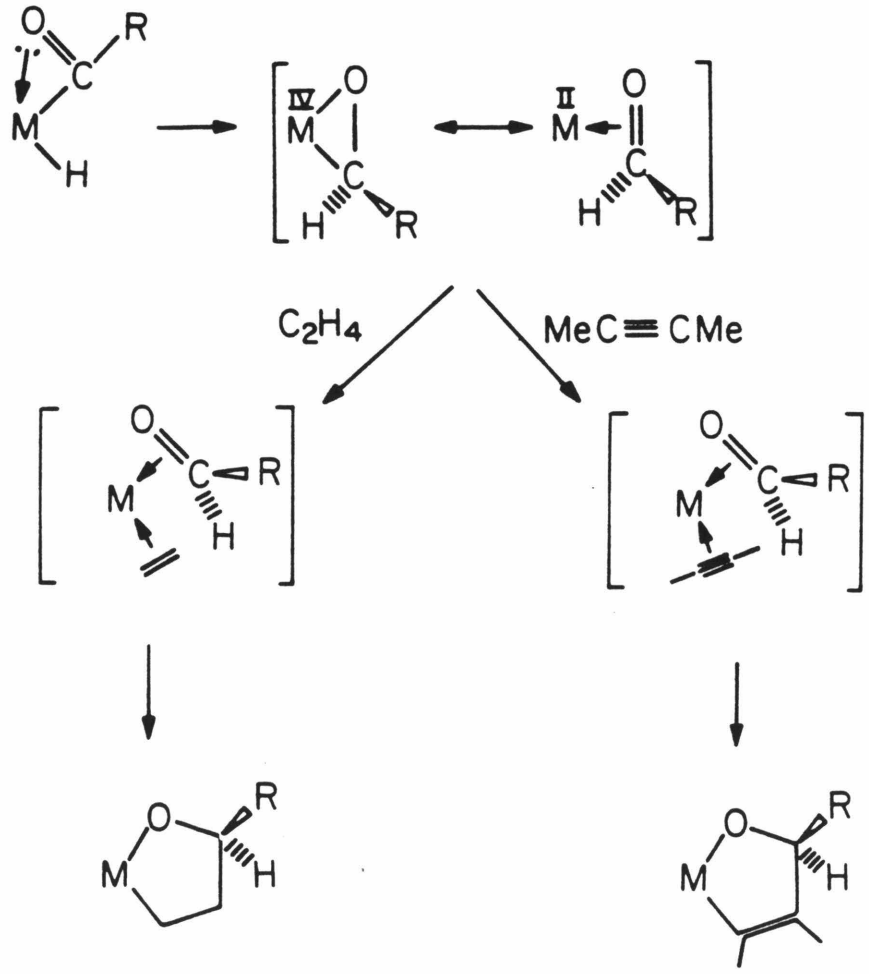

Scheme II

Similarly, the reactions of **1a** with H_2 and $HC{\equiv}C^tBu$ are best viewed as simple oxidative addition reactions, with subsequent hydride transfer to the electrophillic carbonyl center giving the observed alkoxy products (Scheme III).

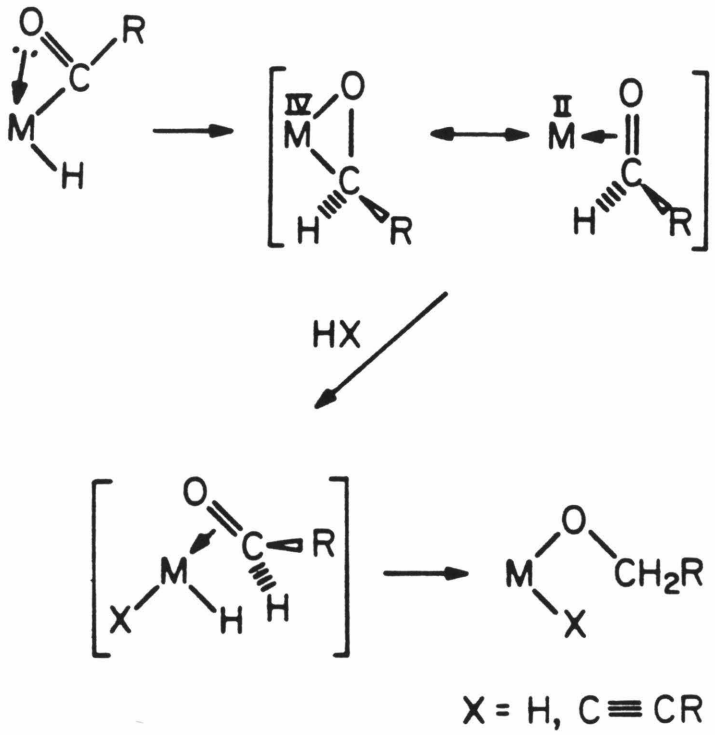

Scheme III

The observed coupling of carbonyl and aldehyde ligands in **4b** to give the enediolate complex 5 (equation 8) is unusual. A reasonable mechanism to account for this transformation is given in Scheme IV.[22] Here, CO inserts into the reactive Hf-C(aldehyde) bond to form an oxyacyl-metallacyclobutane complex **20**, which then undergoes a formal 1,2 hydrogen shift to the carbenoid-like[23] acyl

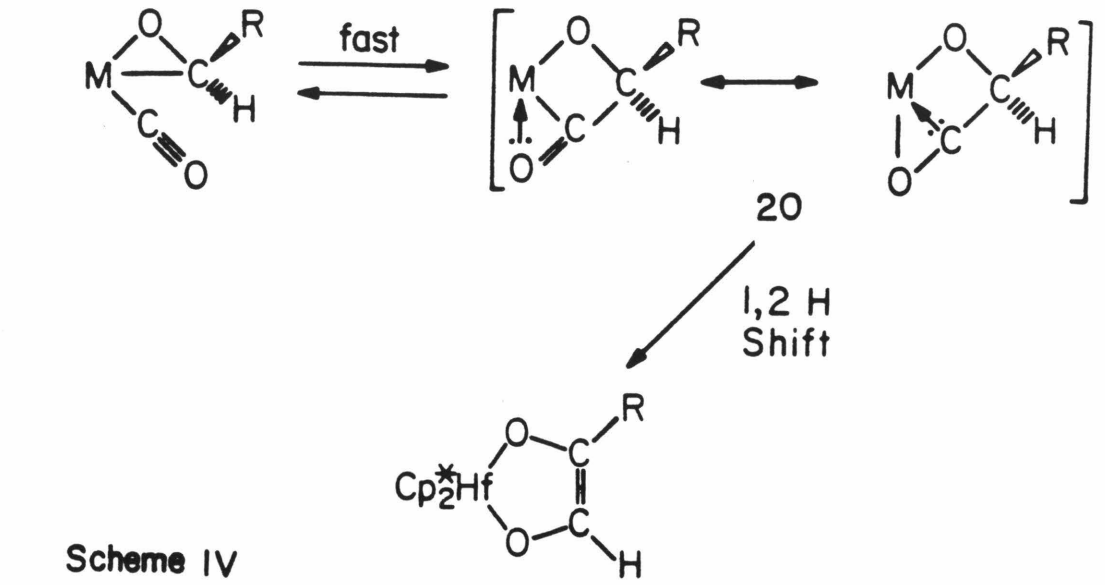

Scheme IV

carbon leading to the observed product. Though unprecedented, an intermediate analogous to 20 has been proposed by Schrock[24] in the carbonylation of $Cp^*TaMe_2(\eta^2\text{-}C(O)Me_2)$ (equation 18).

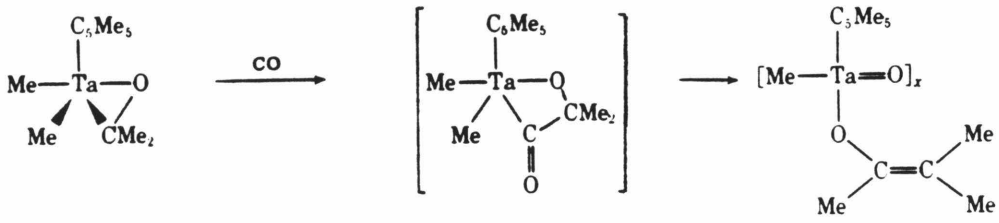

(18)

1,2 hydrogen shift reactions analogous to that proposed in Scheme III have been observed for thorium[25] and zirconium[6c] acyl complexes. Indeed, the thermal rearrangement of acyl

metallacycle **18** (equation 16), which models the proposed intermediate **20**, exhibits a substantial kinetic isotope effect (3.6) consistent with a rate-limiting 1,2 H shift. This observation, together with the observed similar rates of thermolysis of **4b** and **18**, suggests that the rate limiting 1,2 H shift step in Scheme IV is reasonable.

The reaction of **4b** with CO at low temperatures lends further indirect support for the mechanism in Scheme IV. Although the exact nature of the product formed is not known, ^{13}C NMR labeling experiments indicate that incorporation of CO at low temperature to form **6** occurs without dissociation of the carbonyl ligand or isoveraldehyde from **4b**. Since **4b** is coordinatively saturated, insertion to form 16 electron **20** in a facile, reversible equilibrium remains the most likely initial step in this reaction as well as reaction 8 (Scheme V).

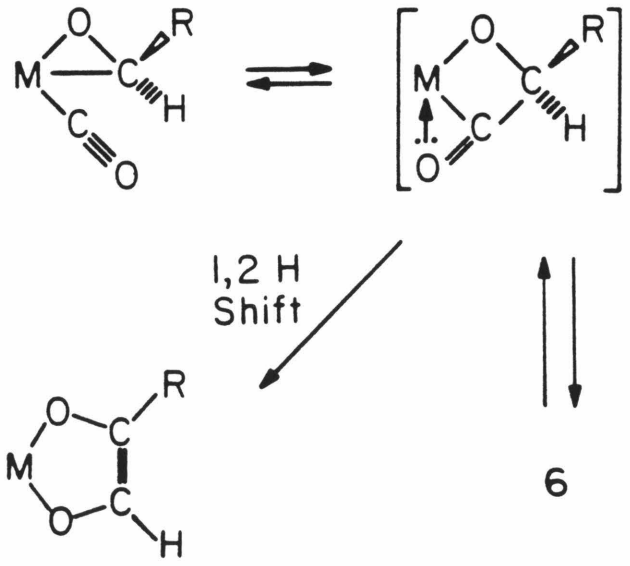

Scheme V

The convenient <u>in situ</u> generation of highly reactive transition metal-aldehyde complexes following Schemes I and II represents a potentially useful synthetic process. Consequently, the extension and generalization of this chemistry to other CO-derived oxygenate complexes was of interest.

The failure to observe a cyclopentanone adduct in the reaction of $Cp^*_2\overline{Hf(CH_2CH_2CH_2CH_2)}$ (9) with excess CO, though disappointing, is not surprising. Consideration of the steric requirements for binding ketone to a Cp^*_2M moiety to form a α,α-disubstituted oxymetallacyclopropane complex suggests that such a complex would be highly destabilized relative to aldehyde complexes such as **4** and **7**. The reactivity observed for **9** parallels that reported for $Cp^*_2ZrMe_2$[4b] and titanacyclobutane[18] complexes (equations 3 and 19).

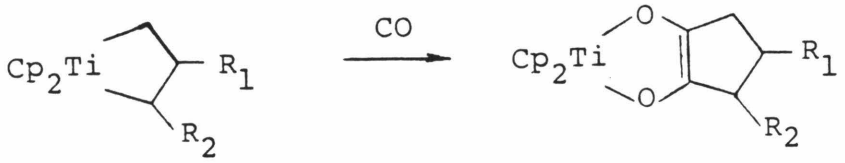

(19)

Although product formation in reaction 3 has been rationalized in terms of an intramolecular coupling of a bis-oxycarbene complex (equation 20), the results

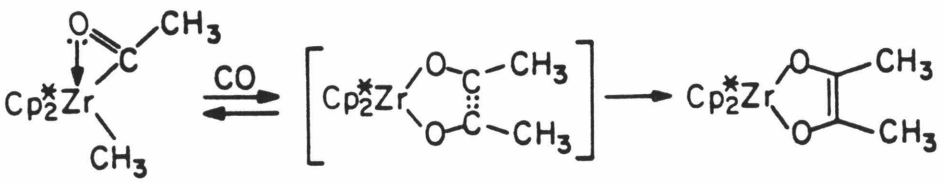

(20)

presented in this chapter suggest an alternative pathway available for these coupling reactions (Scheme VI) similar to that proposed in Scheme IV.

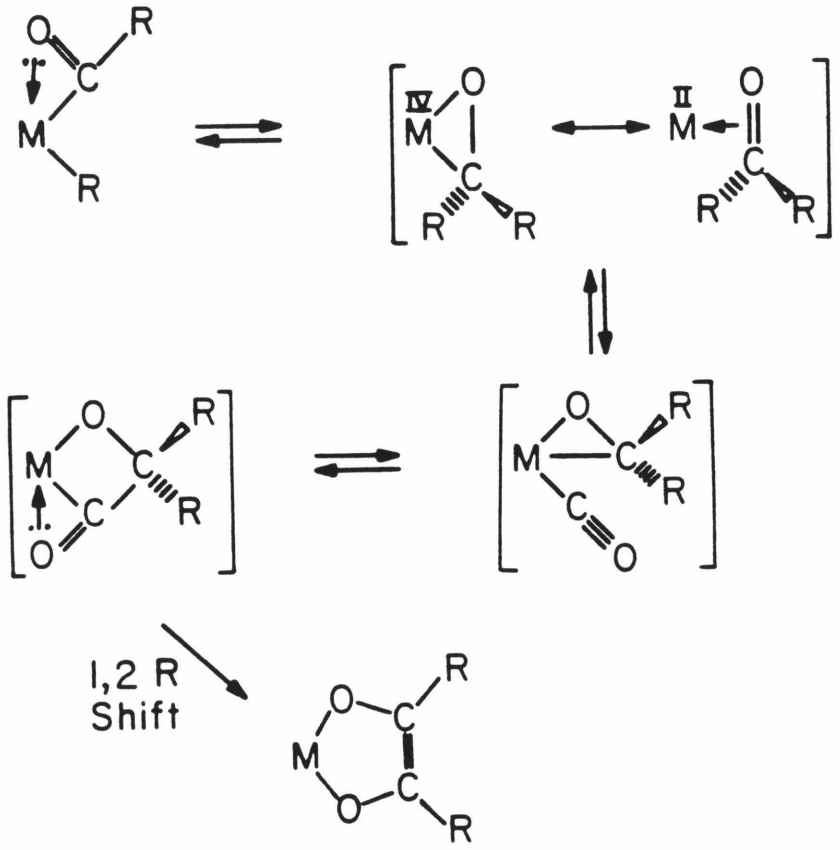

Scheme VI

The final step in the above mechanism entails a 1,2 alkyl shift to an acyl carbon center. Although alkyl migrations to early metal acyls have not been reported, the considerable steric strain present in β,β-disubstituted metallacyclobutane intermediate 21[26] may serve to induce greater acyl carbenoid character, resulting in a more facile 1,2 migration:

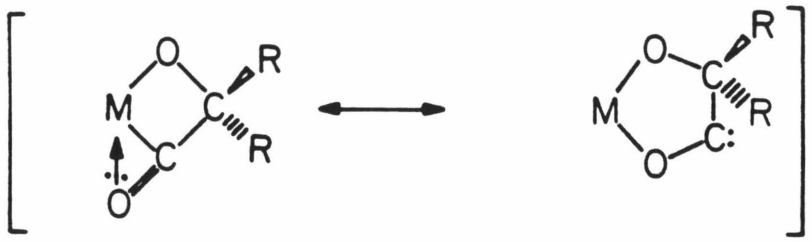

The thermolysis of the vinylacyl hydride **16** in the presence of excess CO similarly failed to generate an aldehyde carbonyl complex analogous to **4**. However, the metallacycle product obtained in this reaction may be rationalized in terms of an intramolecular olefin trapping of an intermediate aldehyde complex **22**, as outlined in Scheme VII.

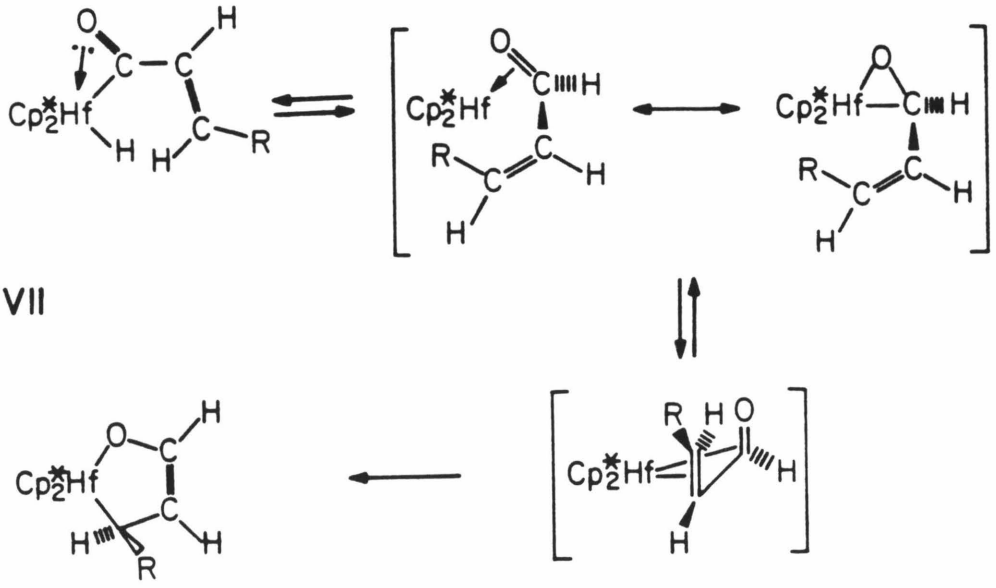

Scheme VII

Coordination of the vinylic group in α,β-unsaturated aldehyde complex **22** to form a η^4-heterobutadiene species **23**,[27] followed by rearrangement to the observed product metallacycle **17** is anticipated to be facile in light of the highly fluxional behavior exhibited by analogous hafnium butadiene complexes.[28]

TABLE I. NMR[a] DATA

Compound	Assignment		Chemical Shift	Coupling
$Cp^*_2ZrH(\eta^2\text{-}C(O)CH_2CHMe_2)$ (1a)	$C_5(C\underline{H}_3)_5$	^1H NMR, -70°C	1.70 s	
	$C(O)CH_2CH\underline{Me}_2$		1.05 d	J = 5.4
	$C(O)C\underline{H}_2CHMe_2$		2.37 d, br	
	$Zr\underline{H}$		3.53 s, br	
$Cp^*_2HfH(\eta^2\text{-}C(O)CH_2CHMe_2)$ (1b)	$C_5(C\underline{H}_3)_5$	^1H NMR, -10°C	1.78 s	
	$C(O)CH_2CH\underline{Me}_2$		1.12 d	J = 6.0
	$C(O)C\underline{H}_2CHMe_2$		2.50 d, br	
	$Hf\underline{H}$		7.03 s	
$Cp^*_2Zr(CO)(\eta^2\text{-}OCHCH_2CHMe_2)$ (4a)	$C_5(C\underline{H}_3)_5$	^1H NMR	1.70, 1.75 s	
	$O{=}CHCH_2CH\underline{Me}_2$		1.23, 1.27 d	J = 6.0
	$O{=}C\underline{H}CH_2CHMe_2$		2.47 d, br	J = 9.5
$Cp^*_2Hf(CO)(\eta^2\text{-}OCHCH_2CHMe_2)$ (4b)	$C_5(C\underline{H}_3)_5$	^1H NMR	1.67, 1.71 s	
	$O{=}CHCH_2CH\underline{Me}_2$		1.18, 1.20 d	J = 6.0
	$O{=}C\underline{H}CH_2CHMe_2$		2.21 d, br	J = 10.0
$Cp^*_2Hf(^{13}CO)(\eta^2\text{-}O^{13}CHCHMe_2)$	$O{=}^{13}\underline{C}HCH_2CHMe_2$	^{13}C NMR	84.22 ddd	$^1J_{CH}$=156.2, $^2J_{CC}$=9.8, $^2J_{CH}$=8.0
	$Hf(^{13}\underline{C}O)$		252.49 d	$^2J_{CC}$ = 9.8

TABLE I (cont'd)

Compound	Assignment		Chemical Shift	Coupling
$Cp^*_2Hf\overline{OC(CH_2CHMe_2)=CHO}$ (5)	$C_5(\underline{CH}_3)_5$	^{1}H NMR	1.89 s	
	$CH_2CH\underline{Me}_2$		1.09 d	J = 6.0
	$OC(CH_2CHMe_2)=C\underline{H}O$		6.30 s	
$Cp^*_2Hf\overline{O^{13}C(CH_2CHMe_2)=^{13}CHO}$	$O^{13}C(CH_2CHMe_2)=^{13}C\underline{H}O$		6.30 dd	$^1J_{CH}$=177, $^2J_{CH}$=21.5
	$O^{13}\underline{C}(CH_2CHMe_2)=^{13}CHO$	^{13}C NMR	146.8 dd, br	$^1J_{CC}$=82.5, $^2J_{CH}$=21.5
	$O^{13}C(CH_2CHMe_2)=^{13}\underline{C}HO$		131.6 dd	$^1J_{CC}$=82.5, $^1J_{CH}$=177
(6)	$C_5(\underline{CH}_3)_5$	^{1}H NMR, -14°C	1.64, 1.68 s	
	$CH_2CH\underline{Me}_2$		0.87, 0.93 d	J = 4.9, 4.9
	$^{13}C\underline{H}O$		4.88 dd	J = 10.1, 2.7
	$^{13}\underline{C}HO$	^{13}C NMR, -30°C	94.4 dddd	J_{CC}=13.6,37.1, $^1J_{CH}$=136.7, $^3J_{CH}$=5.9
	$^{13}\underline{C}=O$		213.6 d	J_{CC}=37.1
	$^{13}\underline{C}=O$		310.6 d	J_{CC}=13.6
$Cp^*_2Hf(CO)(\eta^2\text{-}OCHPh)$ (7)	$C_5(\underline{CH}_3)_5$	^{1}H NMR	1.57, 1.72 s	
	$OCH\underline{Ph}$		7.02 m	
	$OCH\underline{Ph}$		7.33 m	
	$OCH\underline{Ph}$		7.62 m	
	$OC\underline{H}Ph$		3.36 s	

TABLE I (cont'd)

Compound	Assignment		Chemical Shift	Coupling
$Cp^*_2Hf\overline{OC(Ph)=CHO}$ (8)	$C_5(C\underline{H}_3)_5$	^{1}H NMR	1.87 s	
	$OC(\underline{Ph})=CHO$		6.7-7.77 m	
	$OC(Ph)=C\underline{H}O$		7.34 s	
$Cp^*_2Hf\overline{O^{13}C(Ph)=^{13}CHO}$	$O^{13}C(Ph)=^{13}C\underline{H}O$		7.34 dd	$^1J_{CH}$=176.3, $^2J_{CH}$=22.4
	$O^{13}\underline{C}(Ph)=^{13}CHO$	^{13}C NMR	146.42 dd	$^1J_{CC}$=83.5, $^2J_{CH}$=22.4
	$O^{13}C(Ph)=^{13}\underline{C}HO$		134.73 dd	$^1J_{CC}$=83.5, $^1J_{CH}$=176.3
$Cp^*_2Hf(\eta^2\text{-}OCCH_2CH_2CH_2CH_2)$ (10)	$C_5(C\underline{H}_3)_5$	^{1}H NMR, -50°C	1.71 s	
	$O=CCH_2CH_2CH_2C\underline{H}_2$		0.23 m	
	$O=CCH_2C\underline{H}_2C\underline{H}_2CH_2$		1.93 m	
	$O=C\underline{C}H_2CH_2CH_2CH_2$		2.55 m	
	$O=\underline{C}CH_2CH_2CH_2CH_2$	$^{13}C\{^1H\}$	344.0 s	
$Cp^*_2Hf\overline{OCCH_2CH_2CH_2CH_2CO}$ (11)	$C_5(C\underline{H}_3)_5$	^{1}H NMR	1.91 s	
	$OCCH_2C\underline{H}_2C\underline{H}_2CH_2CO$		1.66 m	
	$OC\underline{C}H_2CH_2CH_2CH_2CO$		2.29 m	
	$O\underline{C}CH_2CH_2CH_2C\underline{H}_2CO$	^{13}C NMR	139.82 s	
	$OC\underline{C}H_2CH_2CH_2C\underline{H}_2CO$		31.85 t	J = 125
	$OCCH_2C\underline{H}_2C\underline{H}_2CH_2CO$		24.32 t	J = 125

TABLE I (cont'd)

Compound	Assignment		Chemical Shift	Coupling
$Cp_2^*\overline{ZrOCH(CH_2CHMe_2)CHH'CHH'}$ (12)[b]	$C_5(C\underline{H}_3)_5$	^{1}H NMR	1.85, 1.90 s	
	$OC\underline{H}(CH_2CHMe_2)CHH'CHH'$		4.51 ddt	J = 10.9, 9.3, 3.3
(H' cis to methine H)	$OCH(CH_2C\underline{H}Me_2)CHH'CHH'$		1.004, 1.006 d	J = 6.7
	$OCH(CH_2CHMe_2)C\underline{H}H'CHH'$		2.65 dddd	J = 12.5, 7.4, 3.3, 1.8
	$OCH(CH_2CHMe_2)CH\underline{H}'CHH'$		2.52 dddd	J = 12.5, 12.5, 10.9, 6.4
	$OCH(CH_2CHMe_2)CHH'C\underline{H}H'$		1.51 ddd	J = 12.5, 12.5, 7.4
	$OCH(CH_2CHMe_2)CHH'CH\underline{H}'$		0.12 ddd	J = 12.5, 6.4, 1.8
	$O\underline{C}H(CH_2CHMe_2)CHH'CHH'$	^{13}C NMR	78.20 d	J = 139.1
	$OCH(\underline{C}H_2CHMe_2)\underline{C}HH'\underline{C}HH'$	$^{13}C\{^1H\}$	42.37, 49.98, 50.24	
	$OCH(CH_2\underline{C}HMe_2)CHH'CHH'$		22.88, 24.11, 25.80	
$Cp_2^*\overline{ZrOCH(CH_2CHMe_2)C(CH_3)=C(CH_3)}$ (13)	$C_5(C\underline{H}_3)_5$	^{1}H NMR	1.85, 1.87 s	
	$OC\underline{H}(CH_2CHMe_2)C(CH_3)=C(CH_3)$		4.77 d, br	J = 11.2
	$OCH(CH_2C\underline{H}Me_2)C(CH_3)=C(CH_3)$		1.04, 1.08 d	J = 6.6
	$OCH(CH_2CHMe_2)C(C\underline{H}_3)=C(CH_3)$		1.69 s, br	
	$OCH(CH_2CHMe_2)C(CH_3)=C(C\underline{H}_3)$		1.59 s	
	$O\underline{C}H(CH_2CHMe_2)C(CH_3)=C(CH_3)$	^{13}C NMR	82.3 d	J = 133
	$OCH(\underline{C}H_2CHMe_2)C(CH_3)=C(CH_3)$		46.6 t	J = 125
	$OCH(CH_2CHMe_2)\underline{C}(CH_3)=\underline{C}(CH_3)$		152.1, 184.5 s	
	$OCH(CH_2\underline{C}HMe_2)C(\underline{C}H_3)=C(\underline{C}H_3)$	$^{13}C\{^1H\}$	24.1, 21.2, 19.9, 15.5	

TABLE I (cont'd)

Compound	Assignment		Chemical Shift	Coupling
$Cp^*_2Zr(H)OCH_2CH_2CHMe_2$ (14)	$C_5(C\underline{H}_3)_5$	^1H NMR	1.95 s	
	$OC\underline{H}_2CH_2CHMe_2$		4.13 t	J = 8.0
	$OCH_2CH_2C\underline{H}Me_2$		0.90 t	J = 6.0
	$Zr\underline{H}$		5.69 s	
$Cp^*_2Zr(C{\equiv}C^tBu)OCH_2CH_2CHMe_2$ (15)	$C_5(C\underline{H}_3)_5$		2.00 s	
	$C{\equiv}C^t\underline{Bu}$		1.38 s	
	$OC\underline{H}_2CH_2CHMe_2$		4.17 t	J = 7.0
	$OCH_2CH_2C\underline{H}Me_2$		0.98 d	J = 6.0
$Cp^*_2Hf(H)(\eta^2\text{-}C(O)CH{=}CH^tBu$ (16)	$C_5(C\underline{H}_3)_5$	^1H NMR, -10°C	1.90 s	
	$C(O)C\underline{H}{=}CH^tBu$		7.68 d	J = 15.1
	$C(O)CH{=}C\underline{H}^tBu$		6.59 d	J = 15.1
	$C(O)CH{=}CH^t\underline{Bu}$		0.95 s	
	$Hf\underline{H}$		7.13 s, br	
	$\underline{C}(O)CH{=}CH^tBu$	^{13}C NMR, -10°C	320.34 s	
$Cp^*_2Hf(OCH{=}CHCH^tBu)$ (17)	$C_5(C\underline{H}_3)_5$	^1H NMR	1.86, 1.89 s	
	$OC\underline{H}{=}CHCH^tBu$		6.46 dd	J = 5.3, 3.0
	$OCH{=}C\underline{H}CH^tBu$		5.20 dd	J = 5.3, 6.0
	$OCH{=}CHC\underline{H}^tBu$		0.45 dd	J = 6.0, 3.0
	$OCH{=}CHCH^t\underline{Bu}$		1.30 s	
	$O\underline{C}H{=}CHCH^tBu$	^{13}C NMR	137.32 d	J = 175.2
	$OCH{=}\underline{C}HCH^tBu$		111.27 d	J = 159.3
	$OCH{=}CH\underline{C}H^tBu$		72.86 d	J = 124.5
$Cp^*_2\overline{Hf(OCH{=}CHCH(^tBu)CO)}$ (18)	$C_5(C\underline{H}_3)_5$	^1H NMR	1.81, 1.87 s	
	$OC\underline{H}{=}CHCH(^tBu)CO$		7.10 dd	J = 6.0, 3.0
	$OCH{=}C\underline{H}CH(^tBu)CO$		4.29 dd	J = 6.0, 3.0

TABLE I (cont'd)

Compound	Assignment		Chemical Shift	Coupling
	OCH=CHC<u>H</u>(^{t}Bu)CO		2.90 dd	J = 3.0, 3.0
	OCH=CHCH(^{t}<u>Bu</u>)CO		1.30 s	
	O<u>C</u>H=CHCH(^{t}Bu)CO	^{13}C NMR	148.49 d	J = 177
	OCH=<u>C</u>HCH(^{t}Bu)CO		103.64 d	J = 161
	OCH=CH<u>C</u>H(^{t}Bu)CO		72.92 d	J = 115
	OCH=CHCH(^{t}Bu)<u>C</u>O		307.25 s	
$Cp^*_2Hf(OCH=CHC(^tBu)=CHO$ (19)	$C_5(CH_3)_5$	^{1}H NMR	1.91 s	
	O<u>H</u>=CHC(^{t}Bu)=CHO		7.01 dd	J = 7.2, 0.8
	OCH=C<u>H</u>C(^{t}Bu)=CHO		4.33 dd	J = 7.2, 0.9
	OCH=CHC(^{t}Bu)=C<u>H</u>O		7.05 s, br	
	OCH=CHC(^{t}<u>Bu</u>)=CHO		1.23 s	
	O<u>C</u>H=CHC(^{t}Bu)=CHO			
	OCH=<u>C</u>HC(^{t}Bu)=CHO			
	OCH=CH<u>C</u>(^{t}Bu)=CHO			
	OCH=CHC(^{t}Bu)=<u>C</u>HO			

(a) ^{1}H (90 MHz) and ^{13}C (22.5 MHz) NMR spectra taken in benzene-<u>d</u>$_6$ at ambient temperature; low temperature NMR spectra obtained in toluene-<u>d</u>$_8$. Chemical shifts are reported in δ relative to internal TMS or residual protons or carbons in solvent. Coupling constants are reported in Hz. Long range ^{13}C-^{1}H coupling is reported only when a coupling constant could be determined.

(b) ^{1}H NMR spectrum obtained at 500 MHz.

EXPERIMENTAL SECTION

General Considerations. All manipulations were performed using either glove box or high vacuum line techniques. Solvents were purified by vacuum transfer first from $LiAlH_4$ and then from "titanocene".[29] Hexamethyldisiloxane, 2-butyne, and t-butylacetylene were stored under vacuum over activated 4 Å molecular sieves. Hydrogen was purified by passage over MnO on vermiculite[30] and activated 4 Å molecular sieves. Ethylene and carbon monoxide were used directly from the cylinder. Elemental analyses were determined by Alfred Bernhardt and Dornis & Kolbe Analytical Laboratories.

^1H NMR spectra were recorded using Varian EM-390, JEOL FX90Q, and Bruker 500 MHz spectrometers. ^{13}C NMR spectra were obtained using a JEOL FX90Q spectrometer. Infrared spectra were measured on a Beckman 4240 spectrometer as nujol mulls, unless otherwise noted, and are reported in cm^{-1}. Low temperature IR spectra for **6** were obtained using a low temperature IR cell designed by Hinsberg.[31]

Procedures. **$Cp^*_2Zr(\eta^2\text{-}OCHCH_2CHMe_2)$ (4a).** A solution of $Cp^*_2Zr(H)CH_2CHMe_2$ (0.55 g) in 10 ml toluene was cooled to -78^oC, 1 atm CO was admitted, and the solution was allowed to warm slowly to room temperature with vigorous stirring over the course of several hours. Volatiles were removed

in vacuo and the resultant orange oily solid was taken up in ca. 5 ml hexamethyldisiloxane. 80 mg of solid **4a** (85% pure, ^{1}H NMR) was collected, leaving an oily filtrate residue consisting largely (~70%) of unisolated **4a**. IR: 1940(st), 1160, 1027, 920, 845.

$Cp^*_2Hf(\eta^2\text{-}OCHCH_2CHMe_2)$ **(4b).** Moderately pure (80-90%, ^{1}H NMR) **4b** may be prepared following procedures described for **4a**. IR: 1930(st), 1150, 1030, 927, 842. Thermolysis of crude **4b** in benzene at 80°C for 1 hour yielded $Cp^*_2\overline{Hf(OC\text{-}(CH_2CHMe_2)=CHO)}$ **(5)**, isolable as a crude (80%, ^{1}H NMR) orange oil.

$Cp^*_2Hf(\eta^2\text{-}OCHPh)CO$ **(7).** A thick-walled glass reaction vessel with a teflon needle valve was charged with 0.50 g (0.95 mmol) $Cp^*_2Hf(H)Ph$, 10 ml toluene, and 6.25 mmol CO (ca. 3.5 atm) and was stirred for 24 hours at room temperature. Solvent and residual gas were removed, and the orange solid residue was taken up and recrystallized from petroleum ether to give 0.36 g (66%) of light orange **7**. IR: 1956(st), 1600, 1492, 1230, 1120, 1069, 1027, 750, 700. Anal. Calcd. for $C_{28}H_{36}HfO_2$: C, 57.68; H, 6.22; Hf, 30.61. Found: C, 57.76; H, 6.30; Hf, 30.68. Solution molecular weight (C_6H_6) Calcd.: 583; Found: 592.[32]

$Cp^*_2\overline{Hf(OC(Ph)=CHO)}$ **(8).** The procedure for **7** was followed except 0.33 g of $Cp^*_2Hf(H)Ph$, 10 ml toluene, and 6.7 mmol (ca. 3 atm) CO were stirred for 3 days at 80°C. Workup of

the highly soluble orange residue yielded only 67 mg of orange **8**. IR: 1600, 1580, 1563, 1480, 1320, 1295, 1120, 1070, 1046, 1025, 870, 757, 692, 680, 583, 475. Anal. Calcd. for $C_{28}H_{36}HfO_2$: C, 57.68; H, 6.22; Hf, 30.61. Found: C, 57.64; H, 6.16; Hf, 30.70.

$Cp^*_2Hf(OC(CH_2CH_2CH_2CH_2)CO)$ (11). A solution of $Cp^*_2Hf(CH_2CH_2CH_2CH_2CH_2)$ in 10 ml toluene was cooled to -78°C and stirred under 1 atm CO for 2 hours, generating an orange solution of the acyl metallacycle **10**. The solution was allowed to warm slowly to room temperature and the volatiles were removed *in vacuo*. 5 ml of petroleum was distilled and the solution was cooled to -78°C, precipitating orange crystalline **11** (0.11 g, 40%). IR: 1640, 1353, 1210, 1157, 1100, 1025, 900, 720. Anal. Calcd. for $C_{26}H_{38}HfO_2$: C, 55.66; H, 6.83; Hf, 31.81. Found: C, 55.38; H, 6.85; Hf, 31.69.

$Cp^*_2Zr(OCH(CH_2CHMe_2)CH_2CH_2)$ (12). A solution of 0.34 g (0.71 mmol) $Cp^*_2Zr(H)CH_2CHMe_2$ in 10 ml toluene was cooled to -78°C and stirred for one half hour to quantitatively form the acyl hydride **1a** (^{1}H NMR). Excess CO was removed *in vacuo* and ethylene (2.3 mmol) was admitted. The reaction was warmed slowly to room temperature, volatiles were removed, and *ca.* 7 ml petroleum ether was distilled onto the brown residue. Cooling to -78°C, filtering, and washing once with cold petroleum ether afforded 0.165 g

(46%) of white **12**. IR: 1363, 1090, 1078, 1010, 952, 846, 580. Anal. Calcd. for $C_{27}H_{44}OZr$: C, 68.15; H, 9.32; Zr, 19.17. Found: C, 68.11; H, 9.19; Zr, 19.36.

$Cp^*_2Zr(OCH(CH_2CHMe_2)C(CH_3)=C(CH_3))$ **(13).** A -78°C solution of **1a** derived from 0.30 g (0.60 mmol) $Cp^*_2Zr(H)CH_2CHMe_2$ was prepared following the procedure described for **12**. Removal of excess CO and slow warming in the presence of 2-butyne (7.1 mmol) yielded upon petroleum ether workup 0.20 g (57%) of **13**. IR: 1563, 1486, 1365, 1167, 1120, 1090, 1058, 1040, 990, 950, 840, 802. Anal. Calcd. for $C_{29}H_{46}OZr$: C, 69.40; H, 9.24; Zr, 18.17. Found: C, 69.16; H, 9.07; Zr, 18.45.

$Cp^*_2Zr(H)OCH_2CH_2CHMe_2$ **(14).** A solution of **1a** derived from 0.350 g (0.78 mmol) $Cp^*_2Zr(H)CH_2CHMe_2$ was treated with 1 atm H_2 at -42°C and warmed slowly to room temperature with vigorous stirring. Removal of solvents and subliming twice the oily residue (100°C, 10^{-4} torr) afforded 0.235 gm (63%) **14**. IR: 1565 (ν(Zr-H)), 1510, 1230, 1140, 1105, 1026, 986, 857, 765. Anal. Calcd for $C_{56}H_{42}OZr$: C, 66.75; H, 9.41. Found: C, 66.83; H, 9.73.

$Cp^*_2Zr(C{\equiv}C^tBu)OCH_2CH_2CHMe_2$ **(15).** A solution of **1a** prepared from 0.30 g (0.57 mmol) was treated with 7.1 mmol *t*-butylacetylene at -42°C and warmed slowly to room temperature. Removal of volatiles yielded a colorless oil, identified by

IR and ^{1}H NMR as >90% **15**. IR: 2090 (ν(C=C)), 1378, 1246, 1205, 1138, 1105, 1025, 984, 730.

$Cp^*_2\overline{Hf(OCH=CHCH(^tBu))}$ **(17).** A solution of 0.10 g (0.19 mmol) $Cp^*_2Hf(H)CH=CH^tBu$ in 10 ml toluene was stirred at -78°C for 1 hour under 1 atm CO to generate acyl hydride, **16**. Excess CO was removed *in vacuo*, and the bright yellow solution was allowed to warm slowly to room temperature. The solvent was removed, leaving a thermally unstable orange oil identified by ^{1}H NMR at >90% metallacycle **17**. IR: 1545 (ν(C=C)), 1358, 1236, 1159, 1098, 1041, 1023, 870, 800.

$Cp^*_2\overline{Hf(OCH=CHCH(^tBu)CO}$ **(18).** A solution of 0.21 g (0.40 mmol) $Cp^*_2Hf(H)CH=CH^tBu$ in 5 ml petroleum ether was stirred for 1 hour under 1 atm CO at -78°C, then allowed to warm to room temperature. The solution slowly turned deep orange upon warming, precipitating bright orange crystals overnight. Cooling to -78°C and filtering yielded 0.95 g (40%) of acylmetallacycle **18**. IR: 1610 (ν(C-O)), 1590 (ν(C=C)), 1358, 1286, 1260, 1110, 1040, 1024, 968, 838, 752. Anal. Calcd. for $C_{28}H_{42}HfO_2$: C, 57.09; H, 7.19; Hf, 30.30. Found: C, 57.13; H, 7.16; Hf, 30.11.

$Cp^*_2\overline{Hf(OCH=CHC(^tBu)=CHO)}$ **(19).** A thick-walled glass reaction vessel with teflon needle valve was charged with 0.500 g (0.85 mmol) **18**, 10 ml toluene, and 700 torr CO and

heated to 80°C for 6 hours. Petroleum ether workup of the light brown solution yielded 0.300 g (60%) of off-white **19**. IR: (C_6D_6) 1590 (ν(C=C)), 1460, 1423, 1378, 1358, 1311, 1240(st), 1188(st), 1084, 1045, 1022, 883, 763, 587. Anal. Calcd. for $C_{28}H_{42}HfO_2$: C, 57.09; H, 7.19; Hf, 30.30. Found: C, 57.17; H, 7.30; Hf, 30.17.

Kinetic Measurements. The kinetics of thermal rearrangement of **18** to **19** were followed by ^1H NMR spectroscopy, monitoring the ratio of the t-butyl resonances. All of the kinetic runs obeyed first-order kinetics for > 2.5 half lives (see Figure 1). Sealed NMR tubes were thermalized at 80°C(±1), and spectra were taken every 15 minutes. Two runs on **18**-d_o ([**18**-d_o] = 0.18, 0.36M in C_6D_6) yielded rate constants of 1.51 and 1.50×10^{-4} sec^{-1}, and one run on **18**-d_2 gave 0.41×10^{-4} sec^{-1} (k_H/k_D = 3.6).

REFERENCES

(1) (a) Parshall, G. "Homogeneous Catalysis", Wiley-Interscience, 1980. (b) Collman, J. P.; Hegedus, L. S. "Principles and Applications of Organotransition Metal Chemistry", University Science Books: Mill Valley, CA, 1980.

(2) Schwartz, J.; Labinger, J. A. Angew. Chem. Int. Ed. Engl. 1976, 15, 333.

(3) Pine, S. H.; Zahler, R.; Evans, D. A.; Grubbs, R. H. J. Am. Chem. Soc. 1980, 102, 3270.

(4) (a) Berry, D. H.; Bercaw, J. E.; Jircitano, A. J.; Mertes, K. B. J. Am. Chem. Soc. 1982, 104, 4712. (b) Manriquez, J. M.; McAlister, D. R.; Sanner, R. D.; Bercaw, J. E. J. Am. Chem. Soc. 1978, 100, 2716. (c) Wolczanski, P. T.; Bercaw, J. E. Acc. Chem. Res. 1980, 13, 121. (d) Barger, P. T.; Bercaw, J. E., submitted to J. Am. Chem. Soc.. (e) Roddick, D. M.; Fryzuk, M. D.; Seidler, P. F.; Hillhouse, G. L.; Bercaw, J. E., manuscript in preparation.

(5) Chapter 1, this thesis.

(6) (a) Erker, G.; Rosenfeldt, F. Angew. Chem. Int. Ed. Engl. 1978, 17. 605. (b) Ibid., J. Organomet. Chem. 1980, 188, C1. (c) Moore, E. J., Ph.D. Thesis, California Institute of Technology, 1984, Chapter 3.

(7) The structure of **4a,b** as drawn, in the sterically

preferred form with aldehyde carbon coordinated in the central equatorial position, cannot be differentiated from the alternative structure with the aldehyde oxygen occupying the central coordination site on the basis of spectroscopic data alone.

(8) Aldehyde proton chemical shifts typically range from 9.0 to 9.5 δ,[8a] while carbonyl carbon ^{13}C values fall between 190 and 210 ppm.[8b] (a) Dyer, J. R. "Application of Absorption Spectroscopy of Organic Compounds"; Prentice-Hall, Inc., Englewood Cliffs, N.J., 1965. (b) Silverstein, R. M.; Bassler, G. C.; Morrill, T. C. "Spectrometric Identification of Organic Compounds", 4th Ed.; Wiley, N.Y., 1981.

(9) Brunner, H.; Wachter, J.; Bernal, I.; Creswick, M. Angew. Chem. Int. Ed. Engl. 1979, 18, 861.

(10) Marsella, J. A.; Curtis, C. J.; Bercaw, J. E.; Caulton, K. G. J. Am. Chem. Soc. 1980, 102, 7244.

(11) Manriquez, J. M.; McAlister, D. R.; Sanner, R. D.; Bercaw, J. E. J. Am. Chem. Soc. 1976, 98, 6733.

(12) The absence of assignable ν(C-O) bands above 1200 cm^{-1} has been noted previously for late metal π-aldehyde and ketone complexes: Walther, V. D. Z. Anorg. Allg. Chem. 1977, 431, 17.
(b) Ittel, S. D. J. Organomet. Chem. 1977, 137, 223.

(13) Thermolysis of **4a** under 3 atm CO results in an approximately equimolar mixture of enolate hydride

3 and the zirconium analog to 5 (^{1}H NMR).

(14) Cohen, S. A., Ph.D. Thesis, California Institute of Technology, 1982.

(15) (a) Tsuji, J. "Organic Synthesis via Metal Carbonyls", Vol. II, Wender, I.; Pino, P., eds.; John Wiley & Sons, 1977, p. 595.
(b) Walborsky, H. M.; Allen, L. E. J. Am. Chem. Soc. 1971, 93, 5465.

(16) Milstein, D. Organometallics 1982, 1, 1549.

(17) Recently, the synthesis and structural characterization of binuclear bridging formaldehyde and aldehyde complexes of zirconium which exhibit similar chemical reactivity have been reported.
(a) Gambarotta, S.; Floriani, C.; Chiesi-Villa, A.; Guastini, C. J. Am. Chem. Soc. 1983, 105, 1690.
(b) Erker, G.; Kropp, K.; Kruger, C.; Chiang, A.-P. Chem. Ber. 1982, 115, 2447.

(18) Straus, D. A., Ph.D. Thesis, California Institute of Technology, 1983.

(19) Erker, G.; Rosenfeldt, F. J. Organomet. Chem. 1982, 224, 29.

(20) Cohen, S. A., manuscript in preparation.

(21) A related reaction involving ketone and aldehyde addition to (η^4-butadiene)zirconocene has recently been reported: Erker, G.; Engel, K.; Atwood, J. L.; Hunter, W. E. Angew. Chem. Int. Ed. Engl. 1983, 22, 494.

(22) An alternative mechanism involving hydride migration to the CO ligand followed by direct coupling, although less likely, cannot be ruled out.

(23) Oxycarbenoid character for η^2-acyl ligands in early transition metal and actinide complexes, as

C

suggested by resonance structure C, has been invoked to explain much of the CO reaction chemistry observed in these systems.[4b,25]

(24) Wood, C. D.; Schrock, R. R. J. Am. Chem. Soc. 1979, 101, 5421.

(25) Manriquez, J. M.; Fagan, P. J.; Marks, T. J.; Day, C. S.; Day, V. W. J. Am. Chem. Soc. 1978, 100, 7112.

(26) (a) Substantial steric destabilization of $Cp_2TiCH_2C(R)(R')CH_2$ complexes when R,R'=alkyl has been reported,[26b] and has been attributed to unfavorable ring-(β-substituent) interactions. Such interactions are anticipated to be even more unfavorable in permethyl-ring metallocene complexes, such as **20**. (b) Straus, D. A.; Grubbs, R. H. Organometallics 1982, 1, 1658.

(27) A number of transition metal complexes with η^4-(O=C(R)C=CR'R") functionality have been reported.

(a) Schrauzer, G. N. Chem. Ber. 1961, 94, 642. (b) Sacerdoti, M.; Bertolasi, V.; Gilli, G. Acta. Crystallogr. 1980, 36B, 1061. See also reference 12a.

(28) Yasuda, H.; Kajihara, Y.; Mashima, K.; Nagasuna, K.; Lee, K.; Nakamura, A. Organometallics 1982, 1, 388.

(29) Marvich, R. H.; Brintzinger, H. H. J. Am. Chem. Soc. 1971, 94, 2046.

(30) Brown, T. L.; Dickerhoof, D. W.; Bafus, D. A.; Morgan, G. L. Rev. Sci. Instrum. 1962, 33, 491.

(31) Hinsberg, W. D., Ph.D. Thesis, California Institute of Technology, 1980.

(32) Molecular weight determined by isothermal distillation using the Singer method. (a) Singer, R. Justus Liebigs Ann. Chem. 1930, 478, 246. (b) Clark, E. P. Ind. Eng. Chem., Anal. Ed. 1941, 13, 820.

Chapter IV

Synthesis and Reactivity of Mono-Permethylcyclopentadienyl Hafnium Phosphido Complexes. Structural Characterization of $[Cp^*HfMe(\mu\text{-}H)(\mu\text{-}P^tBu_2)]_2$ and $Cp^*HfCl_2(\eta^2\text{-}C(O)P^tBu_2)$

INTRODUCTION

The chemistry of titanium, zirconium, and hafnium complexes with hard donor ligand such as chloride, alkoxide, and dialkyamide has been studied extensively.[1] In contrast, the chemistry of group IV metals with soft dialkylphosphide donor ligands has not been well developed. In particular, until recently only three examples of Zr(IV) dialkylphosphide complexes,[2] and no examples of Hf(IV) dialkylphosphide complexes had been reported.

Phosphide ligands are currently of interest in the field of bimetallic and cluster chemistry[3] because of their pronounced ability to form stable binuclear bridges. This stability is derived in part from the flexible nature of the (μ_2-PR_2) linkages, which can accommodate a range of metal-metal bonding and nonbonding distances.[3a]

Although numerous examples of terminal dialkylamide complexes are known,[4] terminal phosphide complexes are quite rare.[5,6] Terminal phosphide ligands are of interest because of their ability to function as either 1e- or 3e- donor ligands,[6a] thus stabilizing coordinatively unsaturated complexes while at the same time providing a potential mechanism for generation of a vacant coordination site.

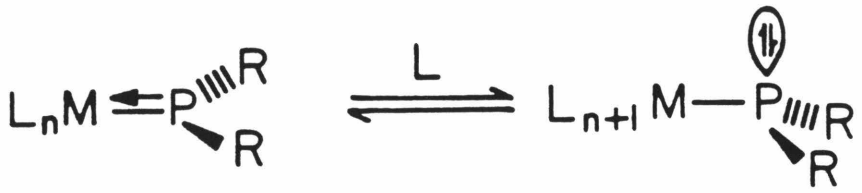

In light of these considerations, we became interested in exploring the chemistry of hafnium (IV) dialkylphosphide complexes. Prior to this work, efforts[7] in our laboratory to prepare reactive zirconium hydrides via hydrogenolysis of Cp^*ZrR_3 (R=alkyl, phenyl) in the presence of free phosphine were unsuccessful, giving instead insoluble, polymeric hydride-containing products. By incorporation of dialkylphosphide ligands, possessing intramolecular phosphine donor functionality, it was hoped that well defined, soluble hydride complexes could be obtained.

Accordingly, this chapter presents the synthesis of the mono and bis-phosphide complexes $Cp^*HfCl_2(P^tBu_2)$ (1) and $Cp^*HfCl(P^tBu_2)_2$ (2) as well as a number of mono-phosphide alkyl and aryl derivatives. Hydrocarbon derivatives of 1 have been prepared by either direct alkylation of 1, or metathesis of Cp*Hf alkyl or aryl chlorides with LiP^tBu_2. The choice of P^tBu_2 as ligand for the study of hafnium phosphide complexes was primarily for steric control.[8,3a] Specifically, it was hoped that

sufficient ligand bulk would favor terminal coordination, as well as stabilize desired hydrido complexes with respect to oligimerization. Hydrogenolysis of hafnium phosphides proved to be a general reaction for cleavage of both Hf-C and Hf-P bonds, yielding insoluble hydridophosphide dimers or, in the case of 1, products derived from initially formed Cp^*HfCl_2H. The product from the reaction of $Cp^*HfMe_2(P^tBu_2)$ (6) and H_2, $[Cp^*Hf(CH_3)(\mu\text{-}H)(\mu\text{-}P^tBu_2)]_2$ (8), has been structurally characterized. Additionally, $Cp^*HfCl_2(P^tBu_2)$ is found to react readily with CO to give the novel, structurally characterized insertion product $Cp^*HfCl_2(\eta^2\text{-}C(O)P^tBu_2)$ (13).

RESULTS AND DISCUSSION

(1) Synthesis of $Cp^*HfCl_2(P^tBu_2)$ (1) and $Cp^*HfCl(P^tBu_2)_2$ (2).

Treatment of Cp^*HfCl_3 with one equivalent LiP^tBu_2 or excess LiP^tBu_2 in diethyl ether afforded deeply-colored phosphide complexes $Cp^*HfCl_2(P^tBu_2)$ (1) and $Cp^*HfCl(P^tBu_2)_2$ (2) respectively, in good yield. Both 1 and 2 are highly moisture sensitive, and lose HP^tBu_2 rapidly upon exposure to air. Solution molecular weight (C_6H_6, calc: 529;

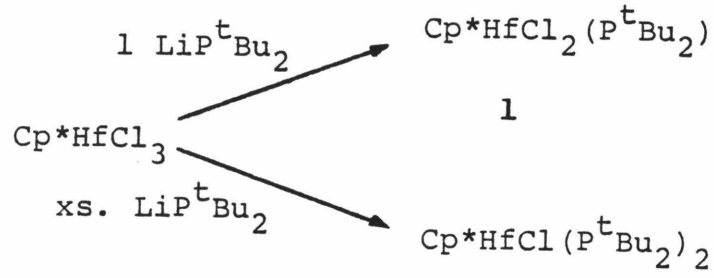

(1)

found: 512) as well as ^1H and ^{31}P NMR (see Table I) and analytical data support the formulation of 1 as a monomeric, terminal phosphide complex of the indicated stoichiometry. The $^{31}P\{^1H\}$ NMR spectra of 1 and 2 exhibit single low field resonances at 209.9 and 261.3 ppm, respectively. Although comparative structural and spectroscopic data are limited, these ^{31}P values fall within the range reported for trigonal planar terminal phosphide complexes (170-320 ppm),[6] and appear indicative

of a π-donor, 3-electron coordination mode for the phosphide ligands of 1 and 2. Both 1 and 2 exhibit magnetically equivalent t-butyl groups in the ^{1}H NMR (1: 18H, δ 1.45.; $^{3}J_{PH}$ = 12.2 Hz. 2: 36H, δ 1.59.; $^{3}J_{PH}$ = 12.6 Hz). The equivalence of t-butyl groups in 1 is consistent with a static structure A, where the t-butyl

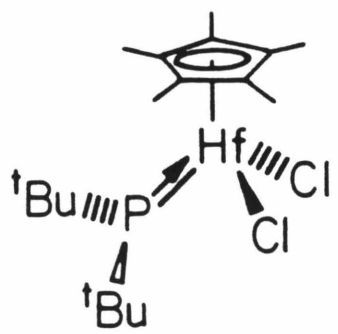

A

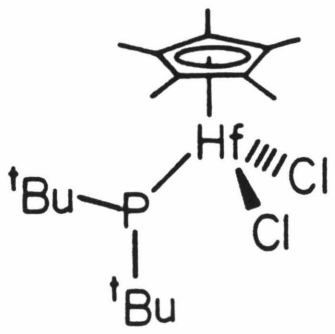

B

groups are related by a mirror plane; however, the observation of a single resonance for the diastereotopic t-butyl groups in 2 and in alkyl derivatives of 1 (Table I) requires equilibration via a fluxional process, and suggests that rotation about the Hf-P bond in these complexes is rapid on the NMR timescale. Only slight broadening of the t-butyl resonances for 1 and 2 was observed down to -94°C, placing an upper limit of ~ 10 kcal on $\Delta G^{\ddagger}$ for site exchange.[9]

(2) Synthesis of $Cp^*HfRR'(P^tBu_2)$ Complexes (R,R'=Cl, alkyl or aryl).

Preparative routes to a number of alkyl and aryl derivatives of **1** and **2** have been examined. Attempts to prepare methyl and phenyl derivatives of **1** by direct methathesis of $Cp^*HfCl_2(P^tBu_2)$ with MeLi, MeMgBr, or PhLi at -78°C were not successful. However, reaction of **1** with one equivalent $LiCH_2CMe_3$ in toluene or KCH_2Ph in ether yielded >90% pure (^1H NMR) $Cp^*HfCl(CH_2CMe_3)(P^tBu_2)$ (**3**) and analytically pure $Cp^*HfCl(CH_2Ph)(P^tBu_2)$ (**4**) as highly colored, crystalline solids (equation 2). The phosphides $Cp^*HfMe_2(P^tBu_2)$ (**5**) and $Cp^*HfCl(Ph)(P^tBu_2)$ (**6**) may be

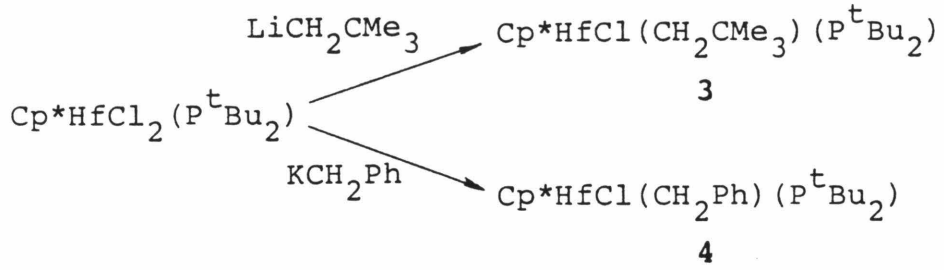

(2)

readily obtained from the reaction of the corresponding chlorides Cp^*HfMe_2Cl and $Cp^*HfPhCl_2$, prepared by metathesis of Cp^*HfCl_3 with MeMgBr or PhLi (see experimental section), with one equivalent LiP^tBu_2 in diethyl ether (equations 3 and 4).

$$Cp^*HfMe_2Cl \xrightarrow{LiP^tBu_2} Cp^*HfMe_2(P^tBu_2) \quad (3)$$

5

$$Cp^*HfPhCl \xrightarrow{LiP^tBu_2} Cp^*HfCl(Ph)(P^tBu_2) \quad (4)$$

6

Efforts to prepare alkyl derivatives of the sterically crowded bis-phosphide 2 were unsuccessful. Neither treatment of 2 with MeLi or MeMgBr, nor reaction of $Cp^*HfMeCl_2$ with excess LiP^tBu_2 yielded any identifiable products.

All of the phosphide derivatives prepared are thermally stable and, like the parent dichloride 1, are quite soluble in aromatic, ethereal, and hydrocarbon solvents. Phosphide $^{31}P\{^1H\}$ NMR resonances for 3-6 (220-225) ppm are comparable to that observed for 1, indicating similar terminal π-donor phosphide coordination.

(3) Reaction of $Cp^*_2HfMe_2(P^tBu_2)$ (5) with Hydrogen

A reaction which has been used with some success for preparation of various cyclopentadienyl hydrides of Zr[7,10] and Hf[10,11] is the hydrogenolysis of the corresponding methyl complex, as shown in equation 5. Therefore, in an

$$Cp'_2M(CH_3)_2 + 2H_2 \longrightarrow Cp'_2MH_2 + 2CH_4 \quad (5)$$

$Cp' = C_5H_nMe_{4-n}R$ (R = alkyl, H)

attempt to generate $Cp^*HfH_2(P^tBu_2)$, the reaction of dimethyl 5 with H_2 was examined. Treatment of benzene solutions of 5 with 2-3 atm H_2 at 25°C induced clean loss of methane (^1H NMR) over the course of several days to form an insoluble, crystalline yellow solid. Acidolysis of the isolated solid with HCl and Toepler analysis of the volatiles yielded 1.63 equivalents of a 1:1 mixture of H_2 and CH_4 which, together with elemental analysis, confirmed a product stoichiometry $Cp^*Hf(H)Me(P^tBu_2)$ (7). The

$$\underset{\mathbf{5}}{Cp^*HfMe_2(P^tBu_2)} \xrightarrow[-CH_4]{H_2} \underset{\mathbf{7}}{[Cp^*Hf(H)Me(P^tBu_2)]_2} \qquad (6)$$

formulation of 7 as a dimer has been verified by its crystal structure (<u>vide infra</u>). Mass spectroscopic analysis of the methane produced in the reaction of 5 with D_2 indicated >95% CH_3D, consistent with a 4-centered hydrogenolysis mechanism as shown in Scheme 1. Analogous

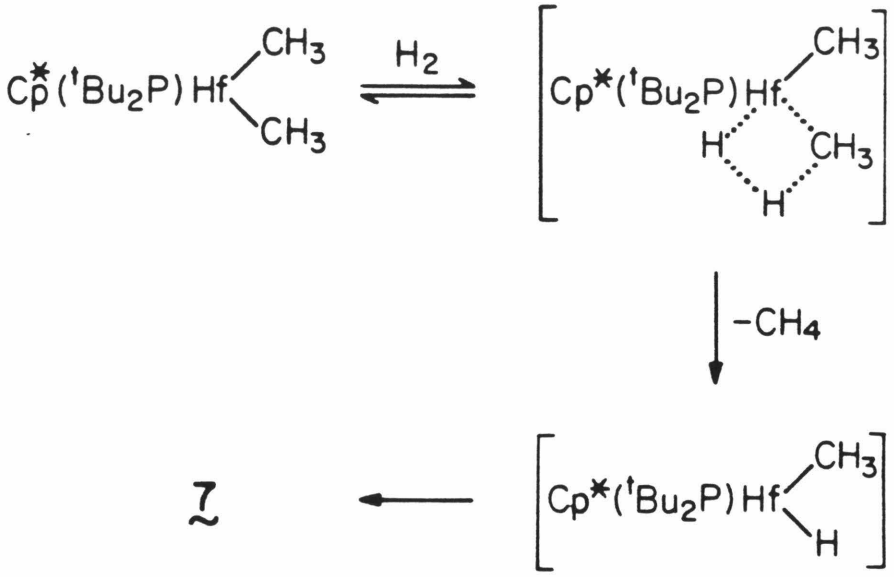

Scheme I

4-center mechanisms have been proposed by Schwartz for the H_2-promoted reductive elimination of alkane from $Cp_2Zr(H)CH_2CH(CH_2)_4CH_2$,[12] and by Andersen for the H-D exchange reactions of thorium and uranium trimethylsilyl complexes.[13]

The presence of hydride ligand in 7 has been confirmed by infrared spectroscopy (ν(Hf-H) = 1510, 760 cm^{-1}; ν(Hf-D) = 1090, 548 cm^{-1}). Comparison of these values with values reported for a number of zirconium and hafnium hydrides (Table II) suggests no clear assignment of hydride ligation mode. The high energy stretch is low for a terminal hydride mode,[14] while comparable values to the low energy 760 cm^{-1} stretch have only been reported for Cp_3MH complexes.[15] Though IR data are most consistent with a terminal hydride complex, the aggregate nature of 7, as indicated by its insolubility, is more suggestive of insoluble bridging hydride oligomers.

TABLE II. Infrared Data for Selected Zr and Hf Hydride Complexes.

Compound	ν(M-H_t) cm^{-1}	ν(M-H_b) cm^{-1}	Ref.
$[Cp^*HfH(CH_3)P^tBu_2]_2$ (7)	1510,760		
$[Cp^*HfH(Cl)P^tBu_2]_2$ (9)	1516,770		
Cp_3ZrH	1609, 752		15
Cp_3HfH	1670, 764		15
$[CpZrH_2]_x$	1520	1300 (br)	16
$[MeCpZrH_2]_2$	1565	1330 (br)	23
$[Cp_2Zr(H)Cl]_x$	1565	1390 (br)	16
$Cp^*_2ZrH_2$	1555	1390 (br)	17
$Cp^*_2HfH_2$	1590	1390 (br)	11
$[Cp^*Zr(BH_4)H(\mu\text{-}H)]_2$	1628	1350-1500 (br)	7
$[Cp^*HfClH_2]_2$	1575	1320 (br)	18
$Cp^*_2Hf(H)CH_2CHMe_2$	1636	1320 (br)	11
$Cp^*_2Hf(H)CH{=}CH(^tBu)$	1620	1320 (br)	11
cis-$[Cp^*_2HfH]_2(\mu\text{-}OCH{=}CHO)$	1655	1320 (br)	11

The structure of 7 is further complicated by the ambidentate nature of the phosphine ligands, which may readily adopt either terminal or bridging geometries. Taken together, at least three possible dimeric structures may be envisioned. In order to address these problems, as well as assess the relative bonding preferences of H and PR_2 (bridging vs. terminal), the structure of 7 has been determined by X-ray diffraction.

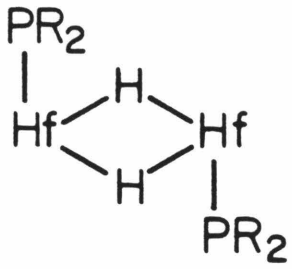

C

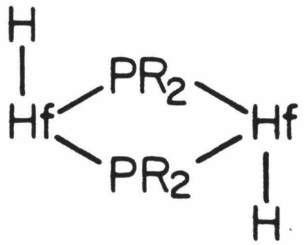

D

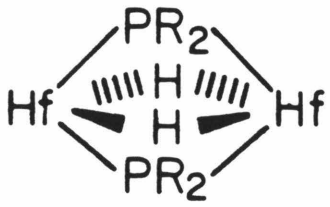

E

(4) Structural Determination of $[Cp^*HfMe(\mu\text{-}H)(\mu\text{-}P^tBu_2)]_2$ (7).

The molecular structure $[Cp^*HfMe(\mu\text{-}H)(\mu\text{-}P^tBu_2)]_2$ (7) is presented in Figure 1, a stereoview in Figure 2, and a skeletal view of the immediate ligation about hafnium with relevant bond distances and bond angles is given in Figure 3.

The molecular structure of 7 consists of two $(\eta^5\text{-}C_5Me_5)HfMe(H)(P^tBu_2)$ units bridged by two 3-center, 4 electron Hf-P-Hf' bonds (Hf-P = 2.805(2) Å, Hf-P' = 2.807(2) Å; P-Hf-P' = 109.2(1)°, Hf-P-Hf' = 70.8(1)°). The overall molecular symmetry of 7 is constrained by a crystallographic center of inversion located between the hafnium atoms, resulting in a trans orientation of methyl and ring groups. The Hf-C(ring) distances range from 2.537(9) to 2.589(9) Å, closely similar to the average values of 2.54, 2.55 Å in $Cp^*Hf(H)(\eta^3\text{-}CH_2CHCH_2)$[19] and somewhat longer than the average value of 2.47 Å for $Cp^*HfCl_2(\eta^2\text{-}C(O)P^tBu_2)$ (vide infra). The Hf-C(σ) bond length, 2.25(9) Å, is intermediate between the reported values of 2.23(1), 2.24(1) Å in Cp_2HfMe_2,[20] 2.30(1) Å in $[Cp_2HfMe]_2(\mu_2\text{-}O)$[21] and 2.33(1) Å in $(\eta^5\text{-}C_9H_7)_2HfMe_2$.[22]

The ligation mode of the hydride ligands in 7 is of primary interest. Although limitations of the data (see Experimental Section) prevented a precise determination of the hydride position, examination of difference Fourier maps of the plane perpendicular to the Hf_2P_2 plane revealed

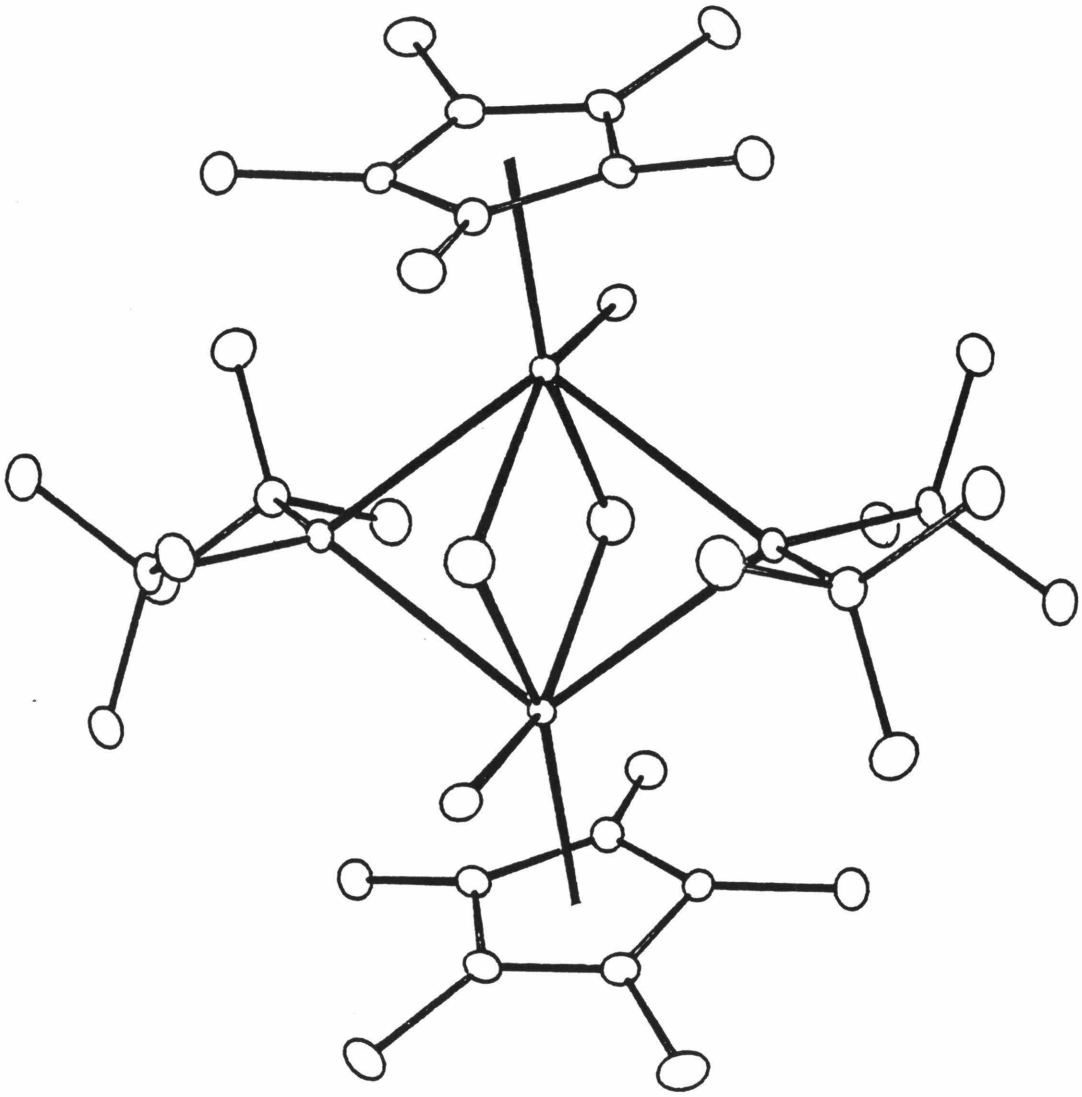

Figure 1. Structure of $[Cp^*HfMe(\mu\text{-}H)(\mu\text{-}P^tBu_2)]_2$ (7).

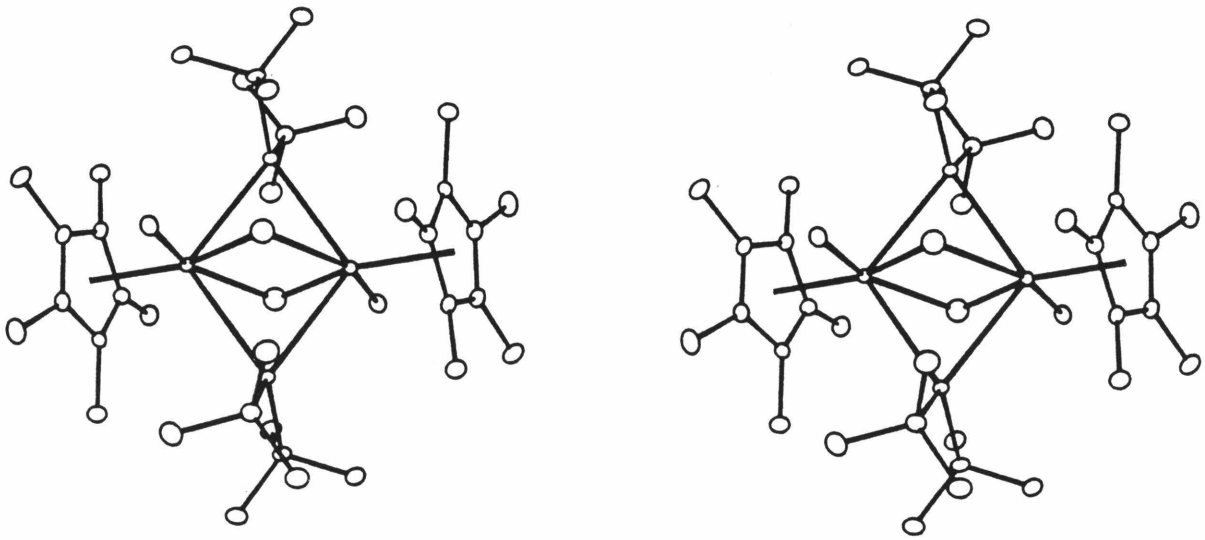

Figure 2. Stereo view of $[Cp^*HfMe(\mu\text{-}H)(\mu\text{-}P^tBu_2)]_2$ (7).

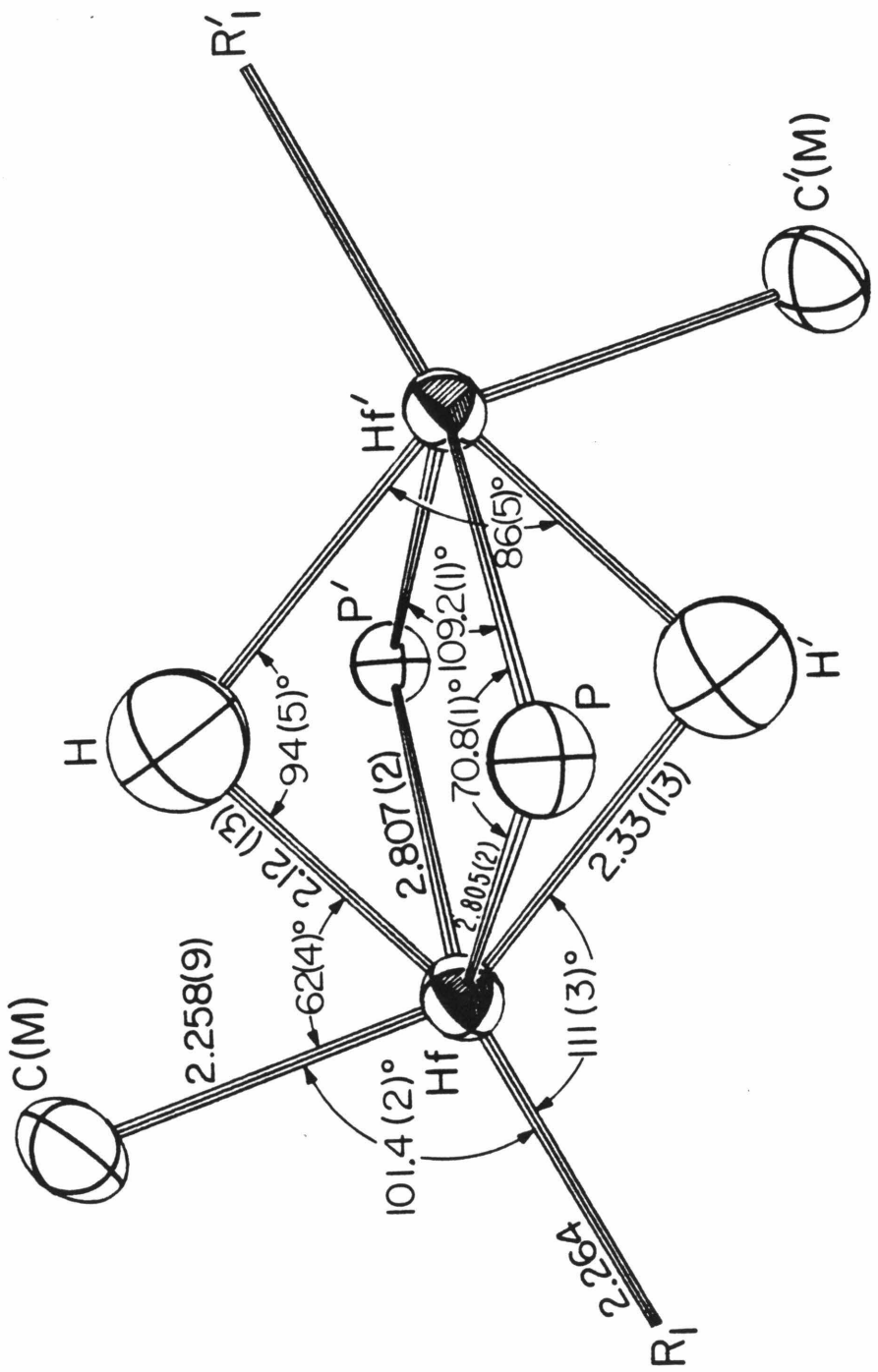

Figure 3. Skeletal view of $[Cp^*HfMe(\mu\text{-}H)(\mu\text{-}P^tBu_2)]_2$ (7), with selected bond distances (Å) and angles (°).

electron density attributable to a bridging hydride ligand; subsequent least-squares refinement of hydride coordinates gave values of Hf-H = 2.12(13) Å, Hf-H' = 2.33(13) Å, Hf-H-Hf' = 94(5)°, and H-Hf-H' = 86(5)°. The observed asymmetry of the Hf_2H_2 unit is consistent with structural data for the related complex $[(C_5H_4Me)_2ZrH_t(\mu\text{-}H_b)]_2$ ($Zr\text{-}H_t$ = 1.78(2) Å, $Zr\text{-}H_b$ = 1.94(2) Å, $Zr\text{-}H_b'$ = 2.05(3) Å).[23] The mean Hf-H bond length in 7 of 2.2 Å is somewhat greater than values for hafnium complexes $(C_5H_4Me)_2Hf(BH_4)_2$ (2.069(7), 2.120(8) Å)[24] and $Hf(BH_4)_4$ (2.06(2) Å),[25] and significantly longer than the terminal Hf-H bond length of 1.85(7) Å for $Cp^*_2Hf(H)(\eta^3\text{-}CH_2CHCH_2)$.[26,27]

The crystallographic data for 7 are in accord with the quadruply-bridged dimeric structure E. Additionally, it is evident from this structure that phosphide ligands do not provide a suitable ligand environment for stabilization of monomeric hafnium hydride complexes. In particular, comparison of Hf-P bond lengths (ave. 2.806 Å) in 7 to reported terminal π-donor Hf-P values for $Cp_2Hf(PEt_2)_2$ (2.488 Å)[6a] and $[Li(DME)][Hf(PCy_2)_5]$ (2.533, 2.475, 2.504 Å)[6b] indicates that considerable lengthening of the Hf-P bonds occur upon bridging.[29] As a result, no significant steric interactions between the bulky t-butyl phosphide groups and the permethyl rings of 7 are incurred,[30] and dimer formation is not prevented.

(5) Reactivity of $[Cp^*HfX(\mu\text{-}H)(\mu\text{-}P^tBu_2)]_2$ (X=CH_3,Cl).

The chemistry of $[Cp^*Hf(H)Me(P^tBu_2)]_2$ (7 is disappointing. Unlike oligomeric $(Cp_2ZrH_2)_x$ or $(Cp_2Zr(H)Cl)_x$, which are sparingly soluble yet reactive in refluxing benzene, 7 decomposes over the course of several hours at 80°C. At room temperature 7 is completely unreactive towards H_2, CO, or allene, and decomposes in the presence of excess reagent upon warming to 80°C. $[Cp^*HfMe(\mu\text{-}H)(\mu\text{-}P^tBu_2)]_2$ does, however, react slowly with excess ethylene at 25°C to cleanly give (^1H NMR) the ethylene-inserted product, $Cp^*HfMe(Et)(P^tBu_2)$ (8). Attempts to form

$$Cp^*HfMe(\mu\text{-}H)(\mu\text{-}P^tBu_2)]_2 \xrightarrow{C_2H_4} Cp^*HfMe(Et)(P^tBu_2) \quad (7)$$

7 8

soluble, more reactive derivatives of 7 by treatment of the formally 16 electron complex with donor ligands such as PMe_3 or NMe_3 were not successful. Another approach to the problem of enhancing hydride reactivity is to increase the thermal stability of 7 by replacing the potentially reactive CH_3 group with Cl. Treatment of benzene solutions of $Cp^*HfCl(CH_2Ph)(P^tBu_2)$ (4) or $Cp^*HfCl(CH_2CMe_3)(P^tBu_2)$ (3) with H_2 readily afforded insoluble yellow 9, formulated as the hydridochloride dimer $[Cp^*HfCl(\mu\text{-}H)(\mu\text{-}P^tBu_2)]_2$ by virtue of characteristic IR (ν(Hf-H) = 1516, 770 cm^{-1};

(Hf-D) = 1085, 540 cm^{-1}) and analytical data, and by analogy to 7. Unfortunately, 9 proved no more thermally

$$2Cp^*HfCl(R)(P^tBu_2) \longrightarrow [Cp^*HfCl(\mu\text{-}H)(\mu\text{-}P^tBu_2)]_2 \quad (8)$$

9

3, R = CH_2CMe_3

4, R = CH_2Ph

stable than 7 and even less reactive, failing to insert C_2H_4 after prolonged exposure at 25°C.

(6) Reaction of $Cp^*HfCl_2(P^tBu_2)$ and $Cp^*HfCl(P^tBu_2)_2$ (2) with H_2.

During the course of investigating the H_2 reactions of alkyl phosphide complexes, it was found that hafnium-phosphide bonds are also readily susceptible to hydrogenolysis. Reaction of $Cp^*HfCl(P^tBu_2)_2$ (2) with 2-3 atm H_2 is rapid, quantitatively yielding 9 plus one equivalent of free phosphine, HP^tBu_2. Qualitatively, for the series

$$\underset{\textbf{2}}{Cp^*HfCl(P^tBu_2)_2} \xrightarrow{H_2} \underset{\textbf{9}}{[Cp^*HfCl(\mu\text{-}H)(\mu\text{-}P^tBu_2)]_2} + \underset{HP^tBu_2}{} \quad (9)$$

$Cp^*HfCl(R)(P^tBu_2)$ (R = P^tBu_2 (2), CH_2CMe_3 (3), CH_2Ph (4)), the observed relative rate of hydrogenolysis[31] (equations 8 and 9) is 2 > 3 >> 4. Comparison of mean bond dissociation energies for the homleptic alkyls ZrR_4 (R = CH_2CMe_3, D =

54 kcal mol^{-1}; R = CH_2Ph, D = 60 kcal mol^{-1})[32] suggests that the ease of hydrogenolysis of **2**, **3** and **4** may be related to ligand bond strengths, with Hf-CH_2Ph > Hf-CH_2CMe_3 > Hf-P^tBu_2 (complex **2**) for this series.

The parent phosphide complex, $Cp^*HfCl_2(P^tBu_2)$ (**1**), reacts slowly under 3 atm H_2 over the course of several weeks to give disproportionation products Cp^*HfCl_3 and $(Cp^*HfH_2Cl)_x$,[33] plus ~40% decomposition (equation 10).

$$\underset{\mathbf{1}}{Cp^*HfCl_2(P^tBu_2)} \xrightarrow[-HP^tBu_2]{H_2} \underset{\mathbf{10}}{[Cp^*HfCl_2H]} \longrightarrow Cp^*HfCl_3 + (Cp^*HfH_2Cl)_x + \ldots \quad (10)$$

In the presence of one or more equivalents of PMe_3, the hydrogenolysis of **1** is complete within minutes at 25°C to give an uncharacterized mixture of products. The intermediacy of monohydride **10** in equation 10 has been confirmed by trapping with excess ethylene to cleanly give the inserted product, $Cp^*HfCl_2(Et)$. In the presence of excess PMe_3, the reaction of **1** with 3 atm H_2 and excess C_2H_4 is rapid, producing $Cp^*HfCl_2(Et)(PMe_3)$ (**11**) quantitatively, isolable in 71% yield as an off-white, analytically pure crystalline solid (equation 11).

$$\underset{\mathbf{1}}{Cp^*HfCl_2(P^tBu_2)} + C_2H_4 + PMe_3 \xrightarrow{H_2} \underset{\mathbf{11}}{Cp^*HfCl_2(Et)(PMe_3)} + HP^tBu_2 \quad (11)$$

Whereas the origin of the phosphine promoter effect in reactions of 1 with H_2 is not fully understood, it should be noted that no significant effect by added PMe_3 on the rate of hydrogenolysis of the alkyl ligand in $Cp^*HfMeCl_2$ is observed. In light of this, the phosphine effect on hydrogenolysis may be attributed to the loss of the π-donor interaction of the terminal phosphide with the metal center: coordination of phosphine to 1 in a rapid albeit unfavorable equilibrium[34] to form a relatively electron rich, 16 electron complex, may weaken the phosphide lone pair interaction with the hafnium, facilitating cleavage of the remaining sigma bond (Scheme 2). Moreover, localization of the lone pair on phosphorus

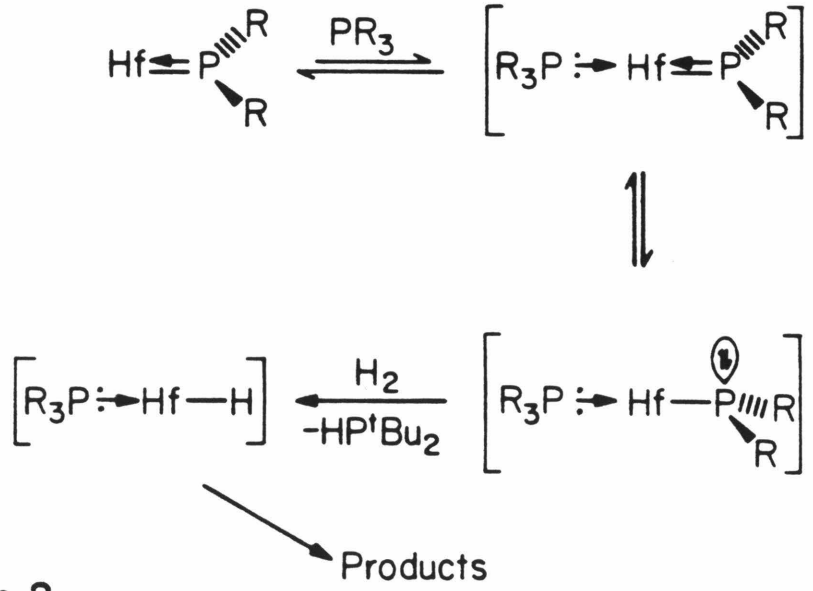

Scheme 2

would be expected to enhance the rate of a heterolytic, four-center mechanism involving a polar intermediate such as:

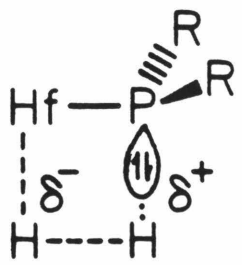

This rationalization is consistent with the observed rapid hydrogenolysis of the bis-phosphide, **2**, which is also formally a 16-electron complex.

(7) Synthesis and Structure of $Cp^*HfCl_2(\eta^2\text{-}C(O)P^tBu_2)$ (12).

The results of the preceding section have shown hafnium-phosphide bonds to be comparable in energy to hafnium-alkyl bonds. In light of the proclivity of group IV alkyl complexes toward CO insertion to give stable η^2-acyl products, it was anticipated that hafnium phosphide complexes should exhibit similar reactivity. Indeed, $Cp^*HfCl_2(P^tBu_2)$ (**1**) reacts with 2 atm CO at 25°C within minutes to give quantitatively (^1H NMR) the carboxyphosphide insertion product $Cp^*HfCl_2(\eta^2\text{-}C(O)P^tBu_2)$ (**12**) (equation 12).

$$Cp^*HfCl_2(P^tBu_2) \xrightarrow{CO} Cp^*HfCl_2(\eta^2\text{-}C(O)P^tBu_2) \qquad (12)$$

1 12

Carboxyphosphide **12**, isolated as a bright yellow analytically pure crystalline solid (73%), has been fully characterized spectroscopically.

The infrared spectrum of **12** exhibits a strong ν(CO) band at 1350 cm^{-1} which shifts to 1320 cm^{-1} upon isotopic substitution with ^{13}CO. This value is markedly lower than ν(CO) values reported for related transition metal and actinide η^2-acyl and η^2-carboxyamide complexes (see Table III), and is more comparable to values reported for exo and endo isomers of $Cp^*_2ZrH(\eta^2\text{-}C(O)CHPMe_3)$ (ν(C-O) = 1427, 1417 cm^{-1}, respectively)[41] in which significant multiple bonding between the C(acyl) and adjacent carbon atom is observed. The $^{13}C\{^1H\}$ spectrum of the labeled complex, $Cp^*HfCl_2(\eta^2\text{-}^{13}C(O)P^tBu_2)$, displays a doublet at 3.03 ppm ($^1J_{PC}$ = 101 Hz), attributable to the carbonyl carbon atom. This observed shift is at considerably higher field than characteristic lowfield, "carbene-like" acyl and carboxyamide values (Table III), and suggests a significant π-interaction of the carbonyl carbon atom with the phosphorus lone pair. Together, these data clearly indicate a substantial contribution of canonical form F to the overall valence bonding description.

TABLE III[a] IR and $^{13}C\{^{1}H\}$ NMR Data of M-(η^2-C(O)R) Complexes.

Compound	IR (cm^{-1})	Acyl ^{13}C Chemical Shift (ppm)	Ref.
$Cp^*_2ThCl(\eta^2\text{-}C(O)CH_2CMe_3)$	1469	360.2	35
c-$Cp_2ZrMe(\eta^2\text{-}C(O)Me)$	1545		36
l-$Cp_2Zr(P\text{-tolyl})(\eta^2\text{-}C(O)(P\text{-tolyl})$	1480	300	37
c-$Cp_2Zr(P\text{-tolyl})(\eta^2\text{-}C(O)(P\text{-tolyl})$	1505	301	37
$Cp_2ZrCl(\eta^2\text{-}C(O)CH_2CMe_3)$	1550	318.7	38
$Cp^*_2ThCl(\eta^2\text{-}C(O)NEt_2)$	1516	248.5	39
$Cp_3U(\eta^2\text{-}C(O)CHPMePh_2)$	1440		40
l-$Cp^*_2ZrH(\eta^2\text{-}C(O)CHPMe_3)$	1427	250.3	41
c-$Cp^*_2ZrH(\eta^2\text{-}C(O)CHPMe_3)$	1417	247.1	41
$Cp^*HfCl_2(\eta^2\text{-}C(O)P^tBu_2)$ (12)	1350	3.03	

[a] l refers to the isomeric form where the acyl oxygen occupies the lateral equatorial site. c refers to the centrally located acyl oxygen isomer.

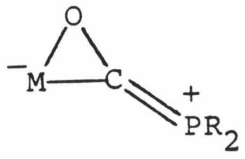

F

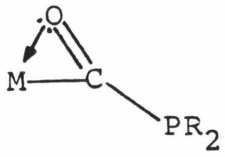

G

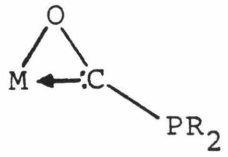

H

The room temperature 90 MHz ^{1}H NMR spectrum of **12** exhibits a single t-butyl methyl resonance at 1.31 ppm ($^{3}J_{PH}$ = 14.2 Hz), indicating that exchange of the inequivalent (vide infra) phosphide t-butyl groups and hence rotation about the C(acyl)-P bond is rapid on the NMR timescale. Upon cooling, the t-butyl doublet broadens and coalesces at -58°C. The slow exchange limit for **12** was not resolved at 90 MHz; however, 500 MHz ^{1}H NMR of **12** at -93°C displays a pair of doublets ($^{3}J_{PH}$ = 10.7, 12.3 Hz) for the inequivalent t-butyl groups with $\Delta\nu$ = 143 ± 2 Hz, corresponding to a frequency separation of 25.7 ± 0.4 Hz at 90 MHz observation frequency. From these values, $G^{=}$ (-58°C) for rotation about the C-P bond is calculated[42] to be 10.7 ± 0.1 kcal mol^{-1}. This observed rotational barrier is somewhat lower than barriers found for transition metal η^{1}-carboxyamides (14-24 kcal mol^{-1}),[43] and is far lower than the rotational barrier estimated for $Cp^{*}_{2}ThCl(\eta^{2}$-

$C(O)NMe_2$) (>23 kcal mol^{-1}).[39] These values reflect the extent of multiple C-E (E=N,P) bonding, and are consistent with trends observed for organic amides and acyl phosphines.[44]

(8) Crystal Structure of $Cp^*HfCl_2(\eta^2\text{-}C(O)P^tBu_2)$ (12).

Complex 12 represents the first example of a metal-ligated carboxyphosphide moiety. In order to substantiate the unusual coordination and ligand geometries suggested by the preceding spectrocopic data, the structure of 12 has been determined by X-ray diffraction. The molecular structure of $Cp^*HfCl_2(\eta^2\text{-}C(O)P^tBu_2)$ is presented in Figure 4, a stereo view in Figure 5, and a skeletal view of the immediate ligation about the hafnium and phosphorus atoms with relevant bond distances and angles is given in Figure 6.

The hafnium coordination geometry may be described as a distorted tetrahedron, if $\eta^5\text{-}C_5(CH_3)_5$ and $\eta^5\text{-}C(O)P^tBu_2$ ligands are considered to each occupy a single geometrical site. The four ring centroid-Hf-X (X = Cl, Y; where Y is defined as the midpoint of the C-O vector) angles vary from 109.7(1)° to 116.1(1)°, and the remaining three angles are Cl(1)-Hf-Cl(2) = 98.0(1)°, Cl(1)-Hf-Y = 101.1°, and Cl(2)-Hf-Y = 112.9°. The Hf-Cl bond lengths of 2.393(2) and 2.383(2) Å are somewhat shorter than Hf-Cl values reported for $(CH_2)_3(C_5H_4)_2HfCl_2$ (2.417)3), 2.429(2) Å[45] and $[(SiMe_3)_3N]_3HfCl$ (2.436(5) Å).[46] Further, Hf-C(ring)

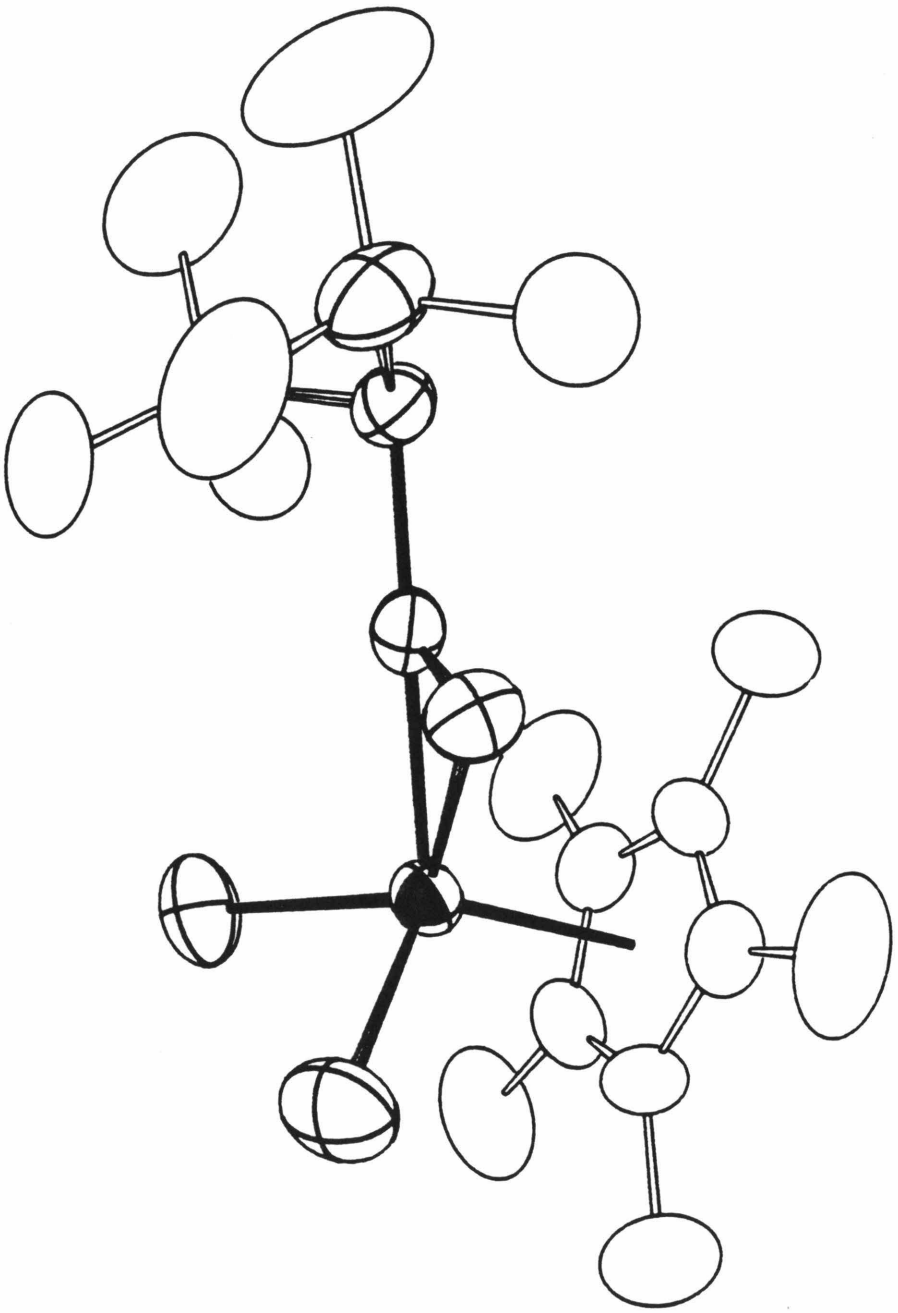

Figure 4. Structure of $Cp^*HfCl_2(\eta^2\text{-}C(O)P^tBu_2)$ (12).

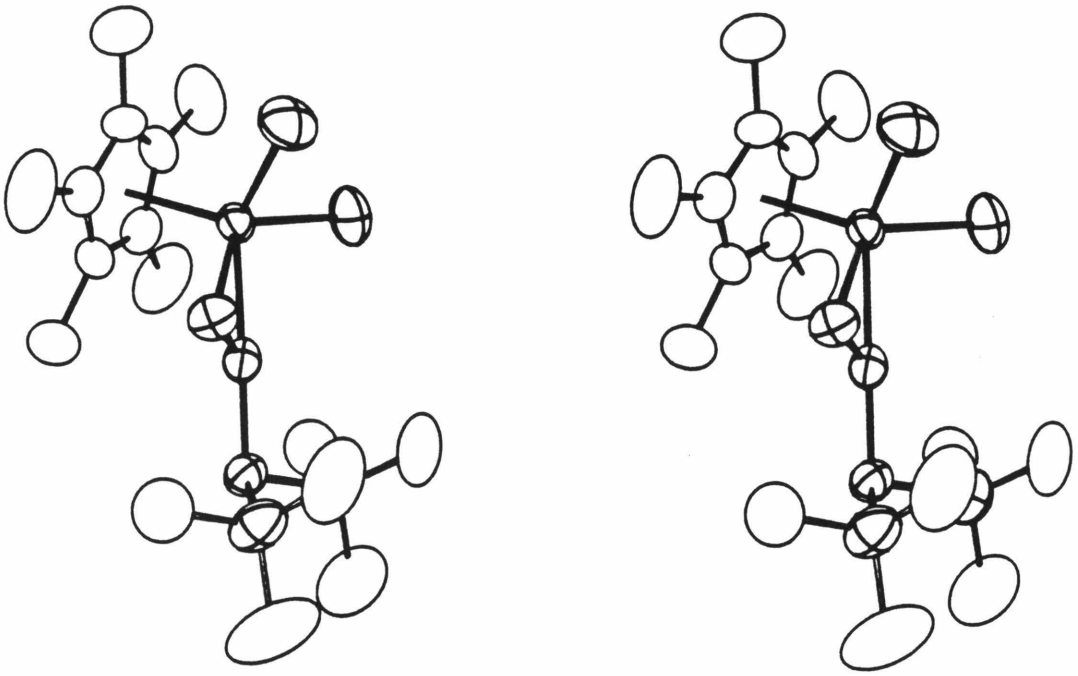

Figure 5. Stereo view of $Cp^*HfCl_2(\eta^2\text{-}C(O)P^tBu_2)$ (12).

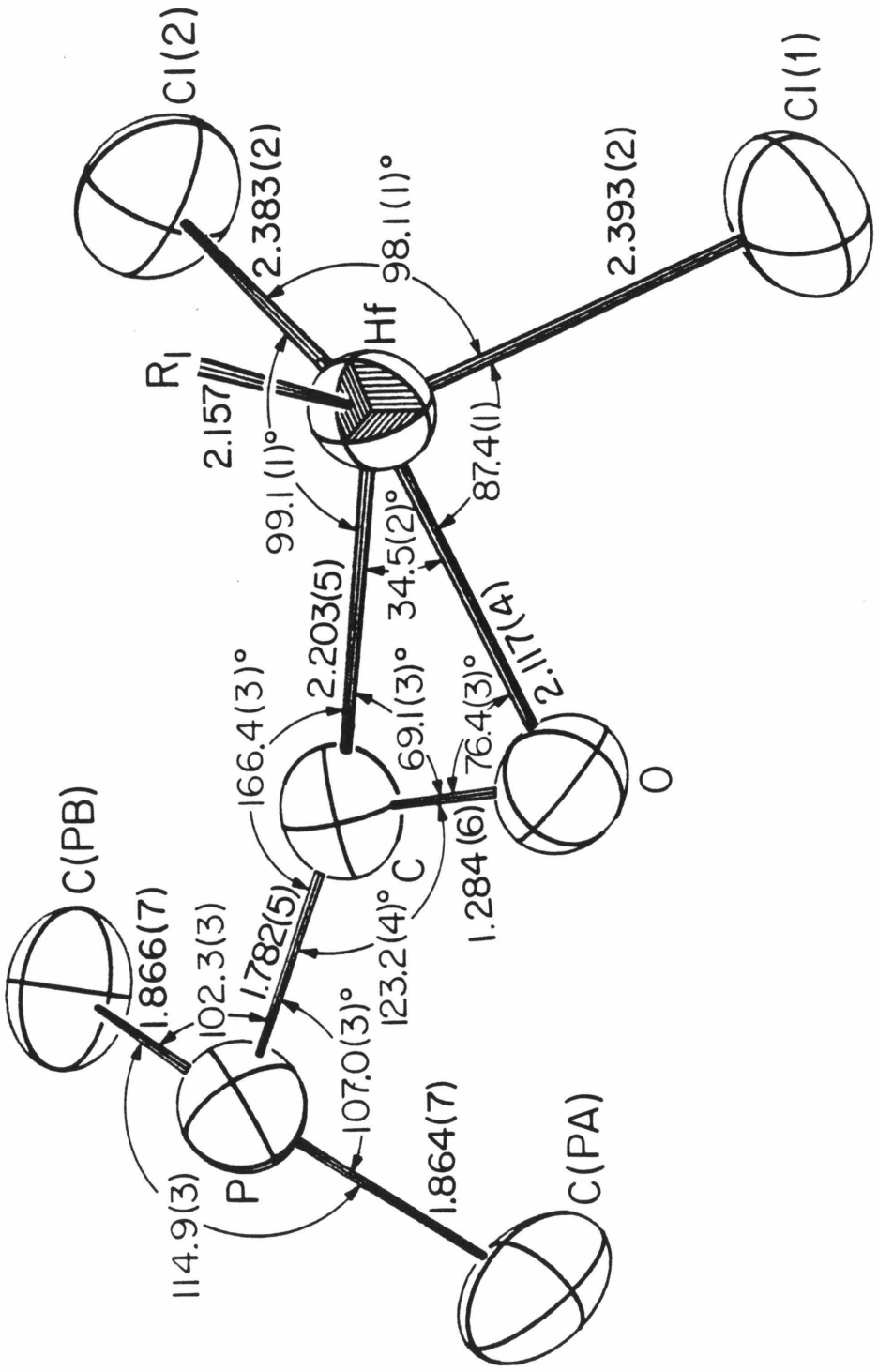

Figure 6. Skeletal view of $Cp^*HfCl_2(\eta^2\text{-}C(O)P^tBu_2)$ (12), with selected bond distances (Å) and angles (°).

values (2.459(6)-2.471(6) Å) are significantly contracted relative to average values for $Cp^*_2Hf(H)(\eta^3\text{-}CH_2CHCH_2)$ (2.54, 2.55 Å)[26] and $[Cp^*HfMe(\mu\text{-}H)(\mu\text{-}P^tBu_2)]_2$ (2.57 Å), and for normal ring complexes Cp_2HfMe_2 (2.50(1) Å)[22] and $[Cp_2HfMe]_2O$ (2.513(5) Å).[21] These observations are consistent with the known dependence of bond lengths on coordination number. Defining the effective coordination number of cyclopentadienyl ligands as three,[46] the coordination numbers of $[(CH_2)_3(C_5H_4)_2]HfCl_2$ and **12** are eight and seven, respectively. Since the effective ionic radius[47] of Hf(IV) (8 coord.) is 0.83 Å and that of Hf(IV) (7 coord.) is 0.76 Å, an approximately 0.07 Å difference in Hf-Cl and Hf-C(ring) bond lengths is anticipated, in reasonable agreement with the observed trend.

The coordination geometry of the carboxyphosphide ligand in **12** is similar to that reported for other dihaptoacyl and η^2-carboxyamide structures. The C-O bond distance for **12**, 1.284(6) Å, is somewhat longer than values reported for simple η^2-acyl $Cp_2ZrMe(\eta^2\text{-}C(O)Me)$ (1.211(8) Å)[36] and $Cp_2ThCl(\eta^2\text{-}C(O)CH_2CMe_3)$ (1.18(3) Å),[35] and is similar to C-O bond distances reported for $\underline{c}\text{-}Cp^*_2ZrH(\eta^2\text{-}C(O)CHPMe_3)$ (1.303(3) Å)[41] and $Cp^*_2U(\eta^2\text{-}C(O)NMe_2)_2$[39] (1.275 Å ave.). The Hf-O distance, 2.117(4) Å, is comparable to reported Hf-O values, 1.94-2.25 Å,[48] and is 0.008 Å shorter than the Hf-C(acyl) bond, reflecting the high oxophillicity of Hf(IV).

Comparison of the carboxyphosphide moiety in **12** with reported acylphosphine structures is revealing. Whereas C(acyl)-P bond distances in $Fe_2(CO)_5[Ph_2PCC(R)=CR']$ (1.918(6) Å),[49] $(^tBu)_2P\overset{O}{\overset{\|}{C}}\overset{O}{\overset{\|}{C}}P(^tBu_2)$ (1.88 Å),[50] and $Me\overset{O}{\overset{\|}{C}}PMe_2$ (1.87(3) Å)[51] are essentially identical to the remaining C(alkyl)-P bond lengths, the C(acyl)-P bond in **12**, 1.782(5) Å, is 0.09 Å shorter, implying significant P=C double bond character in $Cp^*HfCl_2(\eta^2\text{-}C(O)P^tBu_2)$. This observation is in accord with the 10.7 kcal rotational barrier about the P-C(acyl) bond, and is consistent with a contribution of hybrid structure **F** to the composite valence bonding description of **12**. Overall, the η^2-carboxyphosphide ligand is planar to within 0.06 Å, and may best be described as a valence-delocalized three electron ligand.

Conclusion

Although the initial goal of preparing reactive hydridophosphide complexes of hafnium was not realized, the results described in this chapter are enlightening. Unlike the related dialkylamide and alkoxide complexes Cp^*HfMe_2X ($X = n^iPr_2$, NMe_2, O^tBu, O^iPh),[52] which react with H_2 only at elevated temperatures to form uncharacterized product mixtures, the phosphido complexes studied react with H_2 at room temperature to give well defined hydride products in several cases. The origin of the enhanced reactivity is uncertain. One possible explanation is that the presumably weaker interaction of the phosphide lone pair with the hafnium metal center relative to strong amide and alkoxy 3 electron donor ligands affords a level of valence unsaturation more conducive to a 4-center H_2 interaction. Alternatively, the greater polarizability of soft PR_2 ligands compared to hard, first row heteroatom ligands may better stabilize a four-center hydrogenolysis transition state with dipolar character:

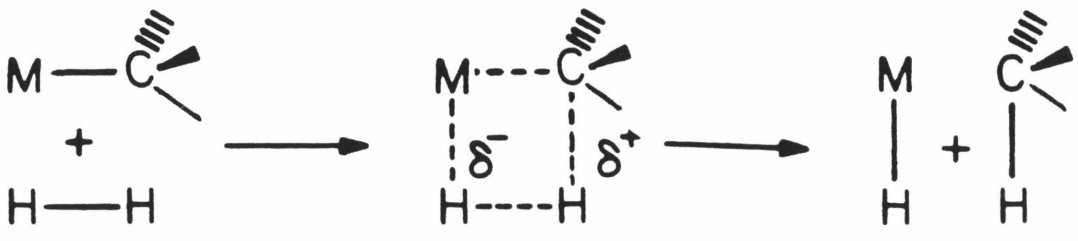

The susceptibility of Hf-P bonds to hydrogenolysis and CO insertion, though unanticipated, is not surprising. Although thermochemical data for M-PR_2 bond dissociation energies is not available, D(Hf-PR_2) is anticipated to be substantially less than the 88 kcal mol^{-1} value reported for D(Hf-NEt_2).[32] Consistent with this ordering, analogous hydrogenolysis and carboxylation reactivity for the related amides Cp*$HfCl_2NR_2$ (R = i-Pr, Me, $SiMe_3$) is not observed.[52] Comparison of Hf-P^tBu_2 and Hf-R (R = alkyl) rates of hydrogenolysis for the complexes Cp*HfCl(X)(P^tBu_2) (X = P^tBu_2, CH_2CMe_3, CH_2Ph), while not a direct measure of relative bond enthalpies, similarly suggests that Hf-PR_2 bonds are relatively weak.

The results of this chapter have some bearing on the proposed use of PR_2 as a stabilizing ligand in bimetallic and cluster chemistry, particularly for early transition metal systems. Our findings on metal PR_2 reactivity suggest that, contrary to what has been proposed,[3] dialkylphosphide ligands may not always function as innocent bridging ligands.

TABLE I. NMR[a] DATA

Compound	Assignment	Nucleus	Chemical Shift	Coupling
$Cp^*HfCl_2P^tBu_2$ (1)	$C_5(C\underline{H}_3)_5$	^1H NMR	2.10 d	J_{PH} = 0.3
	$P(C(C\underline{H}_3)_3)_2$		1.45 d	J_{PH} = 12.2
	$\underline{P}(C(CH_3)_3)_2$	$^{31}P\{^1H\}$ NMR	209.9	
$Cp^*HfCl[P^tBu_2]_2$ (2)	$C_5(C\underline{H}_3)_5$	^1H NMR	2.19 s	
	$[P(C(C\underline{H}_3)_3)_2]_2$		1.59 d	J_{PH} = 12.6
	$[\underline{P}(C(CH_3)_3)_2]_2$	$^{31}P\{^1H\}$ NMR	261.3	
$Cp^*HfCl(CH_2C(CH_3)_3)P^tBu_2$ (3)	$C_5(C\underline{H}_3)_5$	^1H NMR	2.05 s	
	$P(C(C\underline{H}_3)_3)_2$		1.45 d	J_{PH} = 12.9
	$CH_2C(C\underline{H}_3)_3$		1.37 s	
	$C\underline{H}_2C(CH_3)_3$		-0.20 d[b]	J_{HH} = 13.5
	$\underline{P}(C(CH_3)_3)_2$	$^{31}P\{^1H\}$ NMR	213.6	
$Cp^*HfCl(CH_2Ph)P^tBu_2$ (4)	$C_5(C\underline{H}_3)_5$	^1H NMR	2.00 s	
	$P(C(C\underline{H}_3)_3)_2$		1.30 d	J_{PH} = 13.1
	$CH_2C_6\underline{H}_5$		6.8-7.4 m	
	$C\underline{H}_2C_6H_5$		1.74 dd	$^2J_{HH}$=13.2, $^3J_{PH}$=3
	$\underline{P}(C(CH_3)_3)_2$	$^{31}P\{^1H\}$ NMR	222.2	

TABLE I (cont'd)

Compound	Assignment	Nucleus	Chemical Shift	
$Cp^*HfMe_2P^tBu_2$ (5)	$C_5(C\underline{H}_3)_5$	^1H NMR	1.98 s	
	$P(C(C\underline{H}_3)_3)_2$		1.41 d	J_{PH} = 12.9
	$Hf(C\underline{H}_3)_2$		0.26 d	J_{PH} = 2.5
	$\underline{P}(C(CH_3)_3)_2$	$^{31}P\{^1H\}$ NMR	202.5	
$Cp^*HfCl(Ph)P^tBu_2$ (6)	$C_5(C\underline{H}_3)_5$	^1H NMR	2.07 s	
	$P(C(C\underline{H}_3)_3)_2$		1.38 d	J_{PH} = 13.2
	$C_6\underline{H}_5$		8.13 m	
	$C_6\underline{H}_5$		7.20 m	
	$\underline{P}(C(CH_3)_3)_2$	$^{31}P\{^1H\}$ NMR	216.2	
$Cp^*HfMe(Et)P^tBu_2$ (8)	$C_5(C\underline{H}_3)_5$	^1H NMR	1.97 s	
	$P(C(C\underline{H}_3)_3)_2$		1.35 d	J_{PH} = 12.6
	$Hf(C\underline{H}_3)$		0.25 s,br	
	$Hf(C\underline{H}_2CH_3)$		0.39 q	J_{HH} = 8.1
	$Hf(CH_2C\underline{H}_3)$		2.03 t	J_{HH} = 8.1

TABLE I (cont'd)

Compound	Assignment	Nucleus	Chemical Shift	Coupling
$Cp^*HfCl_2(Et)(PMe_3)$ (11)	$C_5(C\underline{H}_3)_5$	^1H NMR	2.00 s	
	$P(C\underline{H}_3)_3$		0.97 d	J_{PH} = 5.0
	$Hf(C\underline{H}_2CH_2)$		0.75 q	J_{HH} = 7.5
	$Hf(CH_2C\underline{H}_3)$		1.80 t	J_{HH} = 7.5
$Cp^*HfCl_2(\eta^2\text{-}C(O)P^tBu_2)$ (12)	$C_5(C\underline{H}_3)_5$	^1H NMR	2.01 s	
	$P(C(C\underline{H}_3)_3)_2$		1.30 d	J_{PH} = 13.5
$Cp^*HfCl_2(\eta^2\text{-}^{13}C(O)P^tBu_2)$	$C_5(C\underline{H}_3)_5$	$^{13}C\{^1H\}$ NMR	11.77 s	
	$\underline{C}_5(CH_3)_5$		122.45 s	
	$P(C(\underline{C}H_3)_3)_2$		31.10 d	J_{PH} = 7.9
	$P(\underline{C}(CH_3)_3)_2$		38.11 d	J_{PH} = 11.9
	$Hf^{13}\underline{C}(O)$		3.03 d	J_{PH} = 101.5
	$\underline{P}(C(CH_3)_3)_2$	$^{31}P\{^1H\}$ NMR	92.6 d	J_{PH} = 101.5

a ^1H (90 MHz), ^{13}C (22.5 MHz), and ^{31}P (36.3 MHz) NMR spectra taken in benzene-$\underline{d}_6$ at ambient temperatures. ^1H and ^{13}C chemical shifts are reported in δ relative to internal TMS or residual protons or carbons in solvent. ^{31}P chemical shifts are reported in δ relative to 85% H_3PO_4 external standard. Coupling constants are reported in Hz.

Experimental Section

General Considerations. All manipulations were performed using either glove box or high vacuum line techniques. Solvents were purified by vacuum transfer first from $LiAlH_4$ or benzophenone ketyl and then from "titanocene".[53] LiP^tBu_2 was prepared by literature methods.[54] Trimethylphosphine (Strem) was stored under vacuum, and distilled prior to use. Hydrogen and Deuterium (Matheson) were purified by passage over MnO on vermiculite[55] and activated 4 Å molecular sieves. Ethylene and carbon monoxide were used directly from the cylinder. Elemental analyses were determined by Alfred Bernhardt, Dornis and Kolbe, Galbraith and C.I.T. Analytical Laboratories.

^1H NMR spectra were recorded using Varian EM-390, JEOL FX90Q, and BRUKER 500 MHz spectrometers. ^{13}C and ^{31}P NMR spectra were obtained using a JEOL FX90Q spectrometer. Infrared spectra were measured on a Beckman 4240 spectrometer as nujol mulls, and are reported in cm^{-1}.

Several reactions were conducted in sealed NMR tubes and monitored by ^1H NMR spectroscopy. A typical example is the reaction of $Cp^*HfCl(CH_2Ph)(P^tBu_2)$ (**4**) with H_2 : **4** (20 mg, 0.04 mmol) was transferred to an NMR tube sealed to a ground-glass joint and fitted with a teflon needle valve adapter. Benzene-$\underline{d}_6$ (0.3 ml) was distilled into the tube

at 77 K, 730 torr H_2 was admitted, and the tube was sealed with a torch.

Procedures. *$Cp^*HfCl_2(P^tBu_2)$ (1).* Cp^*HfCl_3 (4.04 g, 9.6 mmol) and LiP^tBu_2 (1.48 g, 9.7 mmol) were placed in a flask, and *ca.* 40 ml of diethyl ether was distilled in at -78°C. Initially pale yellow, the reaction mixture turned deep green upon warming to room temperature. After stirring at 25°C for 12 hours, the diethyl ether was replaced with 30 ml of petroleum ether, the solution was filtered and the precipitate was washed with petroleum ether. Concentration and crystallization at -78°C, followed by sublimation (90°C, 10^{-4} torr) yielded 2.84 g of deep green 1 (56%). IR: 1360, 1163(et), 1020, 798. Anal. Calcd. for $C_{18}H_{33}Cl_2HfP$: C, 40.81; H, 6.28; P, 5.85; Cl, 13.40. Found: C, 40.38; H, 7.10; P, 5.65; Cl, 13.38. Solution molecular weight (C_6D_6) calcd.: 529; found: 512.[56]

$Cp^*HfCl(P^tBu_2)_2$ (2). Cp^*HfCl_3 (0.50 g, 1.19 mmol) and LiP^tBu_2 (0.452 g, 2.97 mmol) were placed in a flask, and 20 ml of diethyl ether was distilled in at -78°C. The reaction mixture was warmed to room temperature and stirred for 12 hours. The volatiles were removed *in vacuo* and petroleum ether was distilled in. The solution was filtered and concentrated to *ca.* 7 ml; cooling to -78°C afforded 0.485 g (64%) of dark olive green 2. IR: 1361, 1166(st), 1023, 813. Anal. Calcd. for $C_{26}H_{51}ClHfP_2$: C,

48.83; H, 8.04; Cl, 5.54; P, 9.68. Found: C, 48.76; H, 7.93; Cl, 5.48; P, 9.64.

Cp*HfCl(CH_2CMe_3)(P^tBu_2) (3). 30 ml of diethyl ether was distilled onto a mixture of Cp*$HfCl_2$(P^tBu_2) (0.500 g, 0.95 mmol) and $LiCH_2CMe_3$ (0.077 g, 0.99 mmol) at -78°C, and the reaction mixture was warmed slowly to room temperature with stirring. After 12 hours, the diethyl ether was removed and petroleum ether was distilled in. Filtration, washing and crystallization at -78°C yielded only 0.109 g (19%) of highly soluble maroon solid, >90% 3, by ^1H NMR. IR: 1360, 1227(sh), 1215, 1156, 1022.

Cp*HfCl(CH_2Ph)(P^tBu_2) (4). The procedure for 3 was followed except 0.67 g (1.27 mmol) of 1 and 0.17 g (1.31 mmol) of KCH_2Ph were combined in 25 ml diethyl ether. Workup with petroleum ether of the blue-green reaction mixture afforded 0.54 g (73%) of violet, crystalline 4. IR: 1595, 1583(sh), 1484, 1360, 1197, 1162, 1045, 1023, 996, 812(sh), 796, 743(sh), 694(st). Anal. Calcd. for $C_{25}H_{40}ClHfP$: C, 51.28; H, 6.89; Cl, 6.05; P, 5.29. Found: C, 51.21; H, 6.96; Cl, 5.96; P, 5.40. λ_{max} = 580 nm.

Cp*$HfMeCl_2$. Cp*$HfCl_3$ (3.705 g, 8.82 mmol) was placed in a flask, and ca. 100 ml of diethyl ether was distilled in at -78°C. 3.05 ml of 2.9M MeMgBr (8.84 mmol) was syringed into the ether solution at -78°C under argon counterflow,

and the reaction mixture was warmed to room temperature. Workup with petroleum ether after 2 hours[57] afforded 3.05 gm (87%) of white crystalline $Cp^*HfMeCl_2$. IR: 1486, 1424, 1150(st), 1024(st), 799, 540, 460. Anal. Calcd. for $C_{11}H_{18}Cl_2Hf$: C, 33.06; H, 4.54. Found: C, 32.98; H, 4.44.

Cp*HfMe$_2$Cl. The procedure for $Cp^*HfMeCl_2$ was followed except 6.54 g (15.6 mmol) Cp^*HfCl_3 and 11 ml of 2.9 M MeMgBr (31.9 mmol) were combined in 100 ml ether. Workup with petroleum ether after 1 day[59] yielded 5.17 g (88%) of off-white Cp^*HfMe_2Cl. IR: 1485, 1138, 1023, 802. Anal. Calcd. for $C_{12}H_{21}ClHf$: C, 38.00; H, 5.58; Hf, 47.07. Found: C, 37.97; H, 5.66; Hf, 46.99.

Cp*HfPhCl$_2$. The procedure for $Cp^*HfMeCl_2$ was followed except 1.11 g (2.64 mmol) Cp^*HfCl_3 and 1.2 ml of 2.2 M PhLi (2.64 mmol) were combined in 50 ml ether. Workup with petroleum ether gave 0.895 g (73%) of Cp^*PhCl_2. IR: 3050, 1592, 1490(sh), 1480(sh), 1412, 1282, 1064(st), 1028, 991, 890, 730(st), 703(st). Anal. Calcd. for $C_{16}H_{20}Cl_2Hf$: C, 41.62; H, 4.37. Found: C, 42.03; H, 4.47.

Cp*HfMe$_2$(P^{t}Bu$_2$) (5). Cp^*HfMe_2Cl (2.35 g, 6.20 mmol) and LiP^tBu_2 (1.03 g, 6.77 mmol) were placed in a flask and 60 ml of diethyl ether was distilled in. Initially light yellow, the reaction mixture quickly turned purple, and then deep red upon warming to room temperature. After

12 hours, the diethyl ether was replaced with petroleum ether, the solution was filtered and the precipitate was washed thoroughly. Concentration and crystallization at -78°C, followed by sublimation (90°C, 10^{-4} torr) yielded 1.76 g of magenta **6** (58%). IR: 1358, 1166, 1134, 1018. Anal. Calcd. for $C_{20}H_{39}PHf$: C, 49.13; H, 8.04; P, 6.33. Found: C, 48.85; H, 8.45; P, 6.42.

Cp*HfCl(Ph)(P^tBu_2) (6). The procedure for 5 was followed except 0.495 g (1.07 mmol) $Cp^*Hf(Ph)Cl_2$ and 0.165 g (1.08 mmol) LiP^tBu_2 were combined in 30 ml diethyl ether. Workup with petroleum ether afforded 0.275 g (44%) of red-purple Cp*HfCl(Ph)(P^tBu_2). IR: 3050, 1361, 1165, 1063, 1050, 1022, 990, 720, 700. Anal. Calcd. for $C_{24}H_{38}ClPHf$: C, 50.44; H, 6.70. Found: C, 49.35; H, 6.71.

[Cp*HfMe(μ-H)(μ-P^tBu_2)]$_2$ (7). A thick-walled glass reaction vessel with a teflon needle valve, charged with 0.35 g (0.72 mmol) of 5, 10 ml toluene, and ca. 3 atm H_2 was stirred at room temperature for one week. The precipitate was thoroughly washed with petroleum ether and dried in vacuo, yielding 0.21 g (62%) of light yellow 7. IR: 1510(st), 1485(sh), 1352, 1161, 1132, 1077, 1013, 760(st). Anal. Calcd. for $C_{38}H_{74}Hf_2P_2$: C, 48.05; H, 7.85; Hf, 37.58. Found: C, 48.13; H, 7.86; Hf, 37.54.

Reaction of 7 with HCl. To 7 (0.040 g, 0.042 mmol) and 0.3 ml benzene-d_6 in an NMR tube was condensed HCl (ca. 6 equiv.), and the tube was sealed with a torch. Upon warming to room temperature, a vigorous evolution of H_2 and CH_4 (^1H NMR) was observed. The product H_2/CH_4 mixture was passed through a series of liquid N_2 cooled traps and collected via a Toepler pump. H_2 + CH_4 amounted to 0.14 mmol, or 1.7 mmol (H_2 + CH_4)/mmol Hf. This mixture was cycled over CuO at 320°C to convert H_2 to H_2O, which was removed in a liquid N_2 trap. The remaining CH_4 collected amount to 0.070 mmol (0.85 mmol/mmol Hf), or one half of the total gas collected (i.e., H_2:CH_4 = 1:1). The residue obtained after removal of volatiles was not identified.

Structure Determination for [Cp*HfMe(μ-H)(μ-P^{t}Bu$_2$)]$_2$ (7).

Sufficiently large, well formed orange crystals of 7 were obtained from the slow reaction of 5 and H_2 in toluene at 0°C. A single crystal (0.67 x 0.33 x 0.17 mm) was mounted approximately along the b axis in a glass capillary under N_2. A series of oscillation and Weissenberg photographs indicated monoclinic symmetry; the space group $P2_1/c$ was inferred from systematic absences in the diffractometer data (0k0 absent for k odd; h0l absent for l odd). Data were collected on a locally-modified Syntex $P2_1$ diffractometer with graphite monochromator. The unit cell parameters (Table IV) were obtained by least-squares

refinement of 15 2θ values ($46 < 2\theta < 59^{o}$), where each 2θ value was an average of two measurements, at ±2θ. Intensity data was corrected for a 2.3% linear decay, as indicated by the three check reflections, and the data were reduced to F_o^2; the form factors for all atoms were taken from reference 58, and those for Hf and P were corrected for anomalous dispersion. The details on data collection are given in Table IV.

The position of the Hf atom was derived from the Patterson map, and a series of Fourier maps phased on Hf revealed the remaining non-hydrogen atoms of the complex. Least-squares refinement of atom coordinates and U's, minimizing $\Sigma\omega[F_o^2-(F_c/k)^2]^2$, gave R = 0.084. All ring methyl and phosphide t-butyl methyl H-atoms and the hydride atom were located from difference maps; all H-atoms except the hydride were introduced into the model with fixed coordinates and isotropic U's. The refinement of non-hydrogen atoms in the Hf complex with anisotropic U_{ij}'s and the coordinates of the hydride atom with fixed isotropic U using all the data (5678 reflections) led to R = 0.071; the secondary extinction coefficient was refined, giving a value of $0.69(6)\times10^{-6}$. Robust refinement, with 90 reflections deleted having values of $|\Delta F|/\sigma_{F2} > 6$, led to a final R = 0.066. The final ΔF map showed several large features indicative of residual adsorption errors: symmetric pairs of peaks located approximately 0.75 Å from the heavy atoms ($\sim 5e^-/Å^3$ around Hf, $\sim 2e^-/Å^3$ around P).

Final atomic coordinates and U_{ij}'s are given in Table V. Hydrogen atom coordinates are given in Table VI. Bond distances and bond angles are given in Tables VII and VIII, respectively. All calculations were carried out on a VAX 11/780 computer using the CRYRM system of programs.

Cp*$_2$HfMe(Et)(P^{t}Bu$_2$) (8). To 7 (0.025 g, 0.027 mmol) and 0.3 ml benzene-d_6 in an NMR tube was condensed C_2H_4 (0.16 mmol), and the tube was sealed off. After 1½ hours at 80°C the solution was deep red; ^{1}H NMR indicated a single (>90% pure) soluble product, tentatively identified as the ethylene insertion product 8.

[Cp*$_2$HfCl(μ-H)(μ-P^{t}Bu$_2$)]$_2$ (9). A solution of Cp*HfCl(P^{t}Bu$_2$)$_2$ (2) (0.391 g, 0.55 mmol) in 20 ml toluene was stirred under 1 atm H_2 for 3 hours. The solution was filtered, and the light yellow solid was washed thoroughly with toluene and dried *in vacuo*. Yield: 87%. IR: 1517(st), 1483(sh), 1373, 1358, 1162, 1073, 1017, 834, 806, 770. Anal. Calcd. for $C_{36}H_{68}Cl_2Hf_2P$: C, 43.64; H, 6.92. Found: C, 43.90; H, 6.88.

Cp*HfCl(Et)(PMe$_3$) (11). A thick-walled glass reaction vessel with a teflon needle valve was charged with 0.527 g (0.996 mmol) of 1, 10 ml toluene, 6.67 mmol C_2H_4, 5.00 mmol PMe_3, and *ca*. 3 atm H_2 (~3.6 mmol) and stirred at room temperature. After 2 days, petroleum ether workup yielded

0.353 g (72%) of off-white **11**. IR: 1487, 1425, 1302, 1283, 1022, 961(st), 941, 919(sh), 732(st). Anal. Calcd. for $C_{15}H_{29}Cl_2HfP$: C, 36.79; H, 5.97. Found: C, 36.54; H, 5.83.

Cp*HfCl$_2$(η^2-C(O)P^{t}Bu$_2$) (12). A solution of 0.497 g (0.940 mmol) Cp*HfCl$_2$(P^{t}Bu$_2$) (1) in 15 ml petroleum ether was stirred under 900 torr CO for 20 minutes. Filtration, washing with cold petroleum ether, and drying *in vacuo* yielded 0.380 g (73%) of bright yellow **12**. IR: 1400, 1363(sh), 1350(st, ν(C-O)), 1175, 1029, 937, 854, 811, 720, 620, 520. Anal. Calcd. for $C_{19}H_{33}Cl_2HfOP$: C, 40.91; H, 5.96; Cl, 12.71; P, 5.55. Found: C, 41.00; H, 6.03; Cl, 12.74; P, 5.70.

Structure Determination for Cp*HfCl$_2$(η^2-C(O)P^{t}Bu$_2$) (12).

A single crystal (0.33 x 0.75 x 0.33 mm) grown from a pentane/benzene solution was mounted in a glass capillary under N_2. Oscillation and Weissenberg photographs indicated orthorhombic symmetry; the space group $P2_12_12_1$ was inferred from the systematic absences in the photographs and in the diffractometer data (hOO absent for h odd; OkO absent for k odd; OOl absent for l odd). Data were collected on a locally-modified Syntex $P2_1$ diffractometer with graphite monochromator; details on unit cell parameters and the data collection are given in Table IX. Intensity data was corrected for a 1.7% linear

decay, as indicated by the three check reflections, and the data were reduced to F_o^2.[59]

The position of the Hf atom was derived from the Patterson map, and a series of Fourier maps phased on Hf revealed the remaining non-hydrogen atoms of the complex. Least-squares refinement of atom coordinates and U's, minimizing $\Sigma\omega[F_o^2-(F_c/k)^2]^2$, gave R = 0.053. All hydrogens were located from difference maps and introduced into the model with fixed coordinates and isotropic U's. The refinement of non-hydrogen atoms in the Hf complex with anisotropic U_{ij}'s using all the data (5760 reflections) led to R = 0.040 and S = 1.66, with refinement of secondary extinction giving coeff. = 0.58(3) x 10^{-6}.

The final ΔF map showed residual peaks of 1.0 and 1.2 $e^-/\mathring{A}^3$ associated with the Hf atom. Refinement of the structure with form factors corrected for anomalous dispersion led to the correct assignment of the enantiomer by comparison of the goodness-of-fit (f">0 S=2.28; f"<0 S=1.73). The final cycle of refinement was based on coordinates of the correct enantiomer (and f" > 0); these are given in Tables X and XI. Bond distances and bond angles are given in Tables XII and XIII, respectively.

TABLE IV. Crystal and Intensity Collection Data for $[Cp^*HfMe(\mu\text{-}H)(\mu\text{-}P^tBu_2)]_2$ (7).

Formula	$C_{38}H_{74}Hf_2P_2$			
Formula weight	767.02 g/mol			
Space group	$P2_1/c$			
a	11.4848(21) Å			
b	16.4472(52) Å			
c	11.8255(22) Å			
β	118.915(11)°			
V	1955.1 $Å^3$			
Z	4			
D_{calc}	1.61 g/cm^3			
Crystal size	0.67 x 0.33 x 0.17 mm			
λ	0.71069 Å (Mo $K\bar{\alpha}$)			
μ	5.36 mm^{-1}			
Scan range	1.0° below $K\alpha_1$, 1.1° above $K\alpha_2$			
Refln settings	+h, +k, ±l			
2θ range, scan rate,	3.5<2θ<36°	4.88°/min	1.0	3143
backgrd time/scan time,				
number of reflns	35 <2θ<46°	2.02°/min	0.5	6323
Total number of averaged data	5678			
Refinement on	F_o^2			
Final number of parameters	195			

Final cycle:†	Total Data Set	Robust Refinement
R	0.071 (5503)	0.066 (5413)
R'	0.064 (4693)	0.059 (4603)
S	4.02 (5678)	3.55 (5588)

† Typical R-value, number of reflns used in sums given in parentheses. R' refers to R-value calculated for reflns with $F_o^2 > 3\sigma_{F2}$. S is the goodness-of-fit; summations include all reflns. Robust refinement deleted reflns with $|\Delta F|/\sigma_{F2} > 6$.

Table V. Final non-hydrogen atom coordinates ($\times 10^4$) and Gaussian amplitudes ($\times 10^4$).

	x	y	z	U_{11}	U_{22}	U_{33}	U_{12}	U_{13}	U_{23}
Hf	1291.8(3)	544.4(2)	276.8(3)	232(1)	194(1)	235(1)	−3(1)	103(1)	1(1)
P	−1183(2)	605(1)	−1978(2)	270(8)	244(8)	239(8)	27(7)	113(7)	38(7)
C(M)	1172(8)	1709(5)	1226(8)	363(39)	330(39)	362(38)	−57(32)	97(32)	−107(34)
C(1)	3720(7)	204(5)	983(8)	405(41)	386(40)	9(28)	134(30)	112(34)	338(16)
C(2)	3700(8)	1061(5)	1221(8)	331(38)	392(42)	398(42)	−83(33)	164(34)	−23(36)
C(3)	3003(8)	1452(5)	39(9)	6(39)	290(37)	476(45)	−46(29)	223(36)	7(33)
C(4)	2545(8)	873(5)	−968(8)	20(36)	376(39)	339(37)	−49(30)	198(32)	36(32)
C(5)	3013(8)	94(5)	−354(8)	4(36)	360(39)	404(41)	64(30)	222(33)	59(33)
C(1M)	4633(9)	−393(7)	1982(11)	377(45)	556(59)	591(58)	94(40)	205(43)	238(48)
C(2M)	4530(10)	1477(8)	2506(10)	493(53)	733(75)	433(50)	−232(51)	163(43)	−117(51)
C(3M)	2917(11)	2368(6)	−155(10)	654(62)	327(43)	521(53)	−98(42)	251(48)	47(42)
C(4M)	2008(9)	1086(6)	−2361(9)	453(47)	491(50)	400(44)	32(39)	224(39)	106(41)
C(5M)	2991(10)	−685(6)	−1047(10)	466(48)	372(45)	588(55)	−2(36)	294(45)	−46(41)
C(PA)	−1564(9)	140(6)	−3621(7)	434(44)	490(49)	223(33)	−23(37)	137(32)	18(34)
C(PA1)	−2973(11)	−236(7)	−4242(9)	513(56)	614(63)	364(45)	−103(47)	92(42)	−100(46)
C(PA2)	−562(11)	−526(6)	−3367(9)	655(60)	517(53)	413(45)	48(48)	323(45)	−46(45)
C(PA3)	−1490(11)	727(7)	−4599(9)	569(57)	697(70)	334(41)	32(49)	211(41)	120(45)
C(PB)	−1964(8)	1679(5)	−2294(8)	396(40)	282(36)	403(41)	84(32)	144(34)	125(34)
C(PB1)	−1015(10)	2272(6)	−2439(11)	474(50)	350(44)	709(66)	57(39)	220(48)	192(48)
C(PB2)	−2082(11)	1929(6)	−1119(11)	563(56)	348(43)	648(62)	108(40)	325(51)	92(44)
C(PB3)	−3350(10)	1766(7)	−3477(10)	445(48)	514(57)	508(53)	107(42)	150(42)	169(47)

Table VI. Hydrogen atom coordinates ($\times 10^3$).

	x	y	z
H	424(118)	−751(73)	−463(117)
H(1)	2077	1976	1706
H(2)	585	2116	571
H(3)	851	1623	1842
H(4)	−3623	125	−4934
H(5)	−2951	−757	−4689
H(6)	−3237	−350	−3616
H(7)	−883	−1046	−3208
H(8)	290	−386	−2657
H(9)	−459	−608	−4165
H(10)	−654	1030	−4156
H(11)	−2240	1127	−4900
H(12)	−1553	433	−5329
H(13)	−95	2152	−1786
H(14)	−1224	2840	−2315
H(15)	−1093	2230	−3305
H(16)	−1408	2370	−657
H(17)	−2967	2167	−1389
H(18)	−1912	1479	−553
H(19)	−3400	2274	−3957
H(20)	−3524	1304	−4080
H(21)	−4039	1780	−3223
H(22)	4144	−864	2051
H(23)	5075	−125	2879
H(24)	5350	−574	1829
H(25)	4957	1059	3209
H(26)	3981	1829	2751
H(27)	5243	1810	2516
H(28)	3692	2566	−221
H(29)	2101	2504	−968
H(30)	2885	2645	563
H(31)	2700	1397	−2467
H(32)	1803	592	−2888
H(33)	1213	1427	−2680
H(34)	2199	−1016	−1246
H(35)	3793	−1013	−497
H(36)	2994	−572	−1871

Table VII. Bond lengths for $[Cp^*HfMe(\mu\text{-}H)(\mu\text{-}P^tBu_2)]_2$ (Å).

Hf–Hf′	3.250	C(3)–C(4)	1.413(13)
Hf–[a]R_1	2.264	C(4)–C(5)	1.442(12)
Hf–C(M)	2.258(9)	C(1)–C(1M)	1.504(14)
Hf–H′	2.33(13)	C(2)–C(2M)	1.512(15)
Hf–H	2.12(13)	C(3)–C(3M)	1.520(14)
Hf–P	2.805(2)	C(4)–C(4M)	1.495(13)
Hf–P′	2.807(2)	C(5)–C(5M)	1.514(14)
Hf–C(1)	2.557(9)	P–C(PA)	1.931(10)
Hf–C(2)	2.575(9)	P–C(PB)	1.933(9)
Hf–C(3)	2.589(9)	C(PA)–C(PA1)	1.546(15)
Hf–C(4)	2.564(9)	C(PA)–C(PA2)	1.509(15)
Hf–C(5)	2.537(9)	C(PA)–C(PA3)	1.541(15)
C(1)–C(5)	1.396(12)	C(PB)–C(PB1)	1.534(15)
C(1)–C(2)	1.439(13)	C(PB)–C(PB2)	1.517(15)
C(2)–C(3)	1.388(13)	C(PB)–C(PB3)	1.536(14)

[a]$R_1 \equiv$ ring centroid of Cp^*-ring [atoms C(1)—C(5M)].

Table VIII. Bond angles for $[Cp^*HfMe(\mu\text{-}H)(\mu\text{-}P^tBu_2)]_2$ (°).

H–Hf–H′	86 (5)	C(PA1)–C(PA)–P	108.2(7)
P–Hf–P′	109.2(1)	C(PA2)–C(PA)–P	107.9(7)
[a]R_1–Hf–C(M)	101.4(2)	C(PA3)–C(PA)–P	116.1(7)
R_1–Hf–H′	111 (3)	C(PB1)–C(PB)–P	108.3(7)
R_1–Hf–H	162 (4)	C(PB2)–C(PB)–P	108.0(7)
R_1–Hf–P	120.5(1)	C(PB3)–C(PB)–P	116.2(7)
R_1–Hf–P′	120.5(1)	C(2)–C(1)–C(5)	107.1(8)
C(M)–Hf–H′	147 (3)	C(3)–C(2)–C(1)	108.2(8)
C(M)–Hf–H	62 (4)	C(4)–C(3)–C(2)	109.5(8)
C(M)–Hf–P	99.5(2)	C(5)–C(4)–C(3)	106.2(8)
C(M)–Hf–P′	100.4(2)	C(1)–C(5)–C(4)	109.0(8)
H–Hf–P	68 (3)	C(1M)–C(1)–C(5)	127.4(8)
H′–Hf–P′	62 (4)	C(1M)–C(1)–C(2)	123.8(8)
H –Hf–P′	71 (4)	C(2M)–C(2)–C(1)	125.3(9)
Hf–H–Hf′	94 (5)	C(2M)–C(2)–C(3)	125.4(9)
Hf–P–Hf′	70.8(1)	C(3M)–C(3)–C(2)	125.1(9)
C(PA)–P–C(PB)	108.0(4)	C(3M)–C(3)–C(4)	124.8(8)
C(PA)–P–Hf	125.1(3)	C(4M)–C(4)–C(3)	123.9(8)
C(PA)–P–Hf′	112.8(3)	C(4M)–C(4)–C(5)	128.2(8)
C(PB)–P–Hf	112.2(3)	C(5M)–C(5)–C(4)	125.1(8)
C(PB)–P–Hf′	125.2(3)	C(5M)–C(5)–C(1)	124.8(8)
C(PA1)–C(PA)–C(PA2)	109.1(8)	C(PB1)–C(PB)–C(PB2)	108.2(8)
C(PA1)–C(PA)–C(PA3)	108.6(8)	C(PB1)–C(PB)–C(PB3)	108.6(8)
C(PA2)–C(PA)–C(PA3)	106.8(8)	C(PB2)–C(PB)–C(PB3)	107.3(8)

[a]$R_1 \equiv$ ring centroid of Cp^*-ring [atoms C(1)—C(5M).

TABLE IX. Crystal and Intensity Collection Data for $Cp^*HfCl_2(\eta^2\text{-}C(O)P^tBu_2)$ (**12**).

Formula	$C_{19}H_{33}Cl_2HfOP$
Formula weight	557.83
Space group	$P2_12_12_1$
a	14.9191(15) Å
b	9.9521(10) Å
c	15.7794(18) Å
V	2342.8 Å^3
Z	4
D_{calc}	1.64 g/cm^3
Crystal size	0.33 x 0.75 x 0.33 ([100]x[010]x[001])
λ	0.71069 Å (Mo $K\bar{\alpha}$)
μ	4.85 mm^{-1}
Scan range	1.2° below $K\alpha_1$, 1.2° above $K\alpha_2$
2θ limits, scan rate,	4-35° 2.02°/min 1107(+h,+k,±l)
backgrd time/scan time,	17-35° 3.91°/min 738(+h,+k,±l)
number of reflns	34-46° 2.93°/min 2746(+h,+k,±l)
	4-36° 4.88°/min 1881(+h,-k,±l)
	45-50° 2.02°/min 1160(+h,+k,±l)
	45-56° 2.02°/min 1760(+h,+k,±l)
Total number of averaged data	5760
Refinement on	F_o^2
Final number of parameters	218
Final agreement R ($F_o^2 > 0$)	0.040 (5570)†
R'	0.030 (4609)
S	1.66 (5760)

†Typical R-value, number of reflns used in sums given in parentheses. R' refers to R-value calculated for reflns with $F_o^2 > 3\sigma_{F^2}$. S is the goodness of fit.

Table X. Final non-hydrogen atom coordinates ($\times 10^4$) and Gaussian amplitudes ($\times 10^4$).

	x	y	z	U_{11}	U_{22}	U_{33}	U_{12}	U_{13}	U_{23}
Hf	7663.7(1)	6103.5(2)	7536.5(1)	471(1)	395(1)	343(1)	−17(1)	−15(1)	29(1)
P	7541(1)	8745(1)	9407.3(8)	504(10)	392(7)	473(7)	13(7)	25(6)	−10(6)
Cl(1)	8587(1)	6558(2)	6330.2(9)	854(13)	787(11)	515(8)	−72(10)	176(8)	80(8)
Cl(2)	6255(1)	6681(2)	6925(1)	624(11)	827(12)	721(10)	38(10)	−217(8)	149(9)
C	7730(4)	7661(5)	8526(3)	426(32)	417(27)	434(26)	46(27)	−1(27)	84(21)
O	8515(3)	7397(4)	8235(2)	433(25)	504(23)	560(23)	−29(20)	−8(19)	−44(19)
C(1)	7026(4)	4233(6)	8368(4)	604(41)	495(37)	565(35)	53(29)	142(30)	143(27)
C(2)	7863(5)	4539(5)	8736(3)	827(53)	339(28)	383(28)	22(30)	−85(29)	34(22)
C(3)	8527(4)	4242(6)	8151(4)	535(40)	486(37)	628(38)	9(29)	−23(32)	71(29)
C(4)	8112(5)	3731(5)	7418(4)	838(44)	387(27)	428(30)	56(26)	13(34)	−57(36)
C(5)	7182(4)	3729(5)	7554(4)	700(45)	446(28)	542(30)	−98(26)	−241(37)	84(39)
C(1M)	6118(6)	4359(8)	8799(6)	915(68)	887(60)	1597(83)	129(51)	618(61)	508(59)
C(2M)	8030(7)	4989(6)	9649(4)	1767(94)	589(42)	431(34)	117(50)	−71(46)	1(29)
C(3M)	9522(5)	4390(8)	8276(6)	618(55)	881(59)	1575(80)	57(45)	−281(53)	291(56)
C(4M)	8583(7)	3146(8)	6653(5)	1668(96)	649(49)	732(48)	168(57)	374(55)	−55(40)
C(5M)	6494(7)	3213(8)	6945(5)	1432(85)	650(48)	1257(70)	−412(55)	−710(64)	136(48)
C(PA)	8485(4)	9972(6)	9430(5)	523(43)	451(36)	908(50)	−32(30)	−70(36)	−186(33)
C(PA1)	9318(5)	9153(8)	9699(5)	525(44)	920(58)	1015(53)	42(42)	−172(39)	−111(46)
C(PA2)	8685(6)	10627(7)	8572(6)	769(60)	648(48)	1641(82)	−257(44)	7(57)	369(51)
C(PA3)	8312(6)	11038(10)	10085(7)	812(67)	1102(70)	2413(122)	−144(61)	35(72)	−1096(81)
C(PB)	6423(4)	9483(6)	9153(4)	414(37)	653(41)	734(42)	69(33)	78(31)	24(35)
C(PB1)	6168(6)	10486(10)	9821(6)	737(64)	1186(74)	1589(86)	362(60)	203(60)	−311(64)
C(PB2)	5765(5)	8311(8)	9175(5)	543(46)	966(54)	915(51)	−70(43)	35(38)	66(44)
C(PB3)	6371(5)	10165(8)	8296(5)	650(53)	924(57)	1196(66)	143(45)	−135(47)	359(51)

Table XI. Hydrogen atom coordinates ($\times 10^3$).

	x	y	z
H(1)	5885	5341	8806
H(2)	5620	3836	8545
H(3)	6141	4112	9416
H(4)	8414	4289	9949
H(5)	7511	5160	9949
H(6)	8433	5821	9637
H(7)	9773	3673	8620
H(8)	9636	5270	8620
H(9)	9851	4500	7752
H(10)	8528	2134	6654
H(11)	9237	3342	6654
H(12)	8330	3468	6117
H(13)	6276	3936	6564
H(14)	6766	2503	6564
H(15)	5989	2811	7238
H(16)	9198	8188	9563
H(17)	9445	9246	10292
H(18)	9851	9425	9359
H(19)	9369	10739	8513
H(20)	8415	11480	8513
H(21)	8509	10002	8120
H(22)	8740	11760	10094
H(23)	7706	11329	10094
H(24)	8406	10558	10692
H(25)	6531	11327	9790
H(26)	5514	10807	9790
H(27)	6235	10135	10412
H(28)	5199	8475	8879
H(29)	6051	7493	8879
H(30)	5640	8013	9758
H(31)	6916	9960	7955
H(32)	5850	9765	7932
H(33)	6272	11110	8322

Table XII. Bond lengths for $Cp^*HfCl_2(\eta^2\text{-}C(O)P^tBu_2)$ (Å).

Hf–[a]R_1	2.157	C(2)–C(3)	1.386(9)
Hf–Cl(1)	2.393(2)	C(3)–C(4)	1.407(9)
Hf–Cl(2)	2.383(2)	C(4)–C(5)	1.404(8)
Hf–C	2.203(5)	C(1)–C(1M)	1.521(11)
Hf–O	2.117(4)	C(2)–C(2M)	1.528(9)
Hf–C(1)	2.468(6)	C(3)–C(3M)	1.506(11)
Hf–C(2)	2.469(6)	C(4)–C(4M)	1.513(10)
Hf–C(3)	2.456(6)	C(5)–C(5M)	1.497(11)
Hf–C(4)	2.461(6)	C(PA)–C(PA1)	1.546(10)
Hf–C(5)	2.471(6)	C(PA)–C(PA2)	1.533(11)
C–O	1.284(6)	C(PA)–C(PA3)	1.503(12)
P–C	1.782(5)	C(PB)–C(PB1)	1.500(11)
P–C(PA)	1.864(7)	C(PB)–C(PB2)	1.525(10)
P–C(PB)	1.866(7)	C(PB)–C(PB3)	1.516(10)
C(1)–C(5)	1.398(8)		
C(1)–C(2)	1.410(8)		

[a]$R_1 \equiv$ ring centroid of Cp^*-ring [atoms C(1)—C(5M)].

Table XIII. Bond angles for $Cp^*HfCl_2(\eta^2\text{-}C(O)P^tBu_2)$ (°).

[a]R_1–Hf–Cl(1)	116.1(1)	C(1M)–C(1)–C(5)	126.1(6)
R_1–Hf–Cl(2)	114.9(1)	C(1M)–C(1)–C(2)	125.9(6)
R_1–Hf–C	112.7(1)	C(2M)–C(2)–C(1)	126.6(5)
R_1–Hf–O	109.7(1)	C(2M)–C(2)–C(3)	125.0(6)
Cl(1)–Hf–Cl(2)	98.1(1)	C(3M)–C(3)–C(2)	126.7(6)
Cl(1)–Hf–C	113.9(1)	C(3M)–C(3)–C(4)	125.2(6)
Cl(1)–Hf–O	87.4(1)	C(4M)–C(4)–C(3)	126.2(6)
Cl(2)–Hf–C	99.1(1)	C(4M)–C(4)–C(5)	125.4(6)
Cl(2)–Hf–O	126.4(1)	C(5M)–C(5)–C(4)	125.5(6)
C–Hf–O	34.5(2)	C(5M)–C(5)–C(1)	126.8(6)
Hf–C–P	166.4(3)	P–C(PA)–C(PA1)	105.5(5)
Hf–C–O	69.1(3)	P–C(PA)–C(PA2)	114.1(5)
P–C–O	123.2(4)	P–C(PA)–C(PA3)	110.3(5)
Hf–O–C	76.4(3)	C(PA1)–C(PA)–C(PA2)	108.1(6)
C–P–C(PA)	107.0(3)	C(PA1)–C(PA)–C(PA3)	108.8(6)
C–P–C(PB)	102.3(3)	C(PA2)–C(PA)–C(PA3)	109.9(6)
C(PA)–P–C(PB)	114.9(3)	P–C(PB)–C(PB1)	109.8(5)
C(2)–C(1)–C(5)	108.0(5)	P–C(PB)–C(PB2)	105.6(4)
C(3)–C(2)–C(1)	108.1(5)	P–C(PB)–C(PB3)	114.4(5)
C(4)–C(3)–C(2)	108.1(5)	C(PB1)–C(PB)–C(PB2)	109.3(6)
C(5)–C(4)–C(3)	108.0(5)	C(PB1)–C(PB)–C(PB3)	108.4(6)
C(1)–C(5)–C(4)	107.7(5)	C(PB2)–C(PB)–C(PB3)	109.3(6)

[a]$R_1 \equiv$ ring centroid of Cp^*-ring [atoms C(1)—C(5M)].

REFERENCES

(1) (a) Cardin, D. J.; Lappert, M. F.; Raston, C. L.; Riley, P. I. "Comprehensive Organometallic Chemistry"; Wilkinson, G., ed., Pergamon Press: New York, 1982; Vol. 3, 559-634. (b) Wailes, P. C.; Coutts, R. S. P.; Weigold, H. "Organometallic Chemistry of Titanium, Zirconium and Hafnium"; Academic Press: New York, 1974. (c) Andersen, R. A. Inorg. Chem. **1979**, 18, 2928; Ibid. J. Organomet. Chem. **1980**, 192, 189; Planalp,R. P.; Andersen, R. A.; Zalkin, A. Organometallics **1983**, 2, 16. (d) Hillhouse, G. L.; Bercaw, J. E. Ibid. **1982**, 1, 1025.

(2) (a) Ellerman, J.; Poersch, P. Angew. Chem. Int. Ed. Engl. **1967**, 6, 355. (b) Stelzer, O.; Unger, E. Chem. Ber. **1977**, 110, 3430; Johannsen, G.; Stelzer, O. Ibid., 3438.

(3) (a) Jones, R. A.; Wright, T. L.; Atwood, J. L.; Hunter, W. E. Organometallics **1983**, 2, 470. (b) Finke, R. G.; Ganghan, G.; Pierpont, C.; Cass, M. E. J. Am. Chem. Soc. **1981**, 103, 1394. (c) Roberts, D. H.; Steinmetz, G. R.; Breen, M. J.; Shulman, P. M.; Morrison, E. D.; Duttera, M. R.; DeBrosse, C. W.; Whittle, R. R.; Geoffroy, G. L. Organometallics **1983**, 2, 846 and references therein.

(4) (a) Lappert, M. F.; Power, P. P.; Sanger, A. R.; Srivastava, R. C. "Metal and Metalloid Amides"; Ellis Horwood Ltd.,Chichester,1980.

(b) Bradley, D. C.; Chisholm, M. H. Acc. Chem. Res. **1976**, 9, 273.

(5) (a) Domaille, P. J.; Foxman, B. M.; McNeese, T. J.; Wreford, S. S. J. Am. Chem. Soc. **1980**, 102, 4114. (b) Rocklage, S. M.; Schrock, R. R.; Churchill, M. R.; Wasserman, H. J. Organometallics **1982**, 1, 1332.

(6) Quite recently, a number of early transition metal complexes containing terminal phosphido ligands have been reported. (a) Baker, R. T.; Whitney, J. F.; Wreford, S. S. Organometallics **1983**, 2, 1049. (b) Baker, R. T.; Krusic, P. J.; Tulip, T. H.; Calabrese, T C.; Wreford, S. S. J. Am. Chem. Soc. **1983**, 105, 6763. (c) Jones, R. A.; Lasch, J. G.; Norman, N. C.; Whittlesey, B. R.; Wright, T. C. Ibid., 6184.

(7) Wolczanski, P. T.; Bercaw, J. E. Organometallics **1982**, 1, 793.

(8) The steric influence of P^tBu_2 in bridging metal systems has recently been investigated: Jones, R. A.; Stuart,A. L.; Atwood, J. L.; Hunter, W. E.; Rogers, R. D. Organometallics **1982**, 1, 1721; Ibid. **1983**, 2, 874; Atwood, J. L.; Hunter, W. E.; Jones, R. A. Inorg. Chem. **1983**, 22, 993.

(9) Calculated from the Gutowsky-Holm approximation $\Delta G^{\ddagger} \approx 15 + 0.05\ T_c\ (^oC)$, where T_c is the coalescence temperature.

(10) Couturier, S.; Gautheron, B. J. Organomet. Chem. **1978**, 157, C61.

(11) Roddick, D. M.; Fryzuk, M. D.; Seidler, P. F.; Hillhouse, G. L.; Bercaw, J. E., manuscript in preparation.

(12) Gell, K. I.; Schwartz, J. J. Am. Chem. Soc. **1978**, 100, 3246.

(13) Simpson, S. J.; Turner, H. W.; Andersen, R. A. J. Am. Chem. Soc. **1979**, 101, 7728.

(14) Anomalously high bridging hydride stretches have been noted for $[Cp_2TiH]_2$ (1450 cm^{-1})[14a] and binuclear tantalum hydride complexes (1580-1600 cm^{-1}).[14b] (a) Bercaw, J. E.; Brintzinger, H. H. J. Am. Chem. Soc. **1969**, 91, 7301. (b) Belmonte, P. A.; Schrock, R. R.; Day, C. S. J. Am. Chem. Soc. **1982**, 104, 3082.

(15) Lokshin, B. V.; Klemenkova, Z. S.; Ezernitskaya, M. G.; Strunkina, L. I.; Brainina, E. M. J. Organomet. Chem. **1982**, 235, 69.

(16) Wailes, P. C.; Weigold, H. J. Organomet. Chem. **1970**, 24, 405.

(17) Manriquez, J. M.; McAlister, D. R.; Sanner, R. D.; Bercaw, J. E. J. Am. Chem. Soc. **1976**, 98, 6733.

(18) Blenzers, J., Ph.D. Thesis, Ryksuniversiteit te Groningen, **1982**.

(19) Chapter 2 of this thesis.

(20) Hunter, W. E.; Hrncir, D. C.; Vann Bynum, R.; Pentilla, R. A.; Atwood, J. L. Organometallics **1983**, 2, 750.

(21) Fronzek, F. R.; Baker, E. C.; Sharp, P. R.; Raymond, K. N.; Alt, H. G.; Rausch, M. D. Inorg. Chem. **1976**, 15, 2284.

(22) Atwood, J. L.; Hunter, W. E.; Hrncir, D. C.; Samuel, E.; Alt, H. G.; Rausch, M. D. Inorg. Chem. **1975**, 14, 1757.

(23) Jones, S. B.; Petersen, J. L. Inorg. Chem. **1981**, 20, 2889.

(24) Johnson, P. L.; Cohen, S. A.; Marks, T. J.; Williams, J. M. J. Am. Chem. Soc. **1978**, 100, 2709.

(25) Bernstein, E. R.; Hamilton, W. C.; Keiderling, T. A.; Kennelly, W. J.; La Placa, S. J.; Lippard, S. J.; Marks, T. J.; Mayerle, J.J., unpublished results, reported in the Ph.D. dissertation of Keiderling, T. A., Princeton University, **1974**.

(26) Chapter 2 of this thesis.

(27) The ~0.35 Å difference between bridging and terminal hydride bond lengths for 7 and $Cp^*_2Hf(H)(\eta^3\text{-}CH_2CHCH_2)$ is higher than the 0.1-0.2 Å difference normally observed (see reference 28).

(28) Bau, R.; Carroll, W. E.; Teller, R. G.; Koetzle, T. F. J. Am. Chem. Soc. **1977**, 99, 3872.

(29) (a) This ~0.3 Å lengthening going from terminal to $\mu\text{-}PR_2$ coordination contrasts markedly with terminal and bridging Mo-P values for $Mo_2(P^tBu_2)_2(\mu\text{-}P^tBu_2)$[29b] (Mo-P(terminal) = 2.382(1) Å, Mo-P(bridge) = 2.437(1), 2.434(1) Å), which differ by only 0.06 Å. (b) Jones, R. A.; Lasch, J. G.;

Norman, N. C.; Whittlesey, B. R.; Wright, T. C. J. Am. Chem. Soc. **1983**, 105, 6184.

(30) Closest intramolecular nonbonding C-H contacts are C(PB2)-H(22), C(PB3)-H(22) = 2.71 Å.

(31) Defining $t_{1/2}$ as the time at which the P^tBu_2 resonance is half the integral value at t=0, at 25°C, ~3 atm H_2, $t_{1/2} \approx$ 5 min. (**2**), 13 min. (**3**), 7 hr. (**4**).

(32) Lappert, M. F.; Patil, D. S.; Pedley, J. B. J.C.S. Chem. Commun. **1975**, 830.

(33) Tentatively identified by ^1H NMR.

(34) Although no adduct of **1** with PMe_3 was observed down to -70°C, variable temperature ^1H NMR revealed a steady downfield shift ($\Delta\delta$ = 0.3 ppm at -70°C) for the t-butyl resonances, suggestive of an equilibrium involving a metal-phosphine interaction. No similar shift was observed for **1** in the absence of PMe_3.

(35) Fagan, P.J; Manriquez, J. M.; Marks, T. J.; Day, V. W.; Vollmer, S. H.; Day, C. S. J. Am. Chem. Soc. **1980**, 102, 5393.

(36) Fachinetti, G.; Floriani, C.; Marchetti, F.; Merlino, S. J.C.S. Chem. Comm. **1976**, 522.

(37) Erker, G.; Rosenfeldt, F. Angew. Chem., Int. Ed. Engl. **1978**, 17, 605.

(38) Lappert, M. F.; Luong-Thi, N. T.; Milne, C. R. C. J. Organomet. Chem. **1979**, 174, C35.

(39) Fagan, P. J.; Manriquez, J. M.; Vollmer, S. H.; Day, C. S.; Day, V. W.; Marks, T. J. J. Am. Chem. Soc. **1981**, 103, 2206.

(40) Cramer, R. E.; Maynard, R. B.; Paw, J. C.; Gilje, J. W. Organometallics **1982**, 1, 869.

(41) Moore, E. J., Ph.D. Thesis, California Institute of Technology, **1984**.

(42) Using the Eyring equation, with k_c(exchange) rate at coalescence temperature (sec^{-1})) calculated from the Gutowsky-Holm relation: $k_c = \frac{\pi}{\sqrt{2}}\Delta\nu$; Gutowsky, H. S.; Holm, C. H. J. Chem. Phys. **1956**, 25, 1228.

(43) See reference 45 of Marks et. al, reference 39 of this chapter.

(44) Values reported for hindered rotation in organic amides range from 15-30 kcal.[44a] Although direct measurement of acylphosphine rotational barriers has not been reported,[44b] calculations[44c] suggest an upper limit of ~6 kcal. (a) Kessler, H. Angew. Chem., Int. Ed. Engl. **1970**, 9, 219. (b) Egan, W.; Mislow, K. J. Am. Chem. Soc. **1971**, 93, 1805; Kostyanovskii, R. G.; Elnatanov, Y. I.; Zakharov, K. S.; Zagurskaya, L. M. Dokl. Akad. Novk. SSSR (Eng). **1974**, 219, 1021. (c) Dougherty, D. A.; Mislow, K.; Whangbo, M.-H. Tetrahedron Lett. **1979**, 2321.

(45) Saldarriaga-Molina, C. H.; Clearfield, A.; Bernal, I. Inorg. Chem. **1974**, 13, 2880.

(46) Raymond, K. N.; Eigenbrot, Jr., C. W. Acc. Chem. Res. **1980**, 13, 276.

(47) Shannon, R. D. Acta. Crystallogr. **1976**, 32A, 751.

(48) (a) Tranqui, D.; Laugier, J.; Boyer, P.; Vulliet, P. Acta. Crystallogr. **1978**, 34B, 767; Tranqui, D.; Tissier, A.; Laugier, J.; Boyer, P. Ibid. **1977**, 33b, 392. (b) Stutte, B.; Batzel, V.; Boese, R.; Schmid, G. Chem. Ber. **1978**, 111, 1603. (c) Fronczek, F. R.; Baker, E. C.; Sharp, P. R.; Raymond, K. N.; Alt, H. G.; Rausch, M. D. Inorg. Chem. **1976**, 15, 2284.

(49) Smith, W. F.; Taylor, N. J.; Carty, A. J. J.C.S. Chem. Comm. **1976**, 896.

(50) Becker, H.-J.; Fenske, D.; Langer, E.; Prokscha, H. Monatsh. Chem. **1980**, 111, 749.

(51) Khaikin, L. S.; Andrutskaya, L. G.; Grikina, O. E.; Vilkov, L. V.; El'Natov, Y. I.; Kostyanovskii, R. G. J. Mol. Struct. **1977**, 37, 237.

(52) Roddick, D. M., unpublished results.

(53) Marvich, R. H.; Brintzinger, H. H. J. Am. Chem. Soc. **1971**, 94, 2046.

(54) Hoffmann, H.; Schellenbeck, P. Chem. Ber. **1966**, 99, 1134.

(55) Brown, T. L.; Dickerhoof, D. W.; Bafus, D. A.; Morgan, G. L. Rev. Sci. Instrum. **1962**, 33, 491.

(56) Molecular weight determined by isothermal distillation using the Singer method. (a) Singer, R. Justus Liebigs Ann. Chem. **1930**, 478, 246. (b) Clark, E. P. Ind. Eng. Chem., Anal. Ed. **1941**, 13, 820.

(57) Prolonged metathesis resulted in significant Cl $\rightleftharpoons$ Br exchange, as judged by elemental analysis.

(58) International Tables for X-Ray Crystallography, Vol. IV, **1974**, pp. 72-98.

(59) (a) The data were also corrected for absorption by the method of Gaussian quadrature[59b] for the 2120 reflections with multiple observations, the goodness-of-fit was reduced to 3.25 from 3.56 from the correction alone. (b) Busing, W. R.; Levy, H. A. Acta. Crystallogr. **1957**, 10, 180.